# Media access protocols for cable modems

A Thesis

Submitted to the College of Graduate Studies and Research

in Partial Fulfillment of the Requirements

For the Degree of

Master of Science

in the Department of Electrical Engineering

University of Saskatchewan

Saskatoon, Saskatchewan

by

Navjeet Singh Sandhu

November 1997

# Permission To Use

In presenting this thesis in partial fulfillment of the requirements for a Postgraduate degree from the University of Saskatchewan, the author has agreed that the Libraries of this University may make it freely available for inspection. The author further has agreed that permission for copying of this thesis in any manner, in whole or in part, for scholarly purposes may be granted by the professor or professors who supervised this thesis work or, in their absence, by the Head of the Department or the Dean of the College in which this thesis work was done. It is understood that any copying or publication or use of this thesis or parts thereof for financial gain shall not be allowed without the author's written permission. It is also understood that due recognition shall be given to the author and to the University of Saskatchewan in any scholarly use which may be made of any material in this thesis.

Request for permission to copy or to make other use of material in this thesis in whole or part should be addressed to:

Head of the Department of Electrical Engineering
University of Saskatchewan
57 Campus Drive
Saskatoon, Saskatchewan, Canada
S7N 5A9

# Abstract

Cable modems offer qualitatively better performance than either dial-up modems or basic rate ISDN terminal adapters. The cable TV network employs coaxial cable in which the downstream consumes most of the bandwidth from 54 MHz up to the maximum frequency from 600 to 1000 MHz. The upstream is typically assigned to the range from 5 to 42 MHz.

One drawback of cable modems is the lack of standards permitting any cable modem to work with any headend equipment. Work toward a *multimedia cable network system* (MCNS) specification was initiated by Cablelabs, a consortium of Time Warner, Comcast, Cox and Continental Cablevision. This specification defines the physical layer, media access control (MAC) layer, and operational support capabilities.

In this thesis, MAC protocols are described for the upstream path of the hybrid fiber coax network system. These are *Frequency Division Multiple Access* (FDMA), and *Slotted ALOHA* which are standard methods, and *Dynamic Reservation without Contention* (DRNC), *Dynamic Reservation with Contention* (DRC), *Dynamic Reservation with Limited Contention* (DRLC), and *Modified Dynamic Reservation with Limited Contention* (M-DRLC) which are proposed in this work. Detailed mathematical analysis is done and throughput and performance are compared for all six MAC protocols when the users of the network have a variety of data rates. Simulations are done to corroborate the analysis, and simulation results are presented. The effect of *network delay* on the performance is also analysed. Other phenomena, such as *white noise* and *impulse noise* also affect the performance. Simulations are presented to examine the effects of noise on the cable system performance.

From the analysis and simulation results, it is found that FDMA is a very inefficient protocol and it wastes lots of bandwidth. Slotted ALOHA is a simple way to allocate bandwidth, but it is efficient only at very low channel traffic. DRNC gives higher frame delay because it wastes bandwidth by polling inactive users. DRLC is efficient only at very high channel traffic. DRC is efficient if the number of users is very large and user traffic is bursty. M-DRLC is a combination of the DRC and DRLC protocols and it gives low frame delay even at high channel traffic.

Ingress is a big problem in HFC network systems. Even narrowband ingress can make more than 15% of the upstream spectrum useless. Large round trip delay also degrades the cable system performance. Most of the errors generated by white noise and impulse noise can be controlled by using forward error correcting codes. It was found that system performance does not degrade substantially at $10^{-4}$ random bit error rate.

# Acknowledgements

I would like to thank Dr. Surinder Kumar for his supervision, guidance and constant encouragement during the course of this work. I also like to express my gratitude and appreciation to my supervisor Dr. Hugh Wood, for his advice and financial support from the very beginning of my study.

Many thanks go to Dr. Eric Salt, Prof. David Dodds, Dr. Protap Pramanick and Dr. Tarlochan Sidhu for their valuable comments and suggestions. I would also like to thank my fellow graduate students, Abdulfattah Shamiss and Faizal Djoemadi for their discussion, suggestions and assistance.

Special thanks are extended to my Uncle Kanwaljeet Singh Jawanda who has been so supportive all the way. A special thanks is reserved to my friends Pawan, Ishaque, Bhanu, Ram, Sathish, Narain, and Garry for their constant love and friendship.

Financial support provided by University of Saskatchewan scholorship is thankfully acknowledged.

# Table Of Contents

**Permission To Use** i

**Abstract** ii

**Acknowledgements** iii

**Table Of Contents** iv

**List of Tables** viii

**List of Figures** ix

**List of Symbols and Acronyms** xii

**1 Introduction** 1

1.1 Multimedia Cable Network System (MCNS) . . . . . 1

1.2 Media Access Control protocols . . . . . 2

1.3 The Channel Allocation problem . . . . . 2

1.3.1 Static Channel Allocation . . . . . 2

1.3.2 Dynamic Channel Allocation . . . . . 3

1.4 Assumptions . . . . . 4

1.5 Thesis Objective . . . . . 6

1.6 Performance . . . . . 7

1.7 Organization of Thesis . . . . . 7

**2 The Distribution Network** 9

2.1 Local distribution schemes . . . . . 10

2.1.1 *Asymmetric Digital Subscriber Line* (ADSL) . . . . . 10

2.1.2 *Fiber To The Curb* (FTTC) . . . . . 10

2.1.3 *Fiber To The Home* (FTTH) . . . . . 10

2.1.4 *Hybrid Fiber Coax* (HFC) . . . . . 11

2.2 Hybrid Fiber Coax (HFC) Network Design . . . . . 11

2.2.1 *Low Fiber* HFC network . . . . . 12

2.2.2 *Medium Fiber* HFC network . . . . . 13

2.2.3 *Deep Fiber* HFC network . . . . . 13

2.3 Upstream Path of the HFC network . . . . . 14

2.3.1 Limitations of the Upstream Path of the HFC network . . . . 14

**3 Impairments in the Upstream Channel** 17

3.1 Thermal Noise . . . . . 18

3.1.1 Noise Floor . . . . . 18

3.1.2 Amplifier Noise . . . . . 19

3.2 Narrowband Ingress . . . . . 21

3.2.1 Ingress due to Short-Wave Broadcasting . . . . . 22

3.2.2 Ingress due to Amateur and CB Radio . . . . . 25

3.2.3 Other Services . . . . . 26

3.3 Impulse Noise . . . . . 28

3.3.1 Natural sources . . . . . 28

3.3.2 Human sources . . . . . 28

3.3.3 Model of Impulse Noise . . . . . 29

3.4 Summary . . . . . 30

**4 Media Access Protocols For Cable Modems** 31

4.1 *Fixed assignment* FDMA/TDMA . . . . . 31

4.1.1 Frame Delay for FDMA . . . . . 33
4.1.2 Throughput Analysis for FDMA . . . . . 35
4.2 Slotted ALOHA . . . . . 35
4.2.1 Frame Delay for Slotted ALOHA . . . . . 37
4.3 *Dynamic Reservation without Contention* DRNC . . . . . 39
4.3.1 Frame delay for DRNC . . . . . 41
4.3.2 Throughput Analysis for DRNC . . . . . 43
4.4 *Dynamic Reservation with Contention* DRC . . . . . 44
4.4.1 Frame Delay for DRC . . . . . 45
4.4.2 Throughput Analysis for DRC . . . . . 51
4.5 *Dynamic Reservation with limited Contention* DRLC . . . . . 52
4.5.1 Frame Delay for DRLC . . . . . 52
4.5.2 Throughput Analysis for DRLC . . . . . 54
4.6 *Modified-Dynamic Reservation with Limited Contention* M-DRLC . . 54
4.6.1 Frame Delay for M-DRLC . . . . . 55
4.6.2 Throughput Analysis for M-DRLC . . . . . 58

**5 Simulation, analysis and comparison of MAC protocols for the upstream path of the HFC network system 60**

5.1 Comparison of MAC protocols . . . . . 60
5.2 Network delay . . . . . 63
5.2.1 The effect of network delay on the performance of MAC protocols 64
5.3 Simulation Model for Slotted ALOHA . . . . . 68
5.3.1 Contention Resolution . . . . . 69
5.4 Simulation Model for DRNC and DRLC . . . . . 71
5.5 Simulation Model for DRC protocol . . . . . 73
5.6 Simulation Model for M-DRLC . . . . . 74

**6 The effect of White Noise and Impulse Noise on the performance 76**

6.1 Quadrature Amplitude Modulation (QAM) . . . . . 76
6.1.1 Probability of Error of QAM . . . . . 76
6.2 Error Control . . . . . 78
6.3 Forward Error Correction(FEC) . . . . . 79
6.3.1 Linear Block Codes . . . . . 79
6.3.2 Reed-Solomon(RS) block code . . . . . 80
6.4 Error Detection . . . . . 81
6.5 The effect of White Noise on the performance . . . . . 83
6.6 The effect of Impulse Noise on the performance . . . . . 86
6.7 Summary . . . . . 87

**7 Summary and Conclusions** **90**
7.1 Summary . . . . . 90
7.2 Conclusions . . . . . 91
7.3 Future Work . . . . . 93

**References** **95**

**A Media Access Control Layer** (*From MCNS Specifications*) **98**
A.1 Introduction . . . . . 98
A.1.1 Service ID . . . . . 98
A.1.2 Mini-Slots . . . . . 98
A.2 Frame . . . . . 99
A.2.1 MAC Frame Transport . . . . . 100
A.3 Upstream Bandwidth Allocation . . . . . 100

**B Protocol Example** (*From MCNS Specifications*) **103**

# List of Tables


3.1 Broadcasting Allocation Between 5 and 42 MHz . . . . . 22

3.2 Data Carriers in the Gaps Between Broadcasting Bands(Part 1) . . . 23

3.3 Data Carriers in the Gaps Between Broadcasting Bands(Part 2) . . . 24

3.4 Amateur and Citizens Band Allocations Between 5 and 42 MHz . . . 25

3.5 Data Carriers in the Gaps Between Broadcasting Bands, Amateur and CB Bands (Part 1) . . . . . 26

3.6 Data Carriers in the Gaps Between Broadcasting Bands, Amateur and CB Bands (Part 2) . . . . . 27

4.1 Total raw data rate at the physical layer available for given ingress-free spectrum . . . . . 32

4.2 Raw bit rate available (**in kbit/sec**) at the physical layer to each CM by FDM, while using QPSK modulation . . . . . 32

5.1 *Network distance* in kms and corresponding *network delay* in milli seconds 64

6.1 Comparison of different Block Codes . . . . . 79

A.1 PHY Overhead . . . . . 100

# List of Figures


2.1 The Distribution Network . . . . . 9

2.2 Three different HFC network systems based on the number of subscribers per fiber node . . . . . 12

2.3 *Low Fiber* Hybrid Fiber Coax Network . . . . . 13

2.4 *Medium Fiber* Hybrid Fiber Coax Network . . . . . 14

2.5 *Deep Fiber* Hybrid Fiber Coax Network . . . . . 15

3.1 Upstream Path of the HFC network . . . . . 17

3.2 Example showing relation between thermal noise, amplifier noise and signal carrier level at a given signal to noise ratio . . . . . 20

3.3 Noise due to amplifiers in cascade . . . . . 20

3.4 Example showing impulse noise . . . . . 29

4.1 Performance of FDMA protocol . . . . . 34

4.2 Performance of Slotted ALOHA Protocol at various *frame delay* . . . 38

4.3 Example of DRNC protocol (round trip delay and processing time taken by CMs and CMTS are ignored) . . . . . 39

4.4 Example showing simplified version of DRNC . . . . . 41

4.5 Frame Delay in DRNC as a function of $\lambda$ and $L_{tx}$ ($N_{cm} = 100$) . . . . 43

4.6 Frame Delay in DRNC as a function of $\lambda$ and $N_{cm}$ ($L_{tx} = 100$ bytes) . 43

4.7 Performance of DRNC . . . . . 44

4.8 DRC protocol *(note that it is assumed that round trip and processing time taken by CM & CMTS is negligible)* . . . . . 45

4.9 Fraction of bandwidth used for message transmission for different values of r and $L_{tx}/L_{req}$ . . . . . 48
4.10 $D_1$ and $D_2$ as a function of $\lambda_{req}$ . . . . . 49
4.11 $D$ as a function of $\lambda_{req}$ and $r$ . . . . . 49
4.12 Performance of DRC at various delay . . . . . 51
4.13 Frame Delay ($D$) for various values of $P_A$ and $\lambda$ . . . . . 53
4.14 Performance of DRLC at different delays . . . . . 54
4.15 Performance of M-DRLC for *hyper* CMs . . . . . 56
4.16 Performance of M-DRLC for *slack* CMs . . . . . 57
4.17 Performance of M-DRLC . . . . . 58

5.1 Frame delay vs throughput (part-1) . . . . . 61
5.2 Frame delay vs throughput (part-2) . . . . . 62
5.3 Comparing M-DRLC and DRC . . . . . 63
5.4 Performance of FDMA Protocol at various *network distance* . . . . . 65
5.5 Performance of Slotted ALOHA at various *network distance* . . . . . 65
5.6 Example showing DRNC in presence of *network delay* . . . . . 66
5.7 Effect of *network distance* on DRC . . . . . 67
5.8 Effect of *network distance* on M-DRLC . . . . . 69
5.9 Comparison of Analytical results with Simulation results for Slotted Aloha . . . . . 70
5.10 Simulation results for DRNC and DRLC protocols . . . . . 72
5.11 Simulation results for DRC protocols . . . . . 74
5.12 Simulation results for M-DRLC protocol . . . . . 75

6.1 Probability of a symbol/bit error for QAM-16 and QPSK . . . . . 77
6.2 Data Link Layer and Physical Layer of cable modem . . . . . 82
6.3 Performance of Slotted ALOHA in presence of AWGN noise . . . . . 84
6.4 Effect of white noise on DRC protocol . . . . . 85

6.5 Effect of Impulse noise (type A) on DRC protocol . . . . . 87
6.6 Effect of Impulse noise (type B) on DRC protocol . . . . . 88

A.1 Generic MAC Frame Format . . . . . 99
A.2 Variable Length Packet PDU Frame . . . . . 99
A.3 Upstream MAC/PHY Convergence . . . . . 101
A.4 Allocation Map . . . . . 101

B.1 Protocol Example . . . . . 103

# List of Symbols and Acronyms

| | |
|---|---|
| $A$ | gain of the system |
| $A_{cm}$ | total number of active cable modems |
| ADSL | Asymmetric Digital Subscriber Line |
| ATM | Asynchronous Transfer Mode |
| AWGN | Additive White Gaussian Noise |
| B | bandwidth in Hz |
| $B_h$ | channel utilisation by *hyper* users (in M-DRLC) |
| $B_s$ | channel utilisation by *slack* users (in M-DRLC) |
| BCH | Bose Chaudhuri Hocquenghem |
| BEBA | The Binary Exponential Backoff Algorithm |
| BER | Bit Error Rate |
| $c$ | speed of light |
| CATV | Community Access Television (Cable Television) |
| CCIR | Centre for Communication Interface Research |
| CM | Cable Modem |
| CMTS | Cable Modem Termination System |
| CRC | Cyclic Redundancy Check |
| $d$ | network distance (maximum distance between CM & CMTS) |
| $\hat{d}$ | minimum distance between codes (in bits) |
| $D$ | frame delay |

| | |
|---|---|
| $D_1$ | delay in placing request (in DRC) |
| $D_2$ | queueing plus transmission delay for message frame (in DRC) |
| $D_h$ | average frame delay for *hyper* users, (in M-DRLC) |
| $D_{min}$ | minimum distance between non-binary code words |
| $D_s$ | average frame delay for *slack/inactive* CMs (users) |
| DRC | Dynamic Reservation with Contention |
| DRLC | Dynamic Reservation with Limited Contention |
| DRNC | Dynamic Reservation without Contention |
| $erfc$ | complementary error function |
| $f_h$ | fraction of channel traffic produced by *hyper* CMs (in M-DRLC) |
| $f_s$ | fraction of channel traffic produced by *slack* CMs (in M-DRLC) |
| FDMA | Frequency Division Multiple Access |
| FEC | Forward Error Correction |
| FTTC | Fiber To The Curb |
| FTTH | Fiber To The Home |
| $g$ | normalised frame traffic at one station |
| $G$ | normalised channel traffic at mean $G$ frames per frame time (new traffic plus old traffic due to retransmission of frames that previously suffered collision) |
| $G_n$ | normalised new channel traffic (at Poisson rate of $G_n$ frames per frame time) |
| $G_{req}$ | average number of attempts (new + old) per *request frame* time (in DRC) |
| $G_{tx}$ | number of request arriving at CMTS per message frame time. |
| $H_{cm}$ | number of *hyper* CMs (in M-DRLC) |
| HCS | Header Check Sequence |
| HF | High Frequency (5-30 MHz) |
| HFC | Hybrid Fiber Coax |

| | |
|---|---|
| IE | Information Element |
| ISDN | Integrated Service Digital Network |
| $k$ | Boltzmann's constant |
| $\hat{k}$ | number of information bits in a code |
| $K$ | maximum retransmission delay in frame slots (in Slotted Aloha) |
| $\hat{K}$ | number of information symbols in a non-binary code word |
| $l$ | number of symbols (or bits) not transmitted in shortened code word |
| $L_{req}$ | length of request frame in bytes |
| $L_{tx}$ | length of message frames in bytes |
| LLC | Logical Link Layer |
| $M$ | number of states in a modulation system |
| MAC | Media Access Control |
| MCNS | Multimedia Cable Network System |
| MDU | Multiple Dwelling Unit |
| M-DRLC | Modified-Dynamic Reservation with Limited Contention |
| MPEG | Motion Picture Experts Group |
| $n$ | number of information bits in a codeword |
| $n_f$ | noise figure of the amplifier |
| $n_o$ | total noise at the output of the system |
| $n_x$ | noise at the output of xth amplifier |
| $N$ | length of a non binary code word in symbols |
| $N_{cm}$ | number of cable modem on one Coax Drop |
| N-ISDN | Narrowband - Integrated Service Digital Network |
| OC | Optical Carrier |
| ONU | Optical Network Unit |
| $P_0$ | probability that zero frame are generated |
| $P_c$ | probability of correct decision |

| | |
|---|---|
| $P_n$ | thermal noise threshold (noise floor) |
| $P_r$ | probability that some(r) frames are generated in some interval |
| $P_k$ | probability of transmission requiring exactly k attempts (i.e., k-1 collisions followed by one success) |
| $P_A$ | percentage of *active* CMs |
| $P_H$ | percentage of *hyper* CMs (in M-DRLC) |
| $P_{\sqrt{M}}$ | probability of symbol error in $\sqrt{M}$-ary PAM |
| $P_M$ | probability of symbol error in M-ary QAM |
| $\widehat{P_M}$ | probability of bit error in M-ary QAM |
| $P_S$ | percentage of *slack* CMs (in M-DRLC) |
| PAM | Pulse Amplitude Modulation |
| PDU | Protocol Data Unit |
| $q$ | total different possible symbols in a non-binary code |
| QAM | Quadrature Amplitude Modulation |
| QoS | Quality of Service |
| QPSK | Quadrature Phase Shift Keying |
| $r$ | maximum value of $G_{tx}$ in DRC protocol |
| $\hat{r}$ | number of parity bits in a codeword |
| rms | root mean square |
| $R$ | resistance in ohms |
| $R_c$ | code rate |
| RFI | Radio Frequency Interference |
| RS | Reed Solomon |
| $S$ | throughput |
| $S_{cm}$ | number of *slack* CMs (in M-DRLC) |
| $S_h$ | throughput for *hyper* CMs (in M-DRLC) |

| | |
|---|---|
| $S_{req}$ | throughput per *request frame* time (in DRC) |
| | (number of requests arriving per *request frame* time at CMTS) |
| $S_s$ | throughput for *slack* and *inactive* CMs (in M-DRLC) |
| $S_v(f)$ | noise voltage spectral density |
| SFU | Single Family Unit |
| SID | Service ID |
| SNR | Signal to Noise Ratio |
| SOF | Start Of Frame |
| SONET | Synchronous Optical Network |
| $t$ | correction capability of a code |
| $t_{nd}$ | network delay |
| $t_{max\_sd}$ | maximum value of $t_{sd}$ |
| $t_{pr}$ | total processing time taken by CM and CMTS |
| $t_{rd}$ | round trip delay |
| $t_{req}$ | time spent in polling |
| $t_{sd}$ | slot synchronization time |
| $t_{ttx}$ | frame transmission time |
| $t_{tx}$ | time spent in transmitting all message frames |
| T | absolute temperature |
| $\overline{v_n{}^2}$ | mean-square noise voltage |
| VHF | Very High Frequency (30-300 MHz) |
| $W$ | upstream bandwidth in bit/s |
| $W_a$ | bandwidth given to active CMs (in DRLC) |
| $W_h$ | bandwidth given to *hyper* CMs (in M-DRLC) |
| $W_i$ | bandwidth given to inactive users (in DRLC) |
| $W_{req}$ | bandwidth assigned to request channel (in DRC) |
| $W_s$ | bandwidth given to *slack* and *inactive* CMs (in M-DRLC) |

| | |
|---|---|
| $W_{tx}$ | bandwidth assigned to message channel (in DRC) |
| $x$ | total number of amplifiers contributing to noise |
| $\alpha$ | fraction of bandwidth given to *hyper* CMs. (in M-DRLC) |
| $\gamma_b$ | signal to noise ratio per bit |
| $\theta$ | fraction of bandwidth given to inactive CMs. (in DRLC) |
| $\kappa$ | constant (the value is between 0.2 to 0.9) |
| | It is the ratio of speed of light in coax to speed of light in vacuum |
| $\lambda$ | Poisson traffic at one station (new + old) |
| $\lambda_h$ | Poisson traffic produced by any hyper CM (in M-DRLC) |
| $\lambda_{req}$ | Poisson traffic at one CM (in DRC) |
| $\lambda_s$ | Poisson traffic produced by any slack CM (in M-DRLC) |
| $\tau$ | length of frame in seconds |
| $\tau_{req}$ | length of request frame in seconds |
| $\tau_{tx}$ | length of message frame in seconds |
| $\Lambda$ | channel traffic (new + old) |
| $\Lambda_h$ | total traffic produced by *hyper* CMs (in M-DRLC) |
| $\Lambda_n$ | channel traffic (only new) |
| $\Lambda_{req}$ | mean number of attempts per second at request channel (in DRC) |
| $\Lambda_s$ | total traffic produced by *slack* CMs (in M-DRLC) |
| $\Lambda_{tx}$ | mean number of requests arriving at CMTS per second (in DRC) |

# Chapter 1

# Introduction

The increasing demand for interactive television and data services on one hand, and the liberalisation of many telecommunications markets on the other, are resulting in a growing demand for bandwidth on publicly available networks. High speed data transmission via co-axial cable is one option. The cable TV network employs coaxial cable in which the downstream, from the headend to the customer, consumes most of the bandwidth- from 54 MHz up to the maximum frequency, between 600 and 1000 MHz. The upstream is typically assigned to the range from 5 to 42 MHz.

Most cable TV networks were designed as "tree-and-branch" networks. While broadcasting to the branches works fine, the noise from all the branches converges when users transmit in the upstream direction. A cable TV network acts as a giant antenna, and many sources of interference and noise are present in the upstream portion of the spectrum.

## 1.1 Multimedia Cable Network System (MCNS)

Another drawback to the use of the coaxial cable network is the lack of standards permitting any cable modem to work with any headend equipment. Work toward setting standards for the multimedia cable network system was initiated by Cablelabs, a consortium of Time Warner, Comcast Cable Communications, Cox Communications, Tele-Communications and Continental Cablevision. These specifications define the physical layer, media access control layer, and operational support capabilities. The standard is being cast in silicon by chipset manufacturer Broadcom Corp. and has

received compliance commitments from 3Com, Bay Networks, Cisco Systems, Com21, General Instrument, Hewlett-Packard and Scientific-Atlanta [1, 2].

## 1.2 Media Access Control protocols

Broadcast networks have an additional issue in the data link layer: how to control access to the shared channel. A special sublayer of the data link layer, the media access sublayer, deals with this problem.

The media access control (MAC) protocol governs access to the transmission medium independent of the physical characteristics of the medium, but taking into account the topological aspects of the subnetworks, in order to enable the exchange of data between the nodes. MAC procedures include framing, error protection, and acquiring the right to use the underlying transmission medium.

In this thesis, MAC protocols are described for the upstream path of the hybrid fiber coax network system. These are *Frequency Division Multiple Access* (FDMA), and *Slotted* ALOHA which are standard methods, and *Dynamic Reservation without Contention* (DRNC), *Dynamic Reservation with Contention* (DRC), *Dynamic Reservation with Limited Contention* (DRLC) and *Modified Dynamic Reservation with Limited Contention* (M-DRLC) which are proposed in this work. These protocols are discussed in Chapter 4.

## 1.3 The Channel Allocation problem

The main objective of the MAC layer is to allocate a single broadcast channel among competing Cable Modems (CMs). This can be done by two schemes: static channel allocation and dynamic channel allocation.

### 1.3.1 Static Channel Allocation

The traditional way of allocating a single channel among multiple competing users (CMs) is Frequency Division Multiple Access (FDMA). If there are N users, the bandwidth is divided into N equally sized portions and each user is assigned one

portion. Since each user has a private frequency band, there is no direct interference between users. When there is only a small and fixed number of users, each of which has a heavy load of traffic, FDMA is a simple and efficient allocation mechanism

However, when the number of users is large and continually varying, or traffic is bursty, FDMA is very inefficient. This is discussed in more detail in Section 4.1.

### 1.3.2 Dynamic Channel Allocation

In this case, the cable modem termination system (CMTS) acts as a central controller. It controls and allocates bandwidth on request to all of the attached CMs(cable modems). Dynamic channel allocation can again be subdivided into three basic categories. These are collision-free allocation (contention free), with contention allocation, and with limited contention allocation.

#### Contention Free Allocation

A CM sends a request and message frame to the CMTS on the upstream channel (5-42 MHz). The CMTS sends acknowledgements and control signals to all CMs on the downstream channel (54 MHz to 1000 MHz). It is assumed for the sake of simplicity that the downstream channel is an ideal channel.

Dynamic Reservation Without Contention (DRNC) is a Contention Free Allocation. In this protocol, the CMTS polls all CMs and, depending upon requests received, it then allocates bandwidth to the active CMs. The DRNC protocol is discussed in more detail in Section 4.3.

#### Channel Allocation with Contention

The Slotted ALOHA protocol comes under the category of channel allocation with contention. In this case, the channel is divided by time into fixed frame slots and CMs are free to transmit in any slots. There is a chance that two or more CMs will try to send a frame in the same slot. In this case there will be collisions and all the colliding frames will be garbled.

The coaxial cable system is an analog network system. To transmit digital signals on an analog network, each interface must contain electronics to convert the outgoing bit stream to an analog signal, and the incoming analog signal to a bit stream. The system is also a broadband system; broadband systems are divided into multiple channels where each channel can be used for analog television, digital television, analog audio, digital audio, or a digital bit stream for data services.

In a broadband system, it is extremely difficult to detect collisions, so the CMs have to depend on the CMTS for collision detection. For every successful transmission, the CMTS has to send an acknowledgement. If the CM does not receive an acknowledgement in a certain time, then it has to retransmit the same frame. It then again waits for an acknowledgement, and the process continues until the CM is able to do a successful transmission. Section 4.2 gives more detail about slotted ALOHA.

### Limited Contention Allocation

This allocation mechanism uses both allocation techniques, contention and contention free allocation. DRC, DRLC and M-DRLC protocols are included in this category.

## 1.4 Assumptions

There are five key assumptions, made while doing the analysis for MAC protocols.

1 **Station model.** The model consists of $N_{cm}$ stations (cable modems), each with a program or user that generates frames. Some stations are active and some are inactive. Active stations are producing traffic and inactive stations are silent. Active stations can become inactive at any time and vice versa. All stations are producing new traffic at rate $\Lambda_n$ frames/s. In addition to the new frames, the stations also generate retransmissions of frames that previously suffered collisions. In analysis, it is further assumed that old and new channel traffic combined is also *Poisson* distributed, with mean $\Lambda$ frames per second.

2 **Subsplit Channel Assumptions** The medium used for transmission is broadband coaxial cable. The cable can be used up to 1000 MHz. The broadband cable

channel is split into two sub channels, the upstream channel and downstream channel. In the subsplit system, frequencies from 5 to 42 MHz are used for the upstream channel and frequencies from 50 to 1000 MHz are used for the downstream channel. All CMs send message and request frames to the CMTS using the upstream channel and a CMTS communicates with all the attached CMs using the downstream channel. It is further assumed that the downstream channel is an ideal channel. All stations are equivalent, with no special priorities assigned to any of them.

3 **Collision Assumption.** If two frames are transmitted simultaneously, they overlap in time and the resulting signal is garbled. This event is called a collision. Collided frames must be transmitted again later. If a CM transmits a frame and transmission is successful, then the CMTS must send an acknowledgement for that frame. It is assumed that an acknowledgement sent by the CMTS always reaches the CM with no delay.

4 **Slotted Time.** Time is divided into discrete intervals (frame slots). Frame transmission always begins at the start of a slot. A slot may contain zero, one or more frames, corresponding to an idle slot, a successful transmission, or a collision, respectively.

5 **No Carrier Sense.** As the transmission medium is broadband coaxial cable, it is not possible for stations to sense the channel before trying to use it; they just go ahead and transmit. Only from the acknowledgement received from the CMTS can they determine whether or not a transmission was successful.

This does not mean that all stations are totally blind about the status of the upstream channel. In some protocols, i.e. collision free protocols, all stations have complete information about the upstream channel and all stations will have knowledge in advance when to transmit and when not to transmit. This will be discussed in more detail in Chapter 4.

The MAC sublayer defines a single transmitter for the downstream channel - the CMTS. All CMs listen to all frames transmitted on the downstream channel and

accept those the destination of which match those at the CM. CMs can communicate with other CMs only through the CMTS.

The upstream channel is characterized by many transmitters (CMs) and one receiver (the CMTS). Time in the upstream channel is slotted, providing for Time Division Multiple Access at regulated time ticks. The CMTS provides the time reference and controls the allowed usage for each interval. Intervals may be granted for transmissions by particular CMs, or for contention by all CMs. CMs may contend to request transmission time. To a limited extent, CMs may also contend to transmit actual data. In both of these cases, collisions can occur and retries are used.

With this much background, it is now possible to describe the objectives of this thesis.

## 1.5 Thesis Objective

The objectives of this thesis are as follows:

1. Discuss impairments in the upstream channel of the hybrid fiber/coax cable network system.
2. Develop MAC protocols for the cable modem.
3. Analyse the performance of these protocols when the users of the network have a variety of data rates.
4. Analyse the effect of *narrowband ingress* on the cable system performance
5. Analyse the effect of *round trip* delay on the performance.
6. Simulate the model to verify the analysis.
7. Simulate the effects of *white noise* and *impulse noise* on the performance.

## 1.6 Performance

*Performance* in this thesis is taken to mean how many users (CMs) a cable system can support at a particular frame delay and user traffic under ideal situations. The ideal situation means the channel error and round trip delay are negligible and can be neglected. *Performance*, when there is considerable round trip delay, means how many users (CMs) a cable system can support at a given frame delay, user traffic, and network distance. *Throughput performance* in this thesis means the maximum throughput that a given protocol can provide under a given situation. *Delay performance* means how much frame delay a given protocol causes at a given channel traffic or throughput. *Performance* in the presence of noise means how much *delay performance* degrades by a given noise. *Performance* is considered acceptable if frame delay does not increase by more than 20% in the presence of a given noise.

## 1.7 Organization of Thesis

In addition to this introductory chapter, the thesis is organized as follows. Some common types of distribution networks are described in Chapter 2. Much attention is being paid to hybrid fiber coax (HFC) CATV-networks because of their high penetration level, high available capacity, and good linearity in the downstream channels. The HFC network is discussed in more detail in Section 2.2.

However, upstream channels available in a common CATV-network are far from ideal. Only limited bandwidth is provided, and undesired accumulation of ingress noise and interference occurs due to the partial tree and branch architecture. Limitations of the upstream path are discussed in more detail in Section 2.3 and impairments in the upstream channel are discussed in Chapter 3.

The resulting noise characteristics will determine the choice of modulation and multi-access techniques. The MCNS specification (Section 1.1) describes some MAC protocols for cable modems. MAC protocols are proposed for cable modems in Chapter 4.

MAC protocols are compared for performance in Chapter 5. The effect of *network delay* on the performance is analysed in Section 5.2. Also in this chapter, all six MAC protocols are simulated and the results are compared with analytical ones.

In Chapter 6, the effect of *white noise* and *impulse noise* on performance is discussed. Quadrature Amplitude Modulation (QAM) has emerged as the major contender for the upstream digital transmission on hybrid fiber/coax (Section 6.1). QAM is sensitive to *white noise* and *impulse noise*. Network designers have developed many strategies for dealing with errors. One way to correct errors is by using forward error correcting codes such as Reed Solomon (RS) codes (Section 6.3.2). Simulations are presented to examine the effects of noise on the cable system performance.

Conclusions and suggestions for further study are given in Chapter 7.

# Chapter 2

# The Distribution Network

Multiple access protocols and local distribution networks are very closely related, so in this chapter some types of local distribution networks and especially the hybrid fiber coax network system will be discussed. The distribution network is the set of switches and lines between the source and destination. It consists of a SONET or ATM (or ATM over SONET) backbone connected to a local distribution network. The main requirements imposed on the backbone are high bandwidth and low jitter [3].

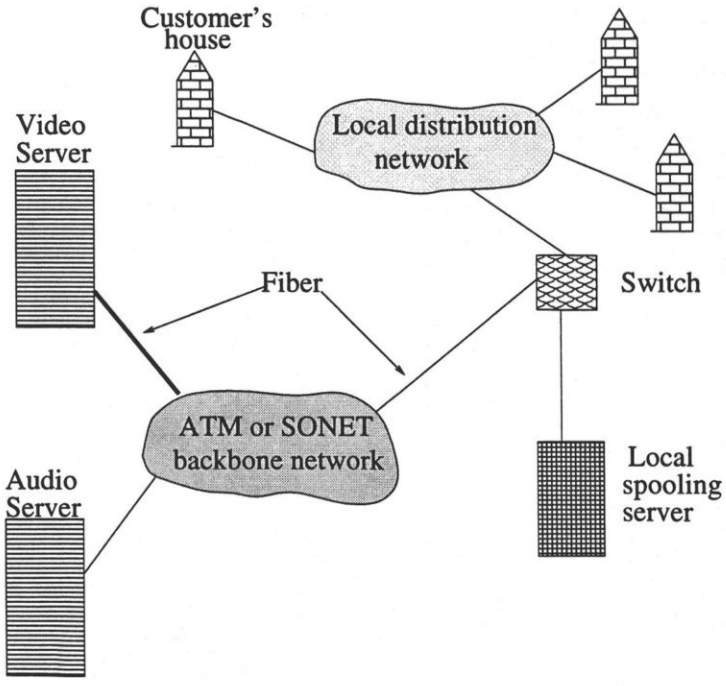


**Figure 2.1:** The Distribution Network

## 2.1 Local distribution schemes

Local distribution is highly chaotic at the present time, with different companies trying out different types of networks in the regions. Telephone companies, cable TV companies, and new entrants are all convinced that whoever gets there first will be the big winner, so there is a proliferation of technologies being installed. There are four main local distribution schemes, as described below.

### 2.1.1 *Asymmetric Digital Subscriber Line* (**ADSL**)

The idea is that virtually every house in North America, Europe and Japan already has a copper twisted pair going into it (for analog telephone service). These wires can be used for video on demand and other interactive services. ADSL-1 offers a 1.536 Mbit/sec downlink channel, but only a single 16 kbit/s uplink channel in addition to the old 4-kHz analog telephone channel (or in some cases, two N-ISDN digital channels).

### 2.1.2 *Fiber To The Curb* (**FTTC**)

In FTTC, the telephone company runs optical fiber from the end office into each residential neighbourhood, terminating in a device called an **ONU** (Optical Network Unit). On the order of 16 copper loops can terminate in an ONU. These loops are now so short that it is possible to run full-duplex T1 or T2 over them, allowing MPEG-1 and MPEG-2 movies respectively. In addition, video-conferencing for home workers and small businesses is now possible because FTTC is symmetric.

### 2.1.3 *Fiber To The Home* (**FTTH**)

In FTTH, the telephone company runs optical fiber from the end office into everyone's house. In this scheme, everyone can have an OC-1, OC-3, or even higher carrier if that is required. FTTH is very expensive and will not happen on a large scale for years but clearly will open a vast range of new possibilities when it finally happens.

### 2.1.4 *Hybrid Fiber Coax* (**HFC**)

ADSL, FTTC, and FTTH are all point-to-point local distribution networks, which is not surprising given how the current telephone system is organised. A completely different approach is HFC, which is the preferred solution currently being installed by cable TV providers.

## 2.2 Hybrid Fiber Coax (HFC) Network Design

The HFC network is a broadband, bi-directional, shared-media transmission system using fiber trunks between the headend and the fiber nodes, and coaxial distribution from the fiber nodes to the customer location. It is a new local distribution network solution currently being installed by cable TV providers. The current 300 to 450 MHz coax cables will be replaced by 750 MHz coax cables, upgrading the capacity from 50 to 75 6-MHz channels to 125 6-MHz channels; 75 of the 125 channels will be used for transmitting analog television. The 50 new channels will each be modulated using QAM-256, which provides about 40 Mbit/sec per channel, giving a total of 2 Gbit/sec of new bandwidth. The headend will be moved deeper into the neighbourhood, so each cable runs past only a few houses.

This development does require the cable providers to replace all the existing cables with 750 MHz coax, install new headends, and remove all the one-way amplifiers–in short, replace the entire cable TV system.

This system is built with coax cable, and designers have to deal with all the impairments of the cable area network. The two main impairments in an HFC plant are noise and ingress. Noise, created mainly by field amplifiers, has not proved to be as large a problem as ingress. Ingress on a CATV plant can come from several sources including poor RFI shielding, damaged coaxial cabling, poor connections/connectors, and unterminated cabling.

One possible solution to ingress and other problems is to take fiber closer to homes (**build fiber deep**). The closer the system is to an all passive network, the more reliable the network becomes and the less vulnerable it will be to ingress and noise.

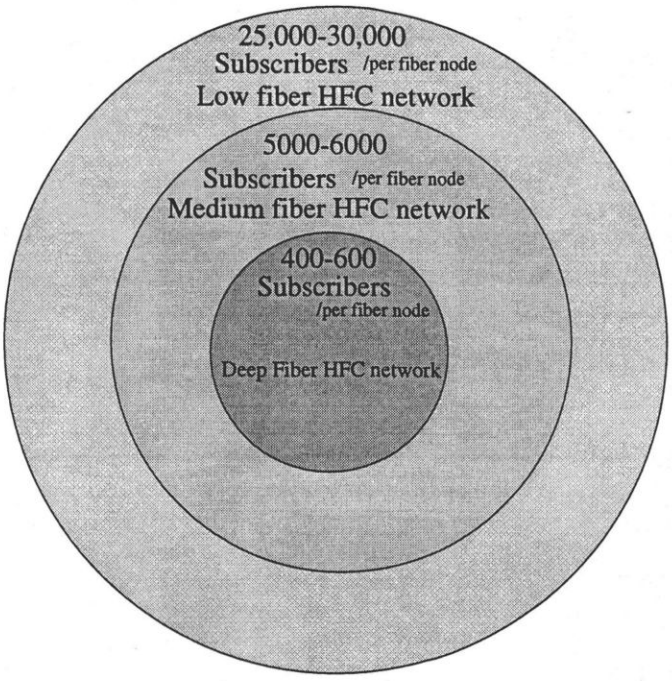


**Figure 2.2:** Three different HFC network systems based on the number of subscribers per fiber node

This would be as a result of reducing or eliminating cascade amplifiers as well as "shortening the antennae" for ingress. As a result, smaller node sizes evolve and fewer subscribers compete for clean bandwidth. But because the majority of interference problems arise in the drop within the home, even building fiber deep will not eliminate all ingress but it will definitely help in reducing it.

The big question is how much investment cable operators are capable of making. Building fiber deep is very expensive and may not be a viable solution. Depending upon the depth of fiber into the network, three types of HFC networks can be constructed.

### 2.2.1 *Low Fiber* HFC network

This is the first phase of HFC network design. In this design, it is assumed that one fiber node will serve 25,000 to 30,000 homes. There will 10-12 coax drops from one fiber node, each coax drop serving 2,500 to 3,000 homes. The maximum number of

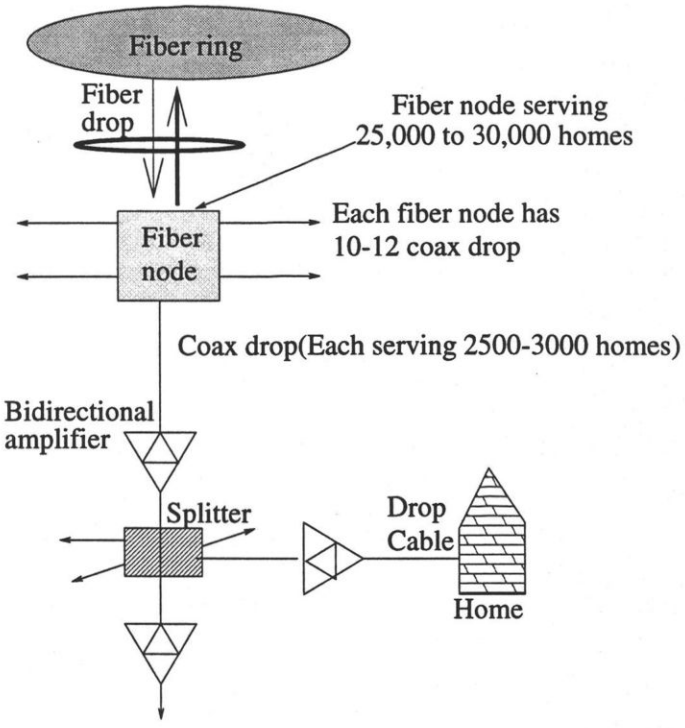


**Figure 2.3:** *Low Fiber* Hybrid Fiber Coax Network

cascade amplifiers will be 16-30; the farthest home from a node is 50-100 kms.

### 2.2.2 *Medium Fiber* HFC network

In the second phase of HFC network design, it is assumed that one fiber node will serve 5,000 to 6,000 homes. There will 5-10 coax drops from one fiber node, each coax drop serving 500-1,000 homes. The maximum number of cascade amplifiers will be 10-20, and the farthest home from a node may be 20-60 kms.

### 2.2.3 *Deep Fiber* HFC network

For more bandwidth, fiber could be pushed closer to the home. In the third phase of HFC network design, it is assumed that one fiber node will serve 200-800 homes. There will be 2-6 coax drops from one fiber node, each coax drop serving 100-150 homes. The maximum number of cascade amplifiers will be 4-16, and the farthest home from a node will be 2-40 kms.

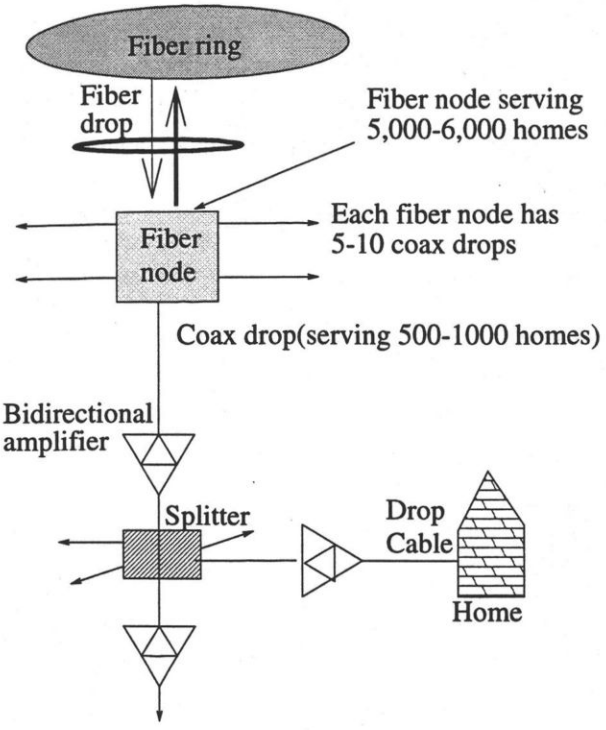


**Figure 2.4:** *Medium Fiber* Hybrid Fiber Coax Network

## 2.3 Upstream Path of the HFC network

The upstream spectrum is limited (between approximately 5 and 42 MHz) and this spectrum is shared by all users connected to a fiber node by the same coax drop. Burst modems, which are more complex than continuous modems, are needed to transmit packets in a time-shared upstream channel [4, 5].

### 2.3.1 Limitations of the Upstream Path of the HFC network

A major limitation of using fiber/coax lies in the upstream path, that portion of the network that travels from the subscriber's home to the central office. The transmission medium within the network uses radio frequencies (RF), much like two-way radio, paging and cellular services. While the RF spectrum is plentiful in the downstream path of the network, the available spectrum for the upstream path is very limited. In addition, the upstream path is subject to ingress interference, which enters the

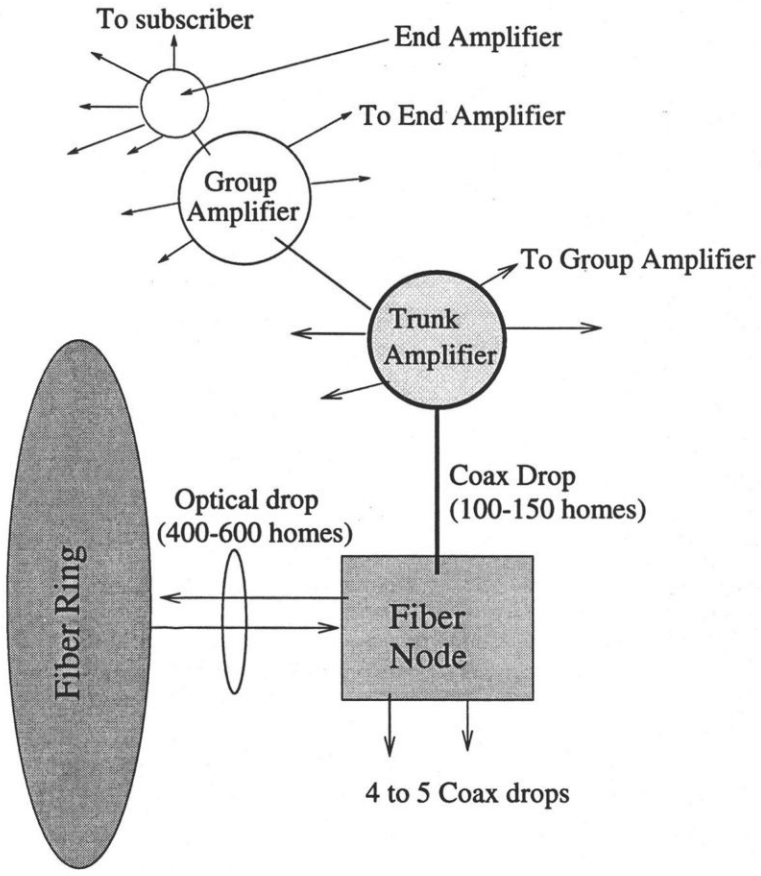


**Figure 2.5:** *Deep Fiber* Hybrid Fiber Coax Network

path and significantly degrades the transmission quality. Ingress interference sources include short-wave transmitters, ham radio transmitters, electric motors, vehicle ignition systems and paging systems, among others. One of the principal entry points of ingress interference into the upstream path is at the customer premise. Here, on-premise cabling to the set-top decoder, TV or VCR acts as an antenna and collects undesired signals from the sources described above. Environmental factors, such as sun spot activity, local weather and seasonal changes can also influence the strength of the interfering signals. Another significant factor is that this type of interference is cumulative. Ingress depends upon the following factors [6, 7, 8].

1. Plant size
2. Plant type (SFU, MDU)

3. Plant construction type (aerial, buried)

4. Plant location

5. Strength of Shortwave Broadcasting signals

6. Time of day

7. Frequency on which data or video carrier is located

8. Weather i.e., thunderstorms, and sunspot activity

Due to the combinatorial effects of these variables, the variation in signal to noise ratio across the channel is in the order of tens of dB. Additional correlational to specific plant portions (trunk, distribution, drop, home wiring) can be conducted by focusing on the specific bridger area. Antenna monitoring in conjunction with ingress monitoring, provides a reference base to compare relative shielding effectiveness. Ingress also depends on node size; it is clear that a reduction in node size reduces the noise funnelling effect.

Availability of the overall spectrum when wider channels are used can be significantly lower than with narrow channels, as each wide channel which becomes unusable due to the presence of one or a few narrow-band interferers will cause a substantial decrease in the payload carrying capacity of the return spectrum. The regions of lower availability are clearly identified where AM short-wave signals are predominant.

The most significant noise sources affecting the receiver at the head-end are non-stationary ingress, common-path noise and various impulse noises. The ingress can be divided into two subparts:

1. Dynamic slowly varying interference such as white noise, narrowband interference due to shortwave transmission and amateur radio.

2. Dynamic fast varying noise such as impulse noise.

In Chapter 3, limitations of the upstream path are discussed in more detail.

# Chapter 3

# Impairments in the Upstream Channel

In Chapter 2, the HFC network system is described and in Section 2.3, some of the limitations of the upstream path are discussed. In this chapter, some of the common impairments in the upstream channel are presented.

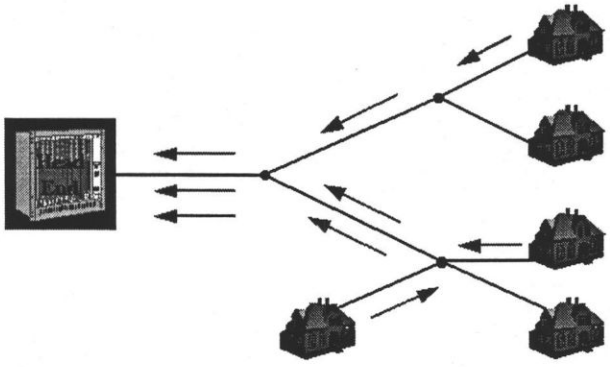

**Figure 3.1:** Upstream Path of the HFC network

The signal arriving at the headend is accompanied by the total of all the interference that has entered the cable from many subscriber homes. This could represent the accumulated interference from hundreds or thousands of homes, and could involve many kilometers of cable. The incidence of ingress levels observed broadly highlights the level of effort required to improve the plant integrity before a variety of services can be supported reliably [9, 10, 11]. Some of the common impairments are thermal noise (Section 3.1), narrowband ingress (Section 3.2) and impulse noise (Section 3.3).

## 3.1 Thermal Noise

A metallic conductor or resistor contains a number of free electrons. Due to thermal agitation, these free electrons are moving continuously in the conductor causing collisions with the atoms and a continuous exchange of energy takes place. This accounts for the resistance property of the conductor and, though there is no current in the conductor on open-circuit, the random motion of electrons in the conductor produces voltage fluctuations across the conductor which accounts for a mean-square noise voltage $\overline{v_n{}^2}$ at its terminals. If the noise voltage spectral density is $S_v(f)$, it can be shown that

$$S_v(f) = 4kTR \tag{3.1}$$

where $k$ is Boltzmann's constant ($k = 1.38 \times 10^{-23} J/K$), R is resistance in ohms and T is the absolute temperature in Kelvin. Noise voltage spectral density depends on T and R but is independent of frequency up to about $10^{13}$ Hz. This implies that thermal noise covers a broad band of frequencies and has a uniform response. Nyquist's investigation of the effect was based on thermo-dynamical reasoning. He showed that the thermal noise power $P_n$ in Watts, associated with any resistor is given by Eq. 3.2.

$$P_n = k \times T \times B \tag{3.2}$$

where B is the bandwidth of the system.

### 3.1.1 Noise Floor

The reference power level of a cable distribution network that must be exceeded to communicate effectively is the *noise floor*. From the *thermal noise*, *noise floor* can be defined. Assuming 4MHz as a bandwidth of the system and 293K as a normal room temperature, then using Eq. 3.2, thermal noise under given above conditions can be calculated.

$$P_n = 1.617 \times 10^{-14}\, W \tag{3.3}$$

The impedance of the television distribution circuit is 75Ω, and a zero reference level has been chosen which corresponds to a voltage of 1 mV appearing across a resistance of 75Ω. This is defined as 0 dBmV. Electrical circuit theory gives this reference level

equivalent to a power of

$$\frac{(1\,mV)^2}{75\,\Omega} = 1.33 \times 10^{-8}\,W\ . \tag{3.4}$$

Noise in dBmV as equivalent to noise in watts of Eq. 3.3 is therefore given by Eq. 3.5.

$$P_n = 10log\frac{1.617 \times 10^{-14}}{1.33 \times 10^{-8}} = -58dBmV \tag{3.5}$$

This is the best (lowest) value that can be obtained in a coaxial distribution network since it considers a negligible length of coaxial cable. As additional coaxial cable is included, network devices are added, electrical/mechanical connections are made, and the network is powered, the *noise floor* increases [6, 7, 12].

### 3.1.2 Amplifier Noise

Amplifier noise also contributes to the *noise floor* of a cable network. All amplifiers generate varying amounts of noise and have a *noise figure* specification that indicates the amount of noise introduced by the amplifier. All practical amplifiers will introduce noise greater than the *noise floor*, and the amount of noise above this threshold is known as the noise figure of the amplifier.

Noise figure($n_f$) = 10log (*SNR at input of amplifier*) - 10log (*SNR at output of amplifier*)

where SNR indicates the signal to noise ratio. From this expression it is clear that the *noise figure* is the number of decibels by which the signal to noise ratio is degraded when signal passes through a amplifier. *Noise figures* between 6 and 10 are common.

#### Example

Consider a case, where there is only one amplifier in a system, and 4MHz is the bandwidth of the system. From Eq. 3.5, thermal noise can be calculated. If an amplifier has a noise figure of 6 dB, then in order to keep a minimum carrier to noise ratio of 62 dB, signal must be sent at +10 dBmV (Fig. 3.2).

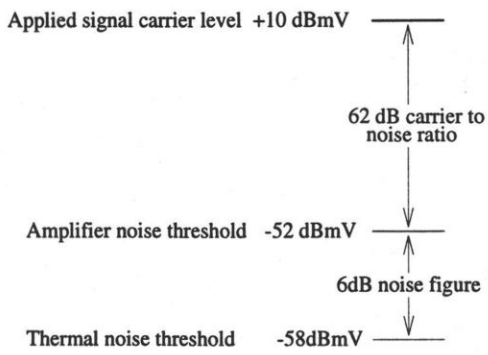


**Figure 3.2:** Example showing relation between thermal noise, amplifier noise and signal carrier level at a given signal to noise ratio

### Noise due to amplifiers in cascade

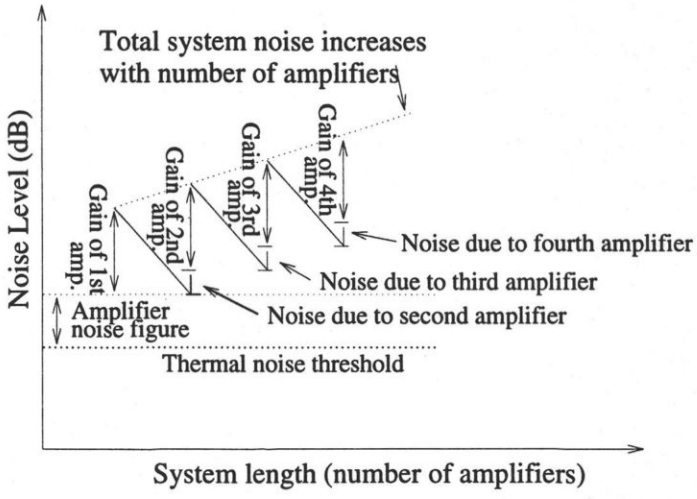


**Figure 3.3:** Noise due to amplifiers in cascade

Noise at the output of the $x^{th}$ amplifier ($n_x$) can be worked out as shown in Fig. 3.3. In Eq. 3.6, it is assumed that gain of each amplifier is unity, and all amplifiers are similar with same noise figure ($n_f$).

$$n_x = n_f + 10Logx \tag{3.6}$$

If $n_o$ is the total noise at the output of the system, $n_f$ is the *noise figure*, $P_n$ is

the *noise floor* of the system, and $A$ is the gain of the system, then Eq. 3.6 can be modified to Eq. 3.7 and the total noise can be represented in terms of thermal noise threshold ($P_n$) and *noise figure*($n_f$).

$$n_o = P_n + A + n_f + 10log(x) \tag{3.7}$$

In the downstream path, x is the number of cascade amplifiers but in the upstream path, x is the total number of amplifiers contributing to noise received at the headend through various branches.

## 3.2 Narrowband Ingress

The main users of the HF radio spectrum (5 MHz to 42 MHz) are the following:

- Broadcasting
- Maritime mobile
- Aeronautical mobile
- Aeronautical navigation
- Fixed(point-to-point)
- Mobile
- Standard frequency and time signals
- Amateur
- Citizen Band
- Satellite Broadcasting
- Amateur satellite

It is found that Shortwave Broadcasting, Amateur and Citizen Band are the main sources of narrowband ingress [1, 6, 7, 8].

### 3.2.1 Ingress due to Short-Wave Broadcasting

The main ingress signals seen on typical HFC systems are short-wave broadcasting signals. The broadcasting service is designed to provide very high field strengths in target markets so that the public can receive clear signals with simple receivers [1, 6]. Thus the service generally has the following characteristics:

1. Amplitude modulated signals
2. Very high transmitter powers
3. High gain directive antenna arrays
4. Simultaneous transmission on multiple frequencies in different parts of the HF spectrum, to combat HF propagation variability
5. Very large field strengths over a wide geographic area, affecting entire cable systems.

The frequencies allocated to the broadcasting services on a world wide basis are shown in Table 3.1:

**Table 3.1:** Broadcasting Allocation Between 5 and 42 MHz

| *Frequency, MHz* | | | |
|---|---|---|---|
| **From** | **To** | **From** | **To** |
| 5.95 | 6.2 | 15.1 | 15.6 |
| 7.1 | 7.3 | 17.55 | 17.9 |
| 9.5 | 9.9 | 21.45 | 21.85 |
| 11.65 | 12.05 | 25.67 | 26.1 |
| 13.6 | 13.8 | | |

### Fitting Data Carrier in the Gaps Between Broadcasting Bands

The modulation rates in this document were chosen to fit in the gaps between the short-wave broadcasting bands, to avoid this significant source of ingress as shown in Table 3.2 and Table 3.3.

**Table 3.2:** Data Carriers in the Gaps Between Broadcasting Bands(Part 1)

| *Non-Broadcast spectrum, kHz* | | | *Modulation rates, kHz* | | | |
|---|---|---|---|---|---|---|
| **From** | **To** | **Gap** | **50** | **100** | **200** | **400** |
| 5,000 | 5,950 | 950 | 19 | 9 | 4 | 2 |
| 6,200 | 7,100 | 900 | 18 | 9 | 4 | 2 |
| 7,300 | 9,500 | 2,200 | 44 | 22 | 11 | 5 |
| 9,900 | 11,650 | 1,750 | 35 | 17 | 8 | 4 |
| 12,050 | 13,600 | 1,550 | 31 | 15 | 7 | 3 |
| 13,800 | 15,100 | 1,300 | 26 | 13 | 6 | 3 |
| 15,600 | 17,550 | 1,950 | 39 | 19 | 9 | 4 |
| 17,900 | 21,450 | 3,550 | 71 | 35 | 17 | 8 |
| 21,850 | 25,670 | 3,820 | 76 | 38 | 19 | 9 |
| 26,100 | 40,000 | 13,900 | 278 | 139 | 69 | 34 |
| Least Gap (kHz) | | 900 | | | | |
| Total carriers | | | 637 | 316 | 154 | 74 |
| Total Bandwidth | | 31,870 | 31,850 | 31,600 | 30,800 | 29,600 |
| Utilization | | | 99.93 | 99.15 | 96.64 | 92.87 |

HF propagation is largely influenced by bending radio waves in the ionosphere, which is the region between about 80 and 250 kms above the earth surface, so the propagation distances can be very large. The bending is caused by the ionization of atmospheric gases, and free electrons. There are several reflecting layers at various heights with different characteristics, so that maximum distance reached depends on the solar ultra-violet radiation produced by solar activity.

**Table 3.3:** Data Carriers in the Gaps Between Broadcasting Bands(Part 2)

| *Non-Broadcast spectrum, kHz* | | | *Modulation rates, kHz* | | |
|---|---|---|---|---|---|
| **From** | **To** | **Gap** | **800** | **1,600** | **3,200** |
| 5,000 | 5,950 | 950 | 1 | 0 | 0 |
| 6,200 | 7,100 | 900 | 1 | 0 | 0 |
| 7,300 | 9,500 | 2,200 | 2 | 1 | 0 |
| 9,900 | 11,650 | 1,750 | 2 | 1 | 0 |
| 12,050 | 13,600 | 1,550 | 1 | 0 | 0 |
| 13,800 | 15,100 | 1,300 | 1 | 0 | 0 |
| 15,600 | 17,550 | 1,950 | 2 | 1 | 0 |
| 17,900 | 21,450 | 3,550 | 4 | 2 | 1 |
| 21,850 | 25,670 | 3,820 | 4 | 2 | 1 |
| 26,100 | 40,000 | 13,900 | 17 | 8 | 4 |
| Least Gap (kHz) | | 900 | | | |
| Total carriers | | | 35 | 15 | 6 |
| Total Bandwidth | | 31,870 | 28,000 | 24,000 | 19,200 |
| Utilization | | | 87.85 | 75.30 | 60.24 |

### Diurnal Variation

During local daytime, higher frequencies (shorter wavelengths) are propagated over large distances and lower frequencies are absorbed. During local night-time, higher frequencies experience diminished propagation and the lower frequencies are propagated over larger distances.

### Solar Cycle

Ionization is at its greatest during the peak of the 11-year sunspot cycle. At the largest sunspot peaks, strong distant signals can be heard across the HF band at most times of the day. At sunspot minima, long-distance propagation can be rare above 15 MHz. Note that the cycle is currently at a minimum, so ingress is likely to

**Table 3.4:** Amateur and Citizens Band Allocations Between 5 and 42 MHz

| *Frequency, MHz* | | | |
|---|---|---|---|
| **From** | **To** | **From** | **To** |
| 7.0 | 7.3 | 21.0 | 21.45 |
| 10.1 | 10.15 | 24.89 | 24.99 |
| 13.8 | 14.35 | 26.96 | 27.24 |
| 18.068 | 18.168 | 28.00 | 29.7 |

affect cable systems on an increasing basis and at higher frequencies over the next 6 years.

### 3.2.2 Ingress due to Amateur and CB Radio

The amateur service is of concern, but for different reasons. Amateur transmitters operate at far lower powers than the broadcasting services, but are usually located in residential neighbourhoods close to the cable plant, so they can represent potential localised sources of ingress in different bands across the HF spectrum. Radiation from the upstream cable plant may also cause interference into amateur receivers. The Citizens Band Service operate at powers which are very much lower and are less likely to be sources of ingress. However, CB receivers may be capable of picking up interference from cable plant radiation. Amateur and citizens band allocation between 5 and 42 MHz are shown in Table 3.4

### Fitting Data Carriers in the Gap between Broadcasting, Amateur and CB Bands

The modulation rates in this document were chosen to fit in the gaps between the short-wave broadcasting bands, amateur and citizens band bands to avoid this significant source of ingress as shown in Table 3.5 and Table 3.6.

**Table 3.5:** Data Carriers in the Gaps Between Broadcasting Bands, Amateur and CB Bands (Part 1)

| *Ingress free spectrum, kHz* | | | *Modulation rates, kHz* | | | |
|---|---|---|---|---|---|---|
| **From** | **To** | **Gap** | **50** | **100** | **200** | **400** |
| 5,000 | 5,950 | 950 | 19 | 9 | 4 | 2 |
| 6,200 | 7,000 | 800 | 16 | 8 | 4 | 2 |
| 7,300 | 9,500 | 2,200 | 44 | 22 | 11 | 5 |
| 9,900 | 10,100 | 200 | 4 | 2 | 1 | 0 |
| 10,150 | 11,650 | 1,500 | 30 | 15 | 7 | 3 |
| 12,050 | 13,600 | 1,550 | 31 | 15 | 7 | 3 |
| 13,800 | 14,000 | 200 | 4 | 2 | 1 | 0 |
| 14,350 | 15,100 | 750 | 15 | 7 | 3 | 1 |
| 15,600 | 17,550 | 1,950 | 39 | 19 | 9 | 4 |
| 17,900 | 18,068 | 168 | 3 | 1 | 0 | 0 |
| 18,168 | 21,000 | 2,832 | 56 | 28 | 14 | 7 |
| 21,850 | 24,890 | 3,040 | 60 | 30 | 15 | 7 |
| 24,990 | 25,670 | 680 | 13 | 6 | 3 | 1 |
| 26,100 | 26,960 | 860 | 17 | 8 | 4 | 2 |
| 27,410 | 28,000 | 590 | 11 | 5 | 2 | 1 |
| 29,700 | 40,000 | 10,300 | 206 | 103 | 51 | 25 |
| Least Gap (kHz) | | 140 | | | | |
| No of carriers | | | 568 | 280 | 136 | 63 |
| Bandwidth | | 28,570 | 28,400 | 28,000 | 27,200 | 25,200 |
| Utilization | | | 99.4 | 98.00 | 95.20 | 88.20 |

### 3.2.3 Other Services

The other services in the HF spectrum operate at powers which are lower than broadcasting, and are usually not located in residential areas, so they are not likely to be of concern. In the low VHF region between 30 and 42 MHz, there may be a localised

**Table 3.6:** Data Carriers in the Gaps Between Broadcasting Bands, Amateur and CB Bands (Part 2)

| *Ingress free spectrum, kHz* | | | *Modulation rates, kHz* | | |
|---|---|---|---|---|---|
| **From** | **To** | **Gap** | **800** | **1,600** | **3,200** |
| 5,000 | 5,950 | 950 | 1 | 0 | 0 |
| 6,200 | 7,000 | 800 | 1 | 0 | 0 |
| 7,300 | 9,500 | 2,200 | 2 | 1 | 0 |
| 9,900 | 10,100 | 200 | 0 | 0 | 0 |
| 10,150 | 11,650 | 1,500 | 1 | 0 | 0 |
| 12,050 | 13,600 | 1,550 | 1 | 0 | 0 |
| 13,800 | 14,000 | 200 | 0 | 0 | 0 |
| 14,350 | 15,100 | 750 | 0 | 0 | 0 |
| 15,600 | 17,550 | 1,950 | 2 | 1 | 0 |
| 17,900 | 18,068 | 168 | 0 | 0 | 0 |
| 18,168 | 21,000 | 2,832 | 3 | 1 | 0 |
| 21,850 | 24,890 | 3,040 | 3 | 1 | 0 |
| 24,990 | 25,670 | 680 | 0 | 0 | 0 |
| 26,100 | 26,960 | 860 | 1 | 0 | 0 |
| 27,410 | 28,000 | 590 | 0 | 0 | 0 |
| 29,700 | 40,000 | 10,300 | 12 | 6 | 3 |
| Least Gap (kHz) | | 140 | | | |
| No of carriers | | | 27 | 10 | 3 |
| Bandwidth | | 28,570 | 21,600 | 16,000 | 9,600 |
| Utilization | | | 75.60 | 56.00 | 33.60 |

effect from high-power paging in the vicinity of 35 MHz.

## 3.3 Impulse Noise

Impulse noise consists of the peaks of noise that individually are significantly larger than the rms level of noise on the channel. Generally it is considered to be a voltage increase of 12 dB or more above the rms noise for a period of 12 ms or less. The impulse noise is sporadic in nature and the exact mechanisms involved in impulse noise generation are not completely known. Impulse noise may occur from impulse events generating strong electro-magnetic fields at particular subscriber locations which couple to a particular coaxial drop or feeder cable, or from impulse events generating fields propagated through the atmosphere that couple to the plant at numerous subscriber locations [6, 7, 13].

### 3.3.1 Natural sources

Naturally occurring sources of impulse noise include lightning, atmospherics, galactic noise, and electrostatic discharge. These naturally occurring impulse events cause disturbances which typically extend from 2kHz to 100 MHz.

### 3.3.2 Human sources

Cable operating experience has shown that impulse noise generally results from bad splices (corroded), and cracked/eroded cable. Impulse noise is often generated by human sources such as power-line arcing, arc welding, electrical motors, engine ignitions, discharges across corroded connector contacts, power switching, and house hold appliances. Although these sources generally produce events in the 60 Hz to 2 MHz portion of the spectrum, the harmonics of these events contribute to impulse noise at higher frequencies. These may introduce extreme errors resulting in loss of synchronisation on digital transmission systems. Computers and digital equipment also are sources of impulse noise in the 5-45 MHz portion of the spectrum. CCIR studies on radio noise have shown that there is a strong 1/f dependence on the noise observed (both impulse and background noise) in the atmosphere as well as the dependence on the location, with industrial and urban locations showing higher levels of noise than rural locations. Considering that much of the generated noise is impulsive in nature, there is likely to be a strong component of impulse noise on the return path. The

consequence of impulse noise is that even if narrow-band interference is not present, impulse events may limit the bit error ratio performance of HFC system unless Forward Error Correction (FEC) is employed [1, 14, 15]. Present data indicates that FEC can be employed to correct for the majority of the errors caused by impulse noise, thus impulse noise is not seen to be a limiting factor for HFC communication. In addition to the FEC, filtering techniques to reduce the cumulative ingress will also aid in reducing impulse noise [1, 6, 7]. Impulse noise has some interesting features [6].

1. At very high signal to noise ratio, impulsive noise causes more error than Gaussian noise. At very low signal to noise ratio, Gaussian noise causes more error than impulse noise.

2. Receivers especially designed to reject a particular type of impulse noise perform substantially better than receivers using standard non-suppression techniques.

3. Pairing of errors increases as noise becomes more impulsive.

### 3.3.3 Model of Impulse Noise

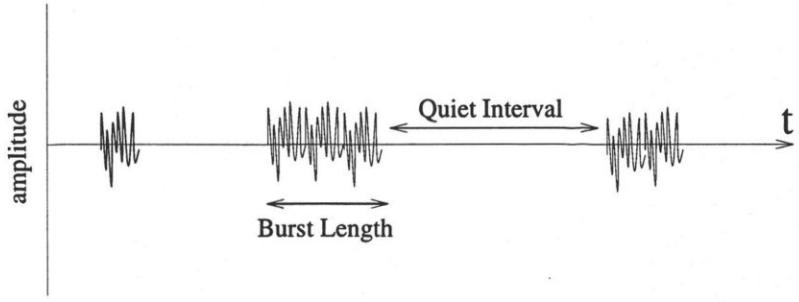


**Figure 3.4:** Example showing impulse noise

For a first approximation, the analysis of impulse noise can include only two parameters, as shown in Fig. 3.4. The parameters are *burst* length and *quiet interval* length [14, 15, 16, 17].

**Burst length** According to assumed upstream RF channel transmission characteristics from MCNS specification [1], the burst length does not exceed more than 100

$\mu$s at a 10 Hz average rate. It is further assumed that the probability density function of *burst length* is *Uniform.*

**Quiet Interval length** According to assumed upstream RF channel transmission characteristics from MCNS specification [1], the quiet interval is usually larger than 0.1 sec and further it is assumed that probability density function of impulse noise *arrival rate* is *Poisson.*

## 3.4 Summary

In this chapter the basic charcteristics of HFC return systems have been examined to evaluate their ability to support bidirectional communications. The above discussion indicates that ingress in the cable return path is primarily due to broadcast signals which accumulate due to the noise-funneling effect of the cable return. White noise is due to many reasons such as thermal noise, amplifier noise and ingress. It is possible to mitigate impulse noise and it can be done by proper maintainance of the cable network. With properly maintained plant, a well designed plant will be highly resistant to ingress problems.

# Chapter 4

# Media Access Protocols For Cable Modems

The need for multi-access protocols arises whenever a resource is shared (and thus accessed) by a number of independent users. In the HFC network, there will be competition between users (CMs) to get maximum upstream bandwidth. Many algorithms for allocating multiple access channels are known, and each algorithm will work efficiently under different traffic load conditions. In this chapter, the following MAC protocols are described for the upstream path of the HFC network. These are FDMA (Section 4.1), and Slotted ALOHA (Section 4.2), DRNC (Section 4.3), DRC (Section 4.4), DRLC (Section 4.5) and M-DRLC (Section 4.6).

## 4.1 *Fixed assignment* FDMA/TDMA

In this algorithm, the *cable modem termination system* (CMTS) divides the bandwidth equally between all CMs. This can be done in a number of different ways; either it can be done through Frequency Division Multiplexing (FDM) or by Time Division Multiplexing (TDM) or by using both, i.e. by first dividing the upstream channel into subchannels by using FDM and then alloting some fixed time slots of the subchannel to each CM.

In this protocol, no CM can request any bandwidth from the CMTS. The CMTS allots certain fixed bandwidth to every CM, whether the CM uses it or not. The fixed bandwidth allocated to all CM, depends upon the following factors:

1. Ingress free upstream spectrum available ($W$).

2. Size of Distribution Network. In other words, how many CMs are attached to one Coax Drop from a CMTS ($N_{cm}$).

**Table 4.1:** Total raw data rate at the physical layer available for given ingress-free spectrum

| Spectrum available | Symbol Rate | Data Rate | |
|---|---|---|---|
| | | QPSK | QAM-16 |
| **MHz** | **Msym/sec** | **Mbit/sec** | |
| 25 | 20 | 40 | 80 |
| 30 | 24 | 48 | 96 |
| 35 | 28 | 56 | 112 |

**Table 4.2:** Raw bit rate available (**in kbit/sec**) at the physical layer to each CM by FDM, while using QPSK modulation

| **upstream spectrum available⟹** | **25 MHz** | **30 MHz** | **35 MHz** |
|---|---|---|---|
| **Number of CMs ($N_{cm}$)** ⇓ | | | |
| **10** | 4,000 | 4,800 | 5,600 |
| **100** | 400 | 480 | 560 |
| **500** | 80 | 96 | 112 |
| **1,000** | 40 | 48 | 56 |
| **1,600** | 25 | 30 | 35 |
| **3,200** | 12.5 | 15 | 17.5 |
| **6,400** | 6.25 | 7.5 | 8.75 |

Nyquist proved that if an arbitrary signal has been run through a low-pass filter of bandwidth B, the filtered signal can be completely constructed by making only $2\,B$ (exact) samples per second. Sampling the line faster than $2\,B$ times per second is

pointless because the higher frequency components that such sampling could recover have already been filtered out [3, 18, 19]. If the QAM signal consists of M discrete levels (M=4 for QPSK, M=16 for QAM-16) , then maximum data rate (W) available for QAM modulated signal is

$$W = B\,log_2 M\ bit/s\,. \tag{4.1}$$

If ingress free spectrum available is 25 MHz, and *raised-cosine* filters are used with *rolloff factor*= 0.8, then $B = 0.8 \times 25$ MHz $= 20$ MHz. The maximum data rate available ($W = 20\,log_2 4$ Mbit/sec) is 40 Mbit/sec as shown in Table 4.1.

### 4.1.1 Frame Delay for FDMA

The average frame delay is defined as the average time from when a frame is generated at the CM until it is successfully received at the CMTS. To analyse frame delay for FDMA, assume that there are $N_{cm}$ CMs and each generates a new fixed-length frame (of $L_{tx}$ bytes). Further assume that upstream channel capacity is $W$ bit/s. Thus with $N_{cm}$ CMs in this FDMA mode, each is assigned a channel of $W/N_{cm}$ bit/s. Loss due to guard bands etc. is neglected, and each channel behaves as an $M/D/1$ queueing system with an average time in the system $D$ (waiting plus transmission) given by Eq. 4.2 [20, 21].

$$D = \underbrace{\frac{(g^2/\lambda)}{2(1-g)}}_{Queueing\ \ Delay} + \underbrace{8\,N_{cm}\,L_{tx}/W}_{transmission\ \ time} \quad seconds \tag{4.2}$$

Simplifying Eq. 4.2,

$$D = \frac{g}{\lambda}\left(1 - \frac{g}{2}\right)\Big/\,(1-g) \quad seconds \tag{4.3}$$

where $\lambda$ is the frame arrival rate at one station according to a *Poisson* process (at mean rate of $\lambda$ frame/s), $g$ is the normalised frame arrival rate at one station according to a *Poisson* process (at rate of $g$ frames per frame time),

$$g = \tau \times \lambda \tag{4.4}$$

and $\tau$ is the transmission time for a message frame

$$\tau = 8\, L_{tx}\, N_{cm} / W \ . \tag{4.5}$$

Eq. 4.3 can be written in a slightly different form,

$$\lambda = (D - \tau) \Big/ (\tau) \left(D - \frac{\tau}{2}\right) \ \ frames/s \ . \tag{4.6}$$

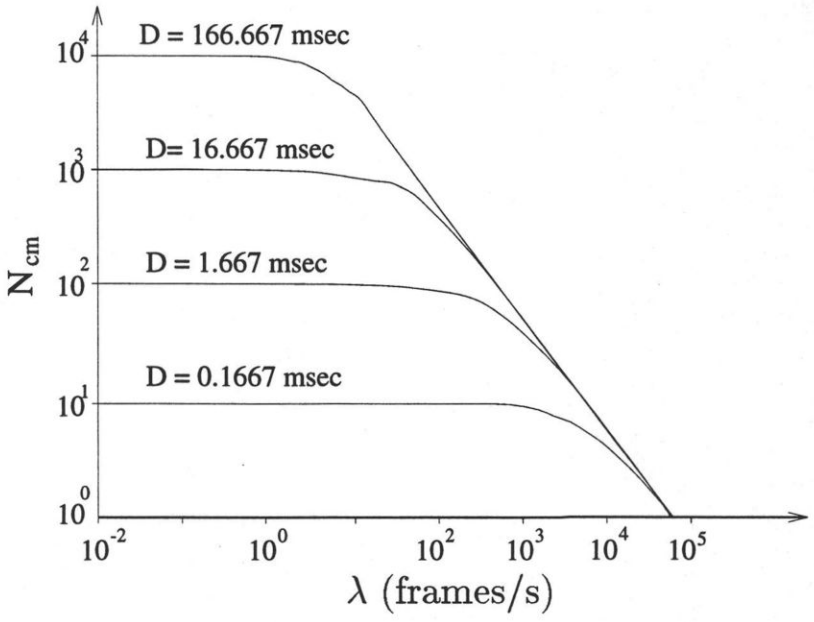


**Figure 4.1:** Performance of FDMA protocol

From Eq. 4.6, it is easy to calculate what should be the input frame rate if frame delay, bandwidth and the number of CMs on a network are given. Fig. 4.1 shows the delay characteristics of FDMA. In this figure, the X-axis represents traffic on any CM ($\lambda$), the Y-axis represents the number of CMs ($N_{cm}$) a particular network can support at a given *frame delay*, the upstream ingress free bandwidth available is 30 MHz, and the average length of a data frame is 100 bytes ($L_{tx}$ = 100 bytes). From Table 4.1, the available bit rate can be calculated when using QPSK modulation ($W$ = 48 Mbit/sec). It is seen that for $D$ = 16.667 ms, the system can support 1000 users as long as $\lambda < 100$, For $\lambda > 100$, the FDMA channel will start saturating.

### 4.1.2 Throughput Analysis for FDMA

There are $N_{cm}$ CMs, out of which only percentage $P_A$ of the CMs are active. So the total number of active CMs is

$$A_{cm} = \frac{P_A\, N_{cm}}{100} \ . \tag{4.7}$$

If each active CM is producing normalised *Poisson* traffic at a mean rate of $g$ frames per frame time, throughput for *Fixed Assignment* can be written as

$$S = \frac{A_{cm}}{N_{cm}} g = \frac{A_{cm}}{N_{cm}} \lambda \tau \ . \tag{4.8}$$

Eq. 4.8 is only valid for $g < 1$ or $\lambda < 1/\tau$.

In computer communication, much of the data traffic is characterised as bursty. Burstiness is a result of the high degree of randomness seen in the generation time and size of the messages and of the relatively low-delay constraint required by the user. Considering the bursty nature of the internet traffic, the FDMA protocol is highly inefficient. Lots of bandwidth is wasted and is not used most of the time. This is because at any given time, the capacity assigned to an inactive user is not utilized, whereas the active users experience relatively long delays due to the low capacity available to each [22].

## 4.2 Slotted ALOHA

In this algorithm, time is divided into discrete intervals, called slots, with each slot corresponding to one frame. This approach requires the CMs to agree to slot boundaries. The CMTS will synchronise all CMs and will transmit the start of each interval like a clock. When a CM is ready to transmit a frame, it waits until the beginning of the next slot.

Whenever two or more frames try to occupy the slot at the same time, there will be a collision and all the colliding frames will be garbled. The CMTS should send acknowledgement of every valid frame received so if there is a collision, the CM will

not receive any acknowledgement. If the CM does not receive any acknowledgement, it waits for random slots and then it transmits the same frame.

Let the frame time ($\tau$) denote the amount of time needed to transmit the standard, fixed-length frame (i.e., frame length divided by the bit rate), so

$$\tau = \frac{8\,L_{tx}}{W} \ . \tag{4.9}$$

It is assumed that an infinite population of users is generating new frames according to a *Poisson* distribution with mean $G_n$ frames per frame time. If $G_n > 1$, the user community is generating frames at a higher rate than the channel can handle, and nearly every frame will suffer a collision.

In addition to the new frames, the stations also generate retransmissions of frames that previously suffered collisions. Assuming that the probability of k transmission attempts per frame time, old and new combined, is also *Poisson*, with mean $G$ per frame time, clearly, $G \geq G_n$. At low load (i.e., $G_n \approx 0$), there will be few collisions, hence few retransmissions, so $G \approx G_n$. At high load there will be many collisions, so $G \geq G_n$. Under all loads, the throughput is just the offered load, G times the probability of a transmission being successful, that is:

$$S = G\,P_0 \tag{4.10}$$

where $P_0$ is the probability that a frame does not suffer a collision. A frame will not suffer collision if no other frames are sent in that slot. The probability that k frames are generated during a given frame time is given by the *Poisson* distribution:

$$Pr[k] = \frac{G^k e^{-G}}{k!} \tag{4.11}$$

The probability that zero frames are transmitted (k=0 in Eq. 4.11) is

$$P_0 = Pr[0] = e^{-G} \ . \tag{4.12}$$

Combining Eq. 4.10 and Eq. 4.12, throughput for slotted ALOHA can be written

as

$$S = Ge^{-G} \ . \tag{4.13}$$

Slotted ALOHA peaks at G=1, with a throughput of S=1/e or about 0.368. If the system is operating at G=1, the probability of an empty slot is 0.368 (from Eq. 4.11). The best that can be obtained from slotted ALOHA is 37 percent empty slots, 37 percent successes, and 26 percent collisions. Operating at higher values of G reduces the number of empties but increases the number of collisions exponentially.

The probability of a transmission requiring exactly k attempts, (i.e., k-1 collisions followed by one success) is

$$P_k = e^{-G}(1 - e^{-G})^{k-1} \ . \tag{4.14}$$

The expected number of transmissions, E per one frame transmission is then

$$E = \sum_{k=1}^{\infty} kP_k = \sum_{k=1}^{\infty} ke^{-G}(1 - e^{-G})^{k-1} = e^{G} \ . \tag{4.15}$$

As a result of the exponential dependence of E upon G, a small increase in the channel load can drastically reduce its performance [3].

### 4.2.1 Frame Delay for Slotted ALOHA

Neglecting the propagation delay, and letting the maximum retransmission delay be an integer number K of frame slots (the retransmission delay being uniformly distributed over the K slots), the transmission delay D in frame slots can be shown to be:

$$D = 1 + \left(\frac{K+1}{2}\right)\left(e^{G} - 1\right) \quad \textit{frame slots} \ . \tag{4.16}$$

If $\Lambda$ is the channel traffic (*Poisson* traffic at mean $\Lambda$ frames/s) then $\Lambda$ and G are related as follows:

$$G = \Lambda\tau \ , \tag{4.17}$$

where $G$ is the normalised channel traffic and $W$ is the upstream bandwidth in bit/s. Eq. 4.16 can be modified and the delay can be written in seconds as follows:

$$D = \left[1 + \left(\frac{K+1}{2}\right)\left(e^{\Lambda\tau} - 1\right)\right]\tau \ \ seconds \ . \tag{4.18}$$

If it is assumed that at a particular instant only a percentage $P_A$ of CMs are in an active state (only active CMs generate traffic), and it is also further assumed that all CMs generate identical *Poisson* traffic with parameter $\lambda$ frames per second, then the total channel traffic ($\Lambda$) is

$$\Lambda = A_{cm}\lambda \ . \tag{4.19}$$

Eq. 4.20 is derived from Eqs. 4.18, 4.7 and 4.19. Fig. 4.2 is plotted using Eq. 4.20. In this figure, the following parameters are used: $W = 48$ Mbit/sec, $P_A = 30\%$ and $L_{tx} = 100$ bytes.

$$\lambda = \frac{100}{P_A N_{cm} \tau} log_e \left[\left(\frac{D}{\tau} - 1\right)\left(\frac{2}{K+1}\right) + 1\right] \tag{4.20}$$

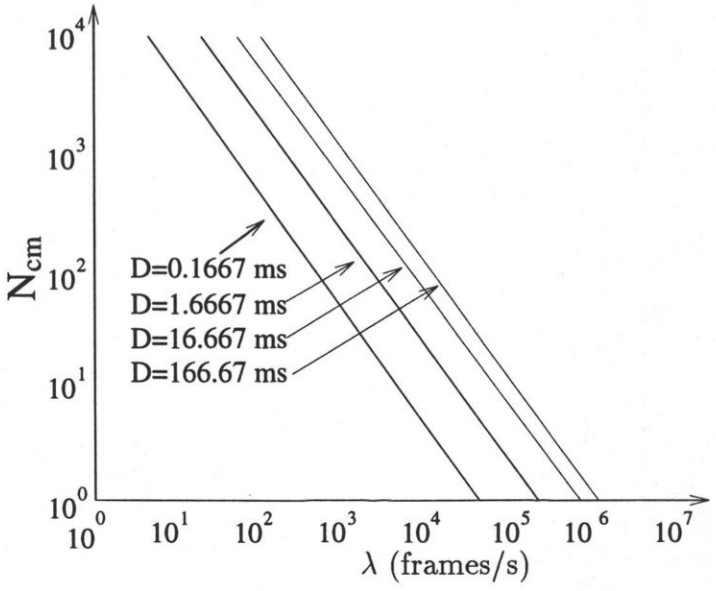


**Figure 4.2:** Performance of Slotted ALOHA Protocol at various *frame delay*

Comparing Fig. 4.1 and Fig. 4.2, it is seen that slotted ALOHA protocol performance is very good at low channel traffic.

## 4.3 *Dynamic Reservation without Contention* DRNC

A more advantageous approach is to provide a single upstream channel to all of the CMs, then demand at any instant will be equal to the sum of the average demands of all CMs. In this protocol, bandwidth is only alloted to a particular CM when it asks for it. The CMTS fixes a slot (CM request opportunity) for every CM after a regular interval. In that slot the CM can ask for some bandwidth. The CMTS then allots Data Grants to CMs depending upon the request. The allocation map is a MAC Management message transmitted by the CMTS on the downstream channel. A given map describes some slots as grants for particular stations to transmit data while other slots are available for requesting bandwidth.

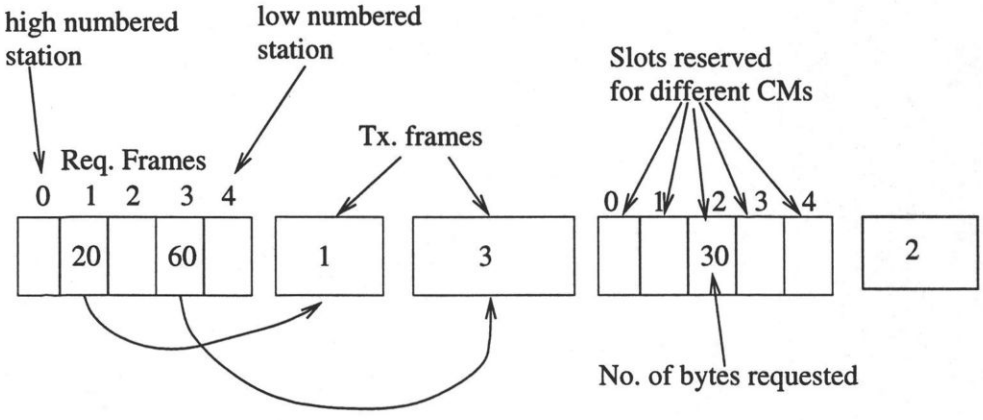


**Figure 4.3:** Example of DRNC protocol (round trip delay and processing time taken by CMs and CMTS are ignored)

### Example of the DRNC Protocol

Some slots are reserved for CM request opportunities and others are reserved for CM transmission opportunities. In the CM request opportunity, the CM requests the bandwidth and in a CM transmission opportunity, it transmits the data. For example in Fig. 4.3, there are five users ($N_{cm} = 5$); stations are numbered as zero, one, two, three and four. The CMTS reserves request frame time for all the five CMs. The CM(0) has no data frame to send, so in its reserved request frame time, it does not place any request. CM(1) has a message frame to send (of 20 bytes long); it places

a request for 20 bytes. Similarly CM(2) and CM(4) do not place any requests and CM(3) places a request for 60 bytes. At this stage, the CMTS has polled all five CMs. It then reserves 20 bytes for CM(1) and 60 bytes for CM(3). After the transmission of message frames by CM(1) and CM(3), the CMTS again polls all CMs and this process continues.

### Slot Synchronisation

The CM can become ready any time for transmission, but it has to wait for its turn to place a request for the desired bandwidth. Time wasted in slot synchronisation (under a random arrival process assumption) is critical. The worst case delay for the high numbered stations and low numbered stations will be determined separately.

### Worst case access latency for high numbered station

Under worst case situations, the high numbered station becomes ready to transmit a frame just after the first reservation slot passed by. In this situation it has to wait $2 \times N_{cm} - 1$ request frame slots plus $A_{cm}$ data frames. The worst situation waiting time ($t_{max\_sd}$) is given by

$$t_{max\_sd} = (2 \times N_{cm} - 1) \times L_{req} + A_{cm} \times L_{tx} \ \ bytes\,, \ \ and \tag{4.21}$$

$$t_{max\_sd} = 8 \times [(2 \times N_{cm} - 1) \times L_{req} + A_{cm} \times L_{tx}] / W \ \ \ seconds\,, \tag{4.22}$$

where $L_{req}$ is the average length of a request frame in bytes.

### Worst case access latency for low numbered station

The prospect for a low numbered station under low load is better. In this case, under the worst situation it has to wait $N_{cm}$ request frame slots. The worst situation waiting time in bytes is given by

$$t_{max\_sd} = N_{cm} \times L_{req} + 2 \times A_{cm} \times L_{tx} \ \ bytes\,, \ \ and \tag{4.23}$$

$$t_{max\_sd} = 8 \times [N_{cm} \times L_{req} + 2 \times A_{cm} \times L_{tx}] / W \quad seconds. \tag{4.24}$$

### 4.3.1 Frame delay for DRNC

The *frame delay* is defined as the time lapse from the moment the frame is ready for transmission to the time the transmission of the frame is completed:

$$D = t_{sd} + t_{ttx} + 2\,t_{nd} + t_{pr} \tag{4.25}$$

where $D$ is the frame delay, $t_{sd}$ is the slot synchronisation time, $t_{ttx}$ is the frame transmission time, and $t_{nd}$ is the *network delay* (time taken by a frame to travel from CM to CMTS). Hence the round trip delay will be two network delay times ($2\,t_{nd}$) and $t_{pr}$ is the total processing time taken by the CM and the CMTS

#### Simplified equation of frame delay (D) for DRNC

To keep the frame delay (D) equation as simple as possible, the network delay ($t_{nd}$) and the processing time taken by the CM and the CMTS ($t_{pr}$) are both ignored, since they are usually very small. Each active CM is producing *Poisson* traffic at a mean rate of $\lambda$ frames/s, and total traffic on the channel is $\Lambda$ (Eq. 4.19). As DRNC is a contention free protocol, and it is also assumed that the channel is error free, then under these conditions, new channel traffic is equal to the total channel traffic.

$$\Lambda = \Lambda_n \tag{4.26}$$

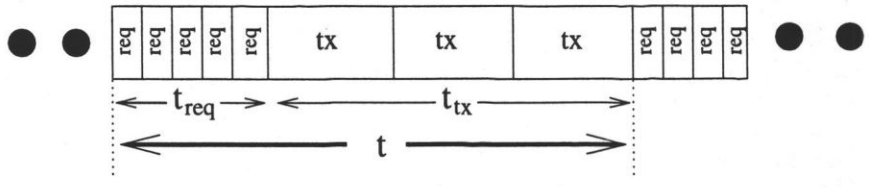


**Figure 4.4:** Example showing simplified version of DRNC

In Fig. 4.4, if $t$ is the time taken for one cycle (requests and transmissions) and

also, in one request, the CM can request as many frames as it needs to transmit, then the total number of requests in time $t$ will be $\Lambda t$ where

$$t = (N_{cm}\, L_{req} + \Lambda\, t\, L_{tx})\, \frac{8}{W}, \tag{4.27}$$

and Eq. 4.27 can be modified to Eq. 4.28:

$$t = \frac{L_{req}\, N_{cm}}{W/8 - \Lambda\, L_{tx}}\,. \tag{4.28}$$

To simplify, *frame delay* (D) can be assumed to be equal to one cycle time (t):

$$D = t = \frac{L_{req}\, N_{cm}}{(W/8 - \Lambda\, L_{tx})}, \tag{4.29}$$

and by using Eq. 4.19, Eq. 4.29 can be modified to:

$$D = \frac{L_{req}\, N_{cm}}{(W/8 - A_{cm}\, \lambda\, L_{tx})}\ \ seconds\,. \tag{4.30}$$

Eq. 4.29 can also be modified, so that $D$ can be written in terms of data (message) frames:

$$D = \frac{N_{cm}\, L_{req}\,/\, L_{tx}}{1 - G}\ \ frames\,, \tag{4.31}$$

where $G$ is the normalised traffic, i.e. number of data frames per data frame time.

Eq. 4.30 can be modified as:

$$\lambda = \left(\frac{100}{P_A\, N_{cm}\, L_{tx}}\right)\left(\frac{W}{8} - \frac{L_{req}\, N_{cm}}{D}\right)\,. \tag{4.32}$$

Fig. 4.5, Fig. 4.6, and Fig. 4.7 are plotted using Eq. 4.30, and Eq. 4.32, and using $W = 48$ Mbit/sec, $L_{tx} = 100$ bytes, $L_{req} = 20$ bytes, $N_{cm} = 100$ and $P_A = 30\%$. In all these figures, the X-axis represent the *Poisson* traffic on any active CM at a mean rate of $\lambda$ frames/s.

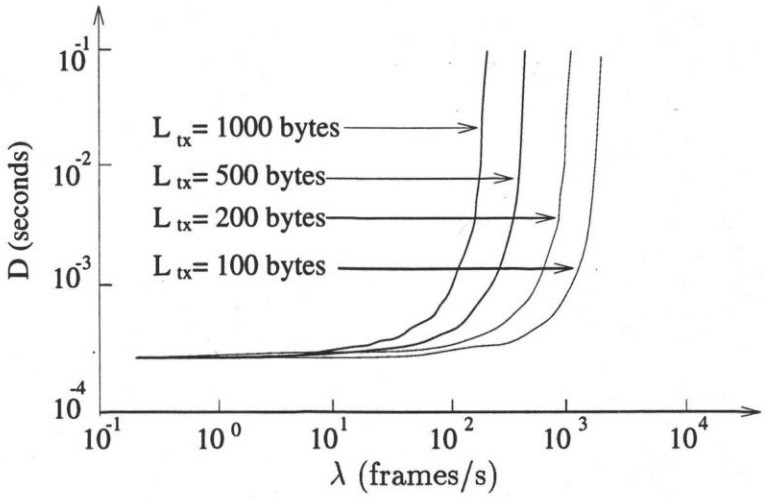


**Figure 4.5:** Frame Delay in DRNC as a function of $\lambda$ and $L_{tx}$ ($N_{cm} = 100$)

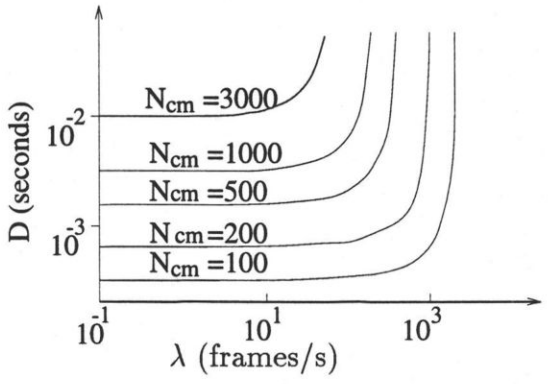


**Figure 4.6:** Frame Delay in DRNC as a function of $\lambda$ and $N_{cm}$ ($L_{tx} = 100$ bytes)

### 4.3.2 Throughput Analysis for DRNC

From Fig. 4.4, channel throughput can be expressed as:

$$S = \frac{\Lambda\, t\, L_{tx}}{N_{cm}\, L_{req} + \Lambda\, t\, L_{tx}}, \tag{4.33}$$

where t is given by Eq. 4.28. Eq. 4.33 can be simplified:

$$S = \frac{8\,\Lambda\, L_{tx}}{W}. \tag{4.34}$$

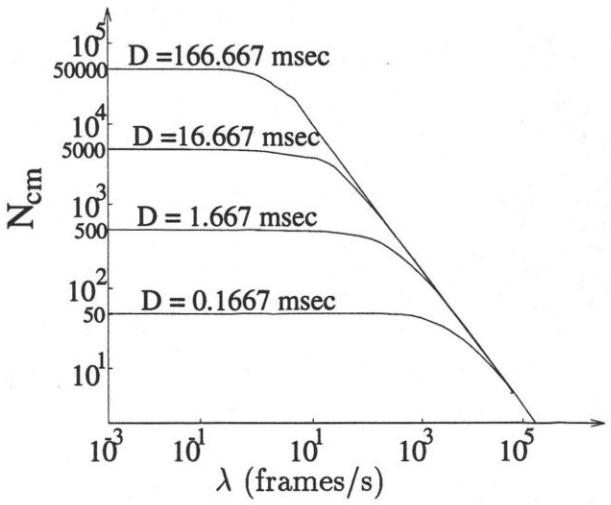


**Figure 4.7:** Performance of DRNC

Note that Eq. 4.34 is valid only when $\Lambda < W/8\,L_{tx}$.

## 4.4 *Dynamic Reservation with Contention* DRC

In the dynamic reservation systems considered in this section, the CM first makes a request for service on the channel whenever it has a message frame to send using the slotted ALOHA mode. It is only when such request is received at the CMTS that the CMTS will schedule the request. The CMTS maintains the queue of the requests and informs the CM of its position in the queue. In order to prevent collisions between the request frames and message frames, the upstream bandwidth is divided into two channels, one used to transmit control (request frames) information and other used for messages themselves.

Consider now a CM with a message frame ready for transmission. To initiate the sending of the message, the CM sends, on the request channel, a request frame containing information about the address of the CM, and the length of the message. At the correct reception of the request frame, the CMTS computes the time at which the backlog on the message channel will empty and then transmits to the CM the time at which it can start transmission (Appendix B).

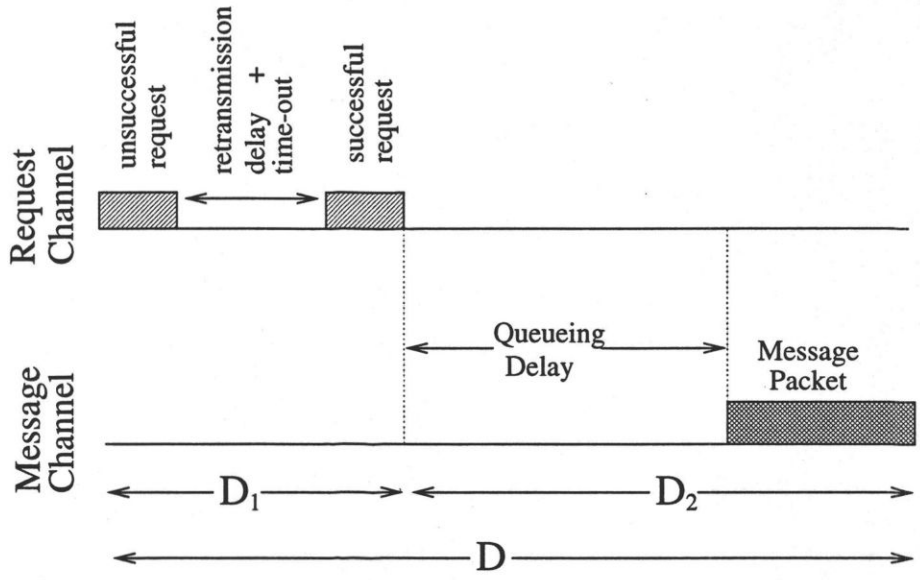


**Figure 4.8:** DRC protocol *(note that it is assumed that round trip and processing time taken by CM & CMTS is negligible)*

### 4.4.1 Frame Delay for DRC

The total message frame delay is defined as the time lapse from the moment the message frame is ready for transmission to the time the transmission of the message frame is complete. This total Delay $D$ is composed of $D_1$, the time for the request frame to be successfully received at the CMTS, and $D_2$, the time between reception of the request frame at the CMTS and the end of the message frame transmission.

Let $W_{req}$ be the bandwidth assigned to the request channel and $W_{tx}$ be the bandwidth assigned to the message channel, then

$$W = W_{req} + W_{tx} \ . \tag{4.35}$$

If $\tau_{req}$ is the length of the request frame in seconds, then

$$\tau_{req} = 8\, L_{req} / W_{req} \tag{4.36}$$

and $\tau_{tx}$, the length of the message frame in seconds, is given by

$$\tau_{tx} = 8\,L_{tx}/\,W_{tx}\ . \tag{4.37}$$

Let $G_{req}$ be the average number of attempts (due to all active CMs) per *request frame* time (this includes the attempts due to new frames plus the time due to frames that previously suffered collisions) and let $S_{req}$ be the throughput per *request frame* time (number of requests arriving per *request frame* time at the CMTS), then

$$S_{req} = G_{req}\,e^{-G_{req}}\ . \tag{4.38}$$

Let $\Lambda_{req}$ be the number of attempts per second at the request channel, then

$$\Lambda_{req} = G_{req}\,/\tau_{req}\ \ , \tag{4.39}$$

and let $\Lambda_{tx}$ be the number of requests arriving at the CMTS per second,

$$\Lambda_{tx} = S_{req}\,/\tau_{req}\ \ . \tag{4.40}$$

Let $G_{tx}$ be the number of requests arriving at the CMTS per message frame time, then

$$G_{tx} = \Lambda_{tx}\,\tau_{tx}\ . \tag{4.41}$$

**Delay in placing request** ($D_1$)

A request for a message frame is placed on the request channel by transmitting a request frame using the slotted ALOHA protocol. If $G_{req}$ is the normalised channel traffic at the request channel, then the expected number of transmissions per transmission can be found by using Eq. 4.15

$$E = e^{G_{req}}\ . \tag{4.42}$$

Neglecting the propagation delay, and letting the maximum retransmission delay be an integer number K of request frame slots(the retransmission delay being uniformly distributed over the K slots), the delay $D_1$ in placing a request can be found by using

Eq. 4.16 and is given by,

$$D_1 = \left[1 + \left(\frac{K+1}{2}\right)\left(e^{G_{req}} - 1\right)\right] \tau_{req} \quad seconds\,. \tag{4.43}$$

**Queueing delay and transmission delay for message frame ($D_2$)**

It is assumed that the CMTS acts as central controller, and it serves all the requests on a first come first served basis. Depending upon the requests, it will allot bandwidth to the CMs, so it can be assumed that the message channel behaves as M/D/1 queueing giving an average time in the system $D_2$ (waiting plus transmission). Using Eq. 4.3, $D_2$ can be written as

$$D_2 = \frac{\left(1 - \frac{G_{tx}}{2}\right)\tau_{tx}}{1 - G_{tx}} \quad seconds\,. \tag{4.44}$$

**Calculating request channel bandwidth ($W_{req}$) and message channel bandwidth ($W_{tx}$)**

The total number of requests per second arriving at the CMTS is

$$\Lambda_{tx} = \frac{S_{req}}{\tau_{req}} = \frac{G_{req}}{\tau_{req}} e^{-G_{req}}\,. \tag{4.45}$$

From Eq. 4.45, the average number of requests per message frame time is

$$G_{tx} = \Lambda_{tx}\,\tau_{tx} = \frac{G_{req}\,\tau_{tx}}{\tau_{req}} e^{-G_{req}}\,. \tag{4.46}$$

From Eq. 4.44, it is clear that for finite queueing delay $G_{tx} < 1$. Also $G_{tx}$ is maximum when $G_{req} = 1$, so Eq. 4.46 can be modified to

$$\underbrace{G_{tx}}_{maximum\ value} = \frac{\tau_{tx}}{\tau_{req}} e^{-1}\,. \tag{4.47}$$

Let $\underbrace{G_{tx}}_{maximum\ value} = r$, then

$$r = \frac{\tau_{tx}}{\tau_{req}} e^{-1} = \frac{L_{tx}\,W_{req}}{L_{req}\,W_{tx}} e^{-1}\,. \tag{4.48}$$

Solving Eq. 4.48

$$W_{req} = \frac{r\, e^{\frac{L_{req}}{L_{tx}}}}{1 + r\, e^{\frac{L_{req}}{L_{tx}}}} W \ , \tag{4.49}$$

and similarly,

$$W_{tx} = \frac{1}{1 + r\, e^{\frac{L_{req}}{L_{tx}}}} W \ . \tag{4.50}$$

### Fraction of bandwidth used for message transmission

Eq. 4.50 can be written as

$$\frac{W_{tx}}{W} = \frac{1}{1 + r\, e^{\frac{L_{req}}{L_{tx}}}} \ . \tag{4.51}$$

To have a proper utilization of the request and message channels, r should be close to 1 (i.e. $r \approx 1$). Fig. 4.9 shows the relation between $W_{tx}/\,W$, $r$ and $L_{tx}\,/L_{req}$.

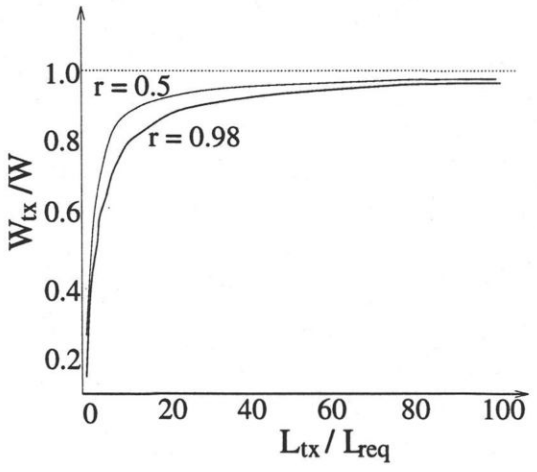


**Figure 4.9:** Fraction of bandwidth used for message transmission for different values of r and $L_{tx}\,/L_{req}$

### Calculating frame delay ($D$) for DRC protocol

The total frame delay is the sum of $D_1$ and $D_2$.

$$D = \left[1 + \left(\frac{K+1}{2}\right)\left(e^{G_{req}} - 1\right)\right] \tau_{req} + \frac{\left(1 - \frac{G_{tx}}{2}\right) \tau_{tx}}{1 - G_{tx}} \ \ seconds \, . \tag{4.52}$$

Since $G_{tx} = \frac{G_{req}\,\tau_{tx}}{\tau_{req}} e^{-G_{req}}$ (Eq. 4.46), $G_{req} = \Lambda_{req}\,\tau_{req}$, then

$$D = \left[1 + \left(\frac{K+1}{2}\right)\left(e^{\Lambda_{req}\,\tau_{req}} - 1\right)\right]\tau_{req} + \frac{\left(1 - \Lambda_{req}\,\tau_{tx}\,e^{-\Lambda_{req}\,\tau_{req}}/2\right)\tau_{tx}}{1 - \Lambda_{req}\,\tau_{tx}\,e^{-\Lambda_{req}\,\tau_{req}}}. \quad (4.53)$$

If it is assumed that there are $A_{cm}$ number of active CMs producing identical *Poisson* traffic at rate $\lambda_{req} = \Lambda_{req}\,/A_{cm}$, where $A_{cm}$ is given by Eq. 4.7 then Eq. 4.53 can be written in terms of $\lambda_{req}$ as

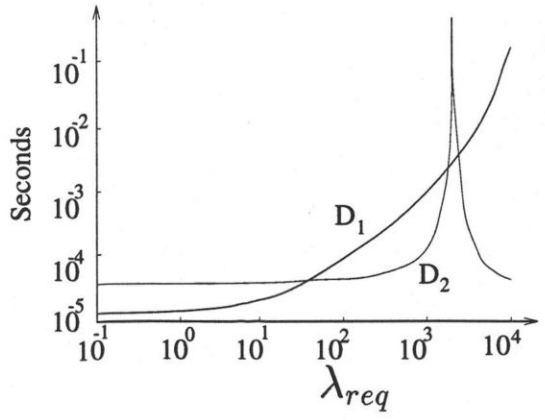


**Figure 4.10:** $D_1$ and $D_2$ as a function of $\lambda_{req}$

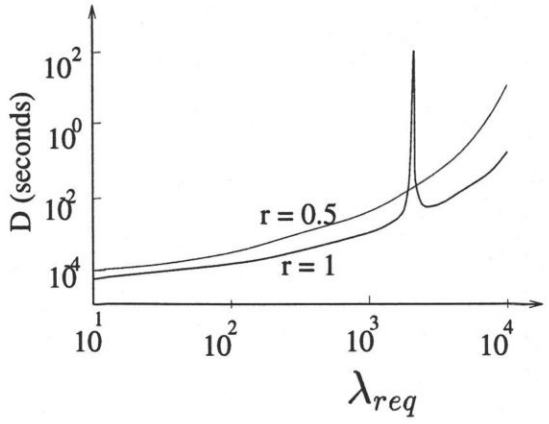


**Figure 4.11:** $D$ as a function of $\lambda_{req}$ and $r$

$$D = \underbrace{\left[1 + \left(\frac{K+1}{2}\right)\left(e^{A_{cm}\,\lambda_{req}\,\tau_{req}} - 1\right)\right]\tau_{req}}_{D_1} + \underbrace{\frac{\left(1 - A_{cm}\,\lambda_{req}\,\tau_{tx}\,e^{-A_{cm}\,\lambda_{req}\,\tau_{req}}/2\right)\tau_{tx}}{1 - A_{cm}\,\lambda_{req}\,\tau_{tx}\,e^{-A_{cm}\,\lambda_{req}\,\tau_{req}}}}_{D_2}. \tag{4.54}$$

If $\Lambda$ is the total channel traffic (new plus old traffic due to retransmissions of frames that previously suffered collision) then total traffic at the request channel is equal to $\Lambda$, which is given by

$$\Lambda = \Lambda_{req} = A_{cm}\,\lambda_{req}\,. \tag{4.55}$$

For $G_{req} < 1$, the request channel mode of DRC will be working under stable slotted ALOHA mode. In this case, in order to maintain equilibrium, new traffic at the request channel will be equal to the throughput of slotted ALOHA ($S_{req}$). In other words, the total number of requests arriving at the CMTS ($\Lambda_{tx}$) will be equal to new traffic ($\Lambda_n$) as long as $G_{req}$ is less than one.

$$\Lambda_n = \Lambda_{tx} \tag{4.56}$$

Using Eq. 4.55, $G_{req}$ can be written as

$$G_{req} = \Lambda_{req}\,\tau_{req} = \Lambda\,\tau_{req}\,, \tag{4.57}$$

and using Eq. 4.56, $G_{tx}$ can be written as

$$G_{tx} = \Lambda_{tx}\,\tau_{tx} = \Lambda_n\,\tau_{tx}\,. \tag{4.58}$$

Eq. 4.52 is simplified to

$$D = \left[1 + \left(\frac{K+1}{2}\right)\left(e^{\Lambda\,\tau_{req}} - 1\right)\right]\tau_{req} + \frac{\left(1 - \frac{\Lambda_n\,\tau_{tx}}{2}\right)\tau_{tx}}{1 - \Lambda_n\,\tau_{tx}} \quad seconds\,. \tag{4.59}$$

In Fig. 4.10 and Fig. 4.11, the X-axis represents traffic on the CM ($\lambda_{req}$) and the Y-axis represents delay in seconds with the following parameters: $W = 48$ Mbit/sec, $r = 1$, $L_{tx} = 200$ bytes, $L_{req} = 20$ bytes, $N_{cm} = 100$, $P_A = 30\%$, and $K = 201$. In

these figures, there are spikes at a certain traffic rate for $r = 1$. At this traffic rate, the request channel is operating at peak efficiency and the CMTS has just enough bandwidth to reserve the bandwidth for all the incoming requests. In other words when $G_{tx} \Rightarrow 1$ then at that traffic rate, $D_2 \Rightarrow \infty$ as shown in Eq. 4.44.

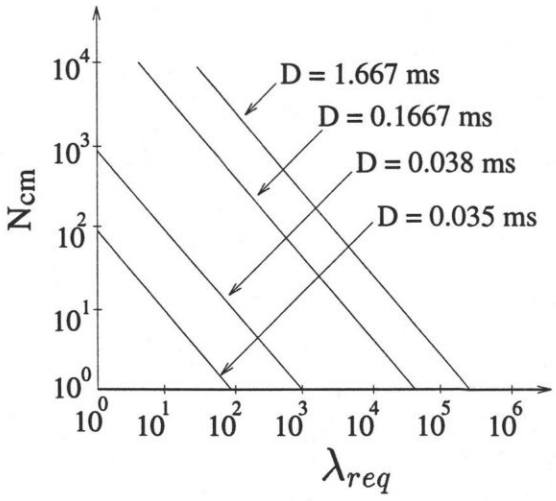


**Figure 4.12:** Performance of DRC at various delay

By comparing Fig. 4.12 and Fig. 4.2, it is seen that the performances are very similar, but in the slotted ALOHA protocol, in order to have the performance as shown in Fig. 4.2, the message frame should be of fixed length, but in the dynamic reservation with contention protocol, there is no such condition on the length of a message frame.

### 4.4.2 Throughput Analysis for DRC

If there are $\Lambda_{tx}$ requests arriving at the CMTS per second, then the throughput (S) will be

$$S = \frac{8\,\Lambda_{tx}\,L_{tx}}{W}, \tag{4.60}$$

and also, similarly

$$\Lambda_{tx} = A_{cm}\,\lambda_{req} e^{-A_{cm}\,\lambda_{req}\,\tau_{req}}, \tag{4.61}$$

and by using Eq. 4.61, Eq. 4.60 can be modified to

$$S = \frac{8\, L_{tx}\, A_{cm}\, \lambda_{req}\, e^{-A_{cm}\, \lambda_{req}\, \tau_{req}}}{W}. \tag{4.62}$$

DRC can be made more efficient than as shown in analysis, if a CM is capable of requesting all its backlog and current traffic by a single request frame. In this case, the load on the request channel will decrease, and more bandwidth can be alloted to the message channel.

## 4.5 *Dynamic Reservation with limited Contention* DRLC

1. *Slotted ALOHA for inactive users.* The CMTS maintains a list of active and inactive CMs. Then it reserves certain bandwidth for inactive users. Inactive CMs request the bandwidth using slotted ALOHA protocol. Once an inactive CM places a request for bandwidth, it no longer remains inactive. It is transferred to the active CMs list.

2. *DRNC for active CMs.* The CMTS reserves certain bandwidth for inactive users and the rest of upstream bandwidth for active CMs. Active CMs place requests using DRNC protocol.

To analyse the performance of DRLC, Fig. 4.4 can be followed, which shows a simplified version of the DRNC protocol.

### 4.5.1 Frame Delay for DRLC

Let $\theta$ be the fraction of bandwidth given to inactive users and $W_i$ be the bandwidth given to inactive users,

$$W_i = \theta\, W\,, \tag{4.63}$$

and if $W_a$ is the bandwidth given to active users, then

$$W_a = (1 - \theta)\; W\,. \tag{4.64}$$

If $t_{req}$ is the time spend in polling all active users

$$t_{req} = 8\, A_{cm}\, L_{req} / W_a\,, \tag{4.65}$$

and let $t_{tx}$ be the time spent in transmitting all message frames, so

$$t_{tx} = 8\, \Lambda\, t\, L_{tx} / W_a\,. \tag{4.66}$$

From Fig. 4.4, it is seen that $t$ is the time period for one cycle,

$$t = t_{req} + t_{tx} = (A_{cm}\, L_{req} + \Lambda\, t\, L_{tx})\, \frac{8}{W_a}\,. \tag{4.67}$$

Simplifying, let frame delay $D = t$. Solving Eq. 4.67 and by using Eq. 4.19, the frame delay for DRLC protocol can be found as

$$D = \frac{A_{cm}\, L_{req}}{(W_a/8 - A_{cm}\, \lambda\, L_{tx})}\,. \tag{4.68}$$

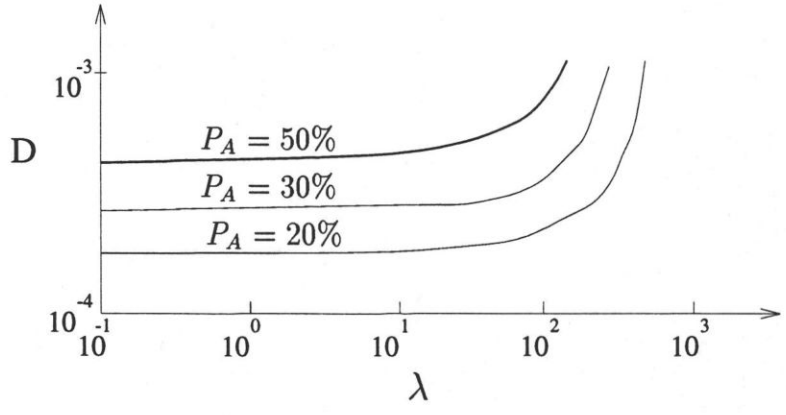


**Figure 4.13:** Frame Delay ($D$) for various values of $P_A$ and $\lambda$

Fig. 4.13 shows $D$ as a function of $P_A$ and $\lambda$. In this figure, $\theta = 0.05$, $W = 4.8 \times 10^6$ Mbit/sec, $L_{tx} = 100$ bytes, and $L_{req} = 20$ bytes. In Fig. 4.14, $P_A = 30\%$ and the rest of the parameters are the same as in Fig. 4.13.

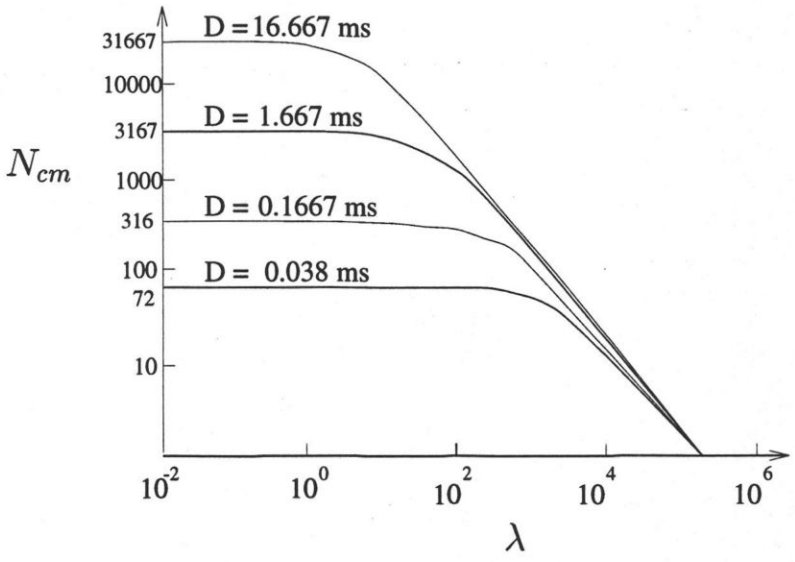


**Figure 4.14:** Performance of DRLC at different delays

### 4.5.2 Throughput Analysis for DRLC

The throughput for DRLC can be calculated by using Eq. 4.34

$$S = \frac{8\,\Lambda\,L_{tx}}{W}, \tag{4.69}$$

and Eq. 4.69 is valid only for $\Lambda < W_a\,/8\,L_{tx}$ .

## 4.6 *Modified-Dynamic Reservation with Limited Contention* M-DRLC

In DRLC, it is assumed that there are two set of users, one active and the other inactive. In the M-DRLC protocol, active users (CMs) are further divided into two categories, *hyper CMs* and *slack CMs* [23, 24, 25, 26].

1. *hyper CMs:* Those CMs who are consuming most of the bandwidth.
2. *slack CMs:* Those CMs, which are active but are consuming much less bandwidth.

*Slack* and *inactive* CMs use the *DRC* protocol to reserve bandwidth; *hyper* CMs use the *DRNC* protocol to reserve bandwidth.

### 4.6.1 Frame Delay for M-DRLC

Let $P_H$ denote the percentage of *hyper* CMs and $P_S$ denote the percentage of *slack* CMs. This means that the total active CMs will be the sum of *hyper* CMs and *slack* CMs.

$$P_A\, N_{cm} = (P_H + P_S)\, N_{cm} \Longrightarrow \{P_A = P_H + P_S\} \tag{4.70}$$

If $H_{cm}$ is the number of *hyper* CMs and $S_{cm}$ is the number of *slack* CMs, then

$$H_{cm} = \frac{P_H\, N_{cm}}{100}\,, \quad and \tag{4.71}$$

$$S_{cm} = \frac{P_S\, N_{cm}}{100}\,. \tag{4.72}$$

Let $f_h$ be the fraction of channel traffic produced by *hyper* CMs, $f_s$ the fraction of channel traffic produced by *slack* CMs, $\Lambda_h$ the total traffic produced by *hyper* CMs, and $\Lambda_s$ the total traffic produced by *slack* CMs, then

$$1 = f_h + f_s\,, \quad and \tag{4.73}$$

$$\Lambda = \Lambda_h + \Lambda_s = f_h\, \Lambda + f_s\, \Lambda\,. \tag{4.74}$$

Further assume that all *hyper* CMs produce identical *Poisson* traffic at mean $\lambda_h$ frames/s and all *slack* CMs produce identical *Poisson* traffic at mean $\lambda_s$ frames/s, then

$$\lambda_h = \frac{\Lambda_h}{H_{cm}}\,, \quad and \tag{4.75}$$

$$\lambda_s = \frac{\Lambda_s}{S_{cm}}\,. \tag{4.76}$$

Let $\alpha$ be the fraction of bandwidth given to *hyper* CMs and $W_h$ be the bandwidth given to *hyper* CMs, then

$$W_h = \alpha\, W\,. \tag{4.77}$$

If $W_s$ is the bandwidth given to *slack* and *inactive* CMs, then

$$W_s = (1 - \alpha)W\,. \tag{4.78}$$

### Frame Delay for hyper CMs

Bandwidth is reserved for *hyper* CMs using the DRNC protocol. Frame delay for *hyper* CMs ($D_h$) can be found by using Eq. 4.30,

$$D_h = \frac{L_{req}\, H_{cm}}{(W_h/8 - H_{cm}\, \lambda_h\, L_{tx})}\,. \tag{4.79}$$

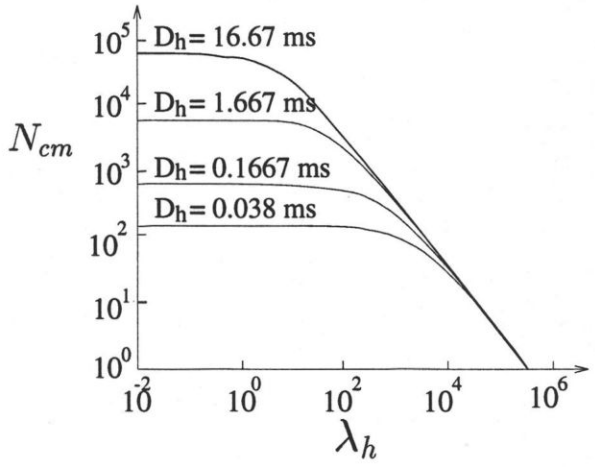


**Figure 4.15:** Performance of M-DRLC for *hyper* CMs

In Fig. 4.15, the performance of M-DRLC for *hyper* CMs is shown. The following parameters are used:
$W = 48$ Mbit/sec, $P_H = 5\%$, $P_S = 25\%$, $\alpha = 0.6$, $L_{req} = 20$ bytes, and $L_{tx} = 200$ bytes. From the figure, it is clear that at low $\lambda_h$ and for $D_h = 0.038$ ms, the M-DLRC protocol can support 136 CMs and for $D_h = 0.1667$ ms, it can support 600 CMs.

### Frame Delay for slack/inactive CMs

*Slack* CMs use the DRC protocol to reserve bandwidth. Using Eq. 4.49, bandwidth

assigned for the request channel ($W_{req}$) can be found as

$$W_{req} = \frac{r\, e\, \frac{L_{req}}{L_{tx}}}{1 + r\, e\, \frac{L_{req}}{L_{tx}}} W_s \tag{4.80}$$

and similarly by using Eq. 4.50, the bandwidth assigned for the message channel ($W_{tx}$) can be found as

$$W_{tx} = \frac{1}{1 + r\, e\, \frac{L_{req}}{L_{tx}}} W_s\,. \tag{4.81}$$

The request frame length in seconds ($\tau_{req}$) and message frame length in seconds ($\tau_{tx}$) can be found by using Eq. 4.36, 4.37, 4.80 and 4.81. If $D_s$ is the average frame delay for *slack/inactive* CMs, then using Eq. 4.54, $D_s$ can be written as

$$D_s = \left[1 + \left(\frac{K+1}{2}\right)\left(e^{S_{cm}\,\lambda_s\,\tau_{req}} - 1\right)\right]\tau_{req} + \frac{\left(1 - S_{cm}\,\lambda_s\,\tau_{tx}\,e^{-S_{cm}\,\lambda_s\,\tau_{req}}/2\right)\tau_{tx}}{1 - S_{cm}\,\lambda_s\,\tau_{tx}\,e^{-S_{cm}\,\lambda_s\,\tau_{req}}}. \tag{4.82}$$

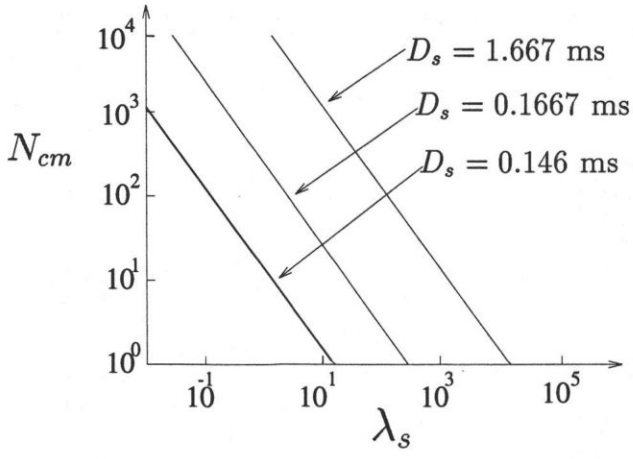


**Figure 4.16:** Performance of M-DRLC for *slack* CMs

In Fig. 4.16, the performance of M-DRLC for *slack* CMs is shown. Parameters used are the same as in Fig. 4.15. In Fig. 4.17, the performance of M-DRLC is shown with the following parameters, $W$ = 48 Mbit/sec, $L_{req}$ = 20 bytes, $L_{tx}$ = 200 bytes, $P_H$ = 5%, $P_S$ = 25%, K=100, r=0.999, $f_h$ = 0.5, $f_s$ = 0.5, and $\alpha$ = 0.5. In this figure the total channel traffic ($\Lambda$) is the sum of new traffic plus the old generated due

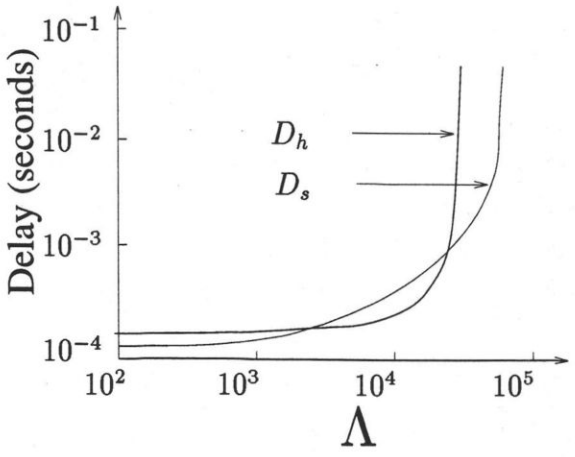


**Figure 4.17:** Performance of M-DRLC

to retransmission and collisions. Only *slack* CMs are using protocol with contention (DRC), so backlog traffic is only produced by *slack* CMs. M-DRLC gives very good frame delay, just slightly more than the DRC but better than any other protocol at low channel traffic. It also gives constant frame delay to *hyper* CMs at high channel traffic and the performance of M-DRLC at high channel traffic is comparable to that of the DRLC. Hence this protocol combines the advantages of both DRLC and DRC protocols. It also limits *hyper* CMs to occupy only a certain fixed bandwidth so that they are prevented from saturating the channel and affecting the performance for other CMs.

### 4.6.2 Throughput Analysis for M-DRLC

Channel utilization by *slack* CMs ($B_s$) can be found from Eq. 4.62

$$B_s = 8\, L_{tx}\, \Lambda_s e^{-\Lambda_s \tau_{req}}\,. \tag{4.83}$$

Let $S_s$ be the throughput for *slack* and *inactive* CMs, then

$$S_s = \frac{B_s}{W_s} = \frac{8\, L_{tx}\, \Lambda_s}{W_s} e^{-\Lambda_s \tau_{req}}\,. \tag{4.84}$$

Channel utilization by *hyper* CMs ($B_h$) is found by using Eq. 4.34 and Eq. 4.29.

$$B_h = \begin{cases} 8\,L_{tx}\,\Lambda_h & for\ \ \Lambda_h < \frac{W_h}{8\,L_{tx}} \\ W_h & for\ \ \Lambda_h \geq \frac{W_h}{8\,L_{tx}} \end{cases} \tag{4.85}$$

Let $S_h$ be the throughput for *hyper* CMs, then

$$S_h = \begin{cases} \frac{8\,L_{tx}\,\Lambda_h}{W_h} & for\ \ \Lambda_h < \frac{W_h}{8\,L_{tx}} \\ 1 & for\ \ \Lambda_h \geq \frac{W_h}{8\,L_{tx}} \end{cases} . \tag{4.86}$$

From Eq. 4.83 and Eq. 4.85 *Throughput* (S) for M-DRLC is

$$S = \begin{cases} \left(8\,L_{tx}\,\Lambda_s e^{-\Lambda_s\,\tau_{req}} + 8\,L_{tx}\,\Lambda_h\right)/\,W & for\ \ \Lambda_h < \frac{W_h}{8\,L_{tx}} \\ \left(8\,L_{tx}\,\Lambda_s e^{-\Lambda_s\,\tau_{req}} + W_h\right)/\,W & for\ \ \Lambda_h \geq \frac{W_h}{8\,L_{tx}} \end{cases} . \tag{4.87}$$

# Chapter 5

# Simulation, analysis and comparison of MAC protocols for the upstream path of the HFC network system

In Chapter 4, various MAC protocols are proposed for the upstream path of the hybrid fiber coax (HFC) network system. In this chapter, the effect of *round trip* delay on the performance will be analysed. Simulation models have been prepared for all the proposed MAC protocols for the upstream path of the HFC network system and their performance at different traffic load conditions is analysed.

## 5.1 Comparison of MAC protocols

In this section it is assumed that network delay is negligible, and there are no errors due to *white* noise and *impulse* noise. In Fig. 5.1, throughput vs delay for FDMA, slotted ALOHA, DRNC, DRC and DRLC protocols are plotted using Eqs. 4.8, 4.13, 4.34, 4.62 and 4.69. The various parameters used are: W=48 Mbit/s, $P_A = 30$, $N_{cm} = 500$, $K = 101$, $L_{tx} = 200$ bytes, $L_{req} = 20$ bytes, $\theta = 0.05$, and $r = 0.9$. It is seen that the DRC gives better *throughput* performance than the slotted ALOHA and better *delay* performance than the DRLC and the DRNC at low throughput. Channel utilization is better for the DRLC and the DRNC than the DRC protocol but at the expense of poor *delay* performance.

In Fig. 5.2, the throughput vs frame delay is plotted for DRC, DRLC and M-DRLC protocols using Eqs 4.62, 4.69, 4.84 and 4.86. The various parameters used are: $f_h = 0.5$, $f_s = 0.5$, $\alpha = 0.5$, $P_H = 5$ and $P_S = 25$ and the other parameters used

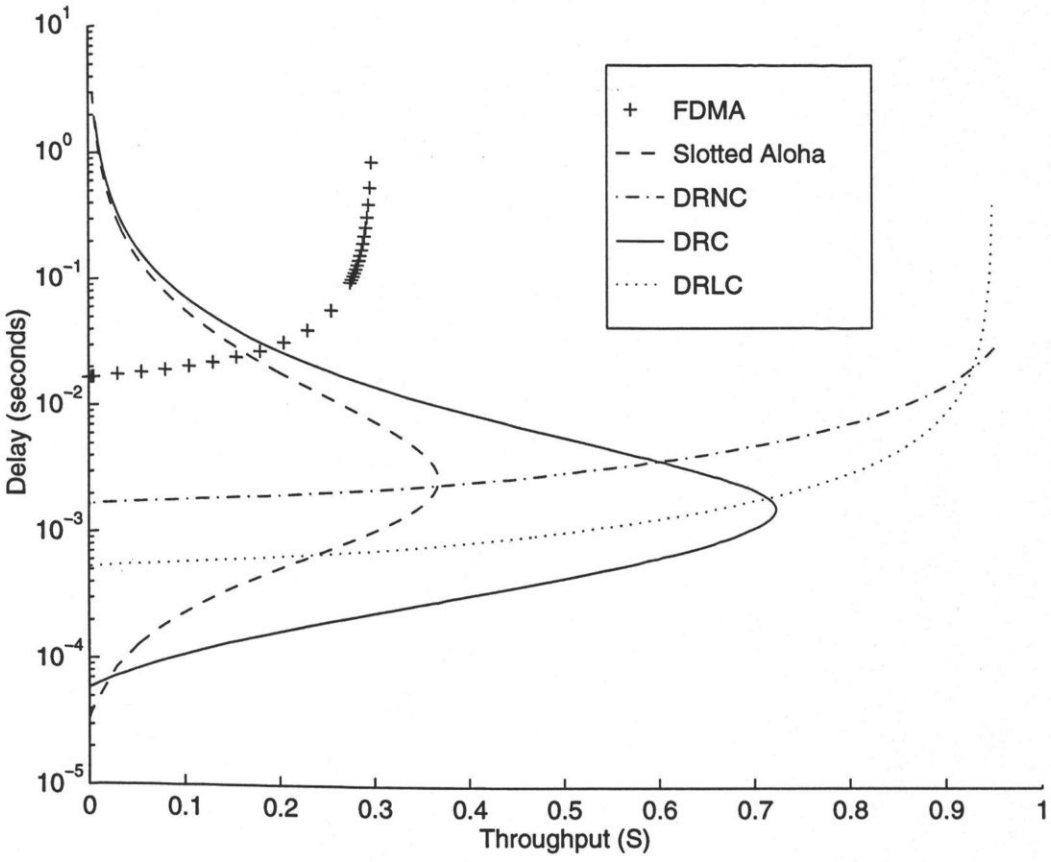


**Figure 5.1:** Frame delay vs throughput (part-1)

are the same as in Fig. 5.1. It is seen that M-DRLC has better *channel utilization* than DRC and better *frame delay* performance than DRLC.

In Fig. 5.3, the value of $r = 0.99$ and $P_H = 5\%$ and other parameters are the same as in Fig. 5.2 and 5.1. Fig. 5.3 does not give an exact comparison. In case of DRC protocol, the CM is producing a new traffic ($\lambda_n$), which is less than total traffic ($\lambda$), because of backlog traffic due to collisions. This situation is the same for the M-DRLC protocol for *slack* CMs. But hyper CMs in M-DRLC protocols use the DRNC protocol, which is a contention free protocol. In that case, there is no backlog traffic due to collisions. Hence new traffic ($\lambda_n$) is equal to the total traffic produced by the CM ($\lambda$).

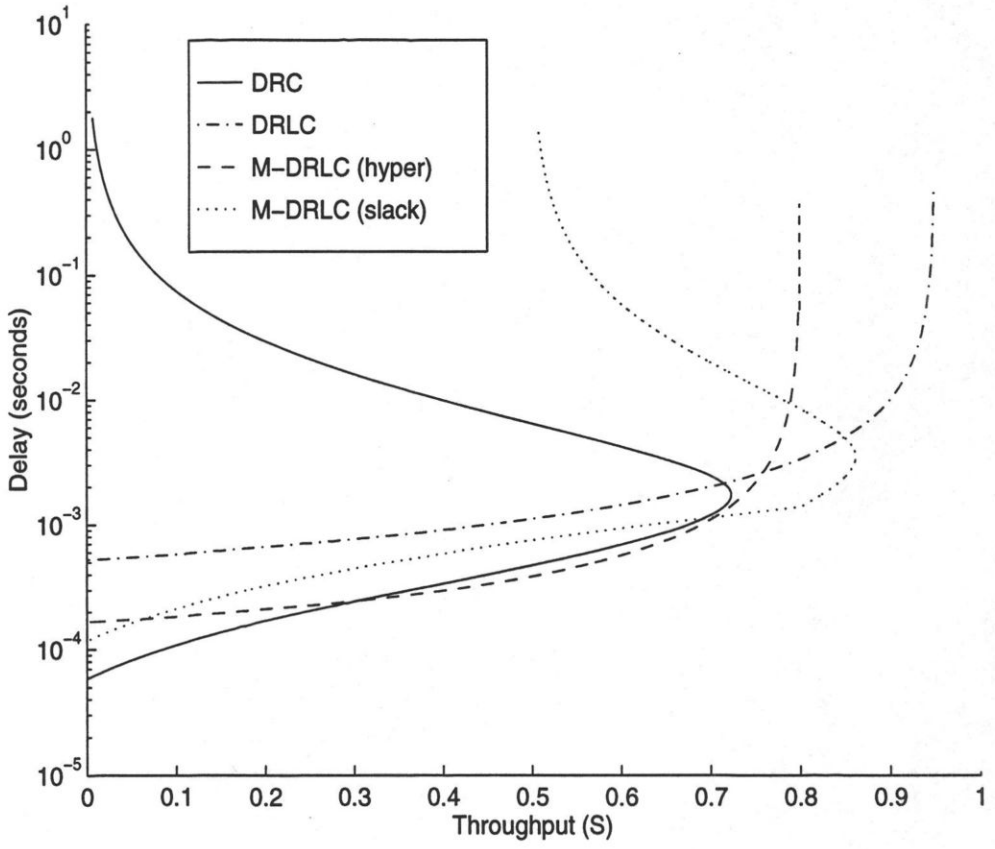


**Figure 5.2:** Frame delay vs throughput (part-2)

It is clear that DRC gives overall low frame delay, but M-DRLC has the advantage in the sense that no single user can saturate the whole channel. Whenever a single user is producing large traffic, it will be immediately transfered to the hyper CM category. In that case, it will not be in position to send requests independently. It will be in the hands of the CMTS to give it some bandwidth for transmitting data frames. This shows that the M-DRLC protocol can prevent the channel saturation, which may occur due to hyper activity of a few users.

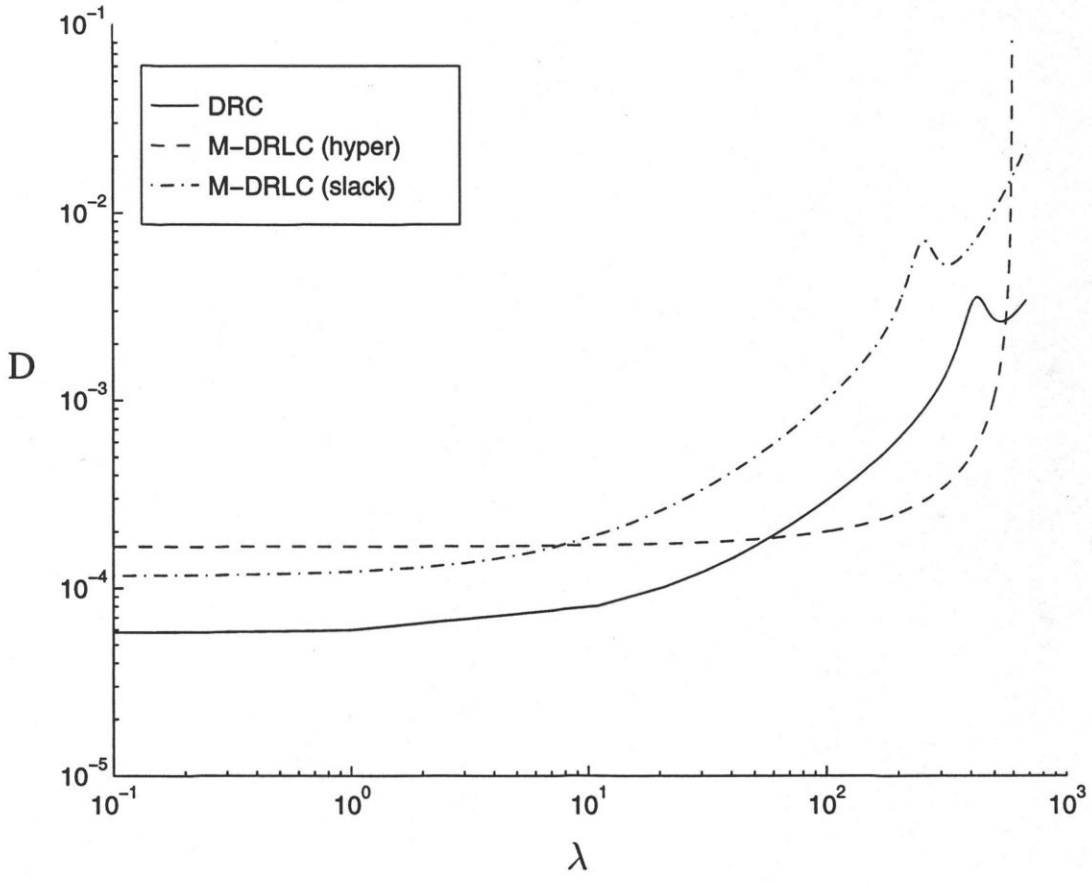


**Figure 5.3:** Comparing M-DRLC and DRC

## 5.2 Network delay

The transit delay from the most distant CM to the CMTS is called *network delay.* If the distance between the CM and the CMTS is known, then the *network delay* can be calculated as shown in Eq. 5.1.

$$t_{nd} = \frac{d}{\kappa\, c} \tag{5.1}$$

where $t_{nd}$ is *network delay* in seconds, $d$ is the *network distance* (maximum distance between the CM and the CMTS) in kms, $c$ is the speed of light in vacuum in km/s ($c = 3 \times 10^5$ km/s) and $\kappa$ is a *constant.* $\kappa$ can have any value between 0.2 to 0.9 depending upon the situation. According to MCNS specifications *network delay*

should be much less then 0.8 ms. See also reference [1] and Section 1.1 for more details. Table 5.1 shows the relation between $d$ and $t_{nd}$. In this table, $\kappa = 0.6$ is assumed. *Network delay* ($t_{nd}$) and *round trip delay* ($t_{rd}$) are related. Eq. 5.2 shows

**Table 5.1:** *Network distance* in kms and corresponding *network delay* in milli seconds

| $d$ **(kms)** | $t_{nd}$ **(ms)** |
|---|---|
| 2 | 0.0111 |
| 10 | 0.0556 |
| 30 | 0.1667 |
| 72 | 0.4 |
| 144 | 0.8 |

the relation between the two.

$$t_{rd} = 2\,t_{nd} \tag{5.2}$$

### 5.2.1 The effect of network delay on the performance of MAC protocols

Eq. 4.2 can be modified to include *network delay* in **FDMA**

$$D = \underbrace{\frac{(G^2/\lambda)}{2(1-G)}}_{Queueing\ Delay} + \underbrace{8\,N_{cm}\,L_{tx}/W}_{transmission\ time} + \underbrace{t_{nd}}_{network\ delay} \tag{5.3}$$

Eq. 5.3 can be simplified to Eq. 5.4

$$D = \frac{G}{\lambda}\left(1 - \frac{G}{2}\right)\Big/\,(1-G) + t_{nd} \tag{5.4}$$

Fig. 5.4 is plotted using Eq. 5.4 at constant frame delay ($D = 1.667$ ms). The X-axis represents traffic on any CM ($\lambda$), and the Y-axis represents the number of CMs a particular network can support at a given *frame delay*. The other parameters are: $L_{tx} = 200$ bytes, $\kappa = 0.6$ (Eq. 5.1) and $W = 48$ Mbit/s. The effect of *network delay* on the performance of **Slotted ALOHA** can be calculated. If it is assumed that processing time ($t_{pr}$) taken by the CM and the CMTS is negligible, then in case of collision of frames, the CM will come to know about this only after $t_{rd}$ seconds.

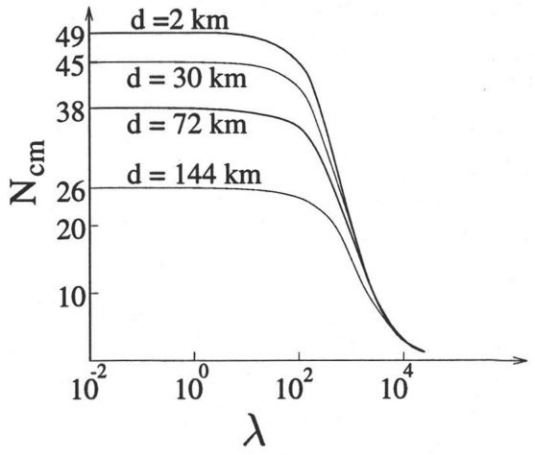


**Figure 5.4:** Performance of FDMA Protocol at various *network distance*

Eq. 4.18 can be modified to include network delay.

$$D = \tau + t_{nd} + \left(\frac{K+1}{2}\tau + 2\,t_{nd}\right)\left(e^{\Lambda\tau} - 1\right) \tag{5.5}$$

Using Eqs. 4.7, 4.19 and 5.5, Fig. 5.5 is plotted for frame delay $D = 1.667$ms.

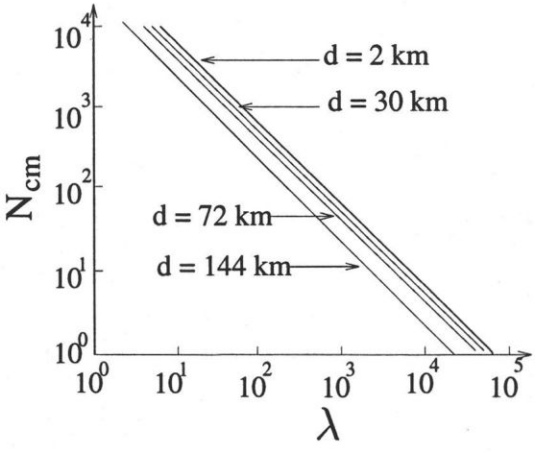


**Figure 5.5:** Performance of Slotted ALOHA at various *network distance*

Parameters used are: $P_A = 30\%$, $K = 101$ and other parameters are the same as in Fig. 5.4. In **DRNC**, the CMTS polls all CMs by alloting fixed size slots for

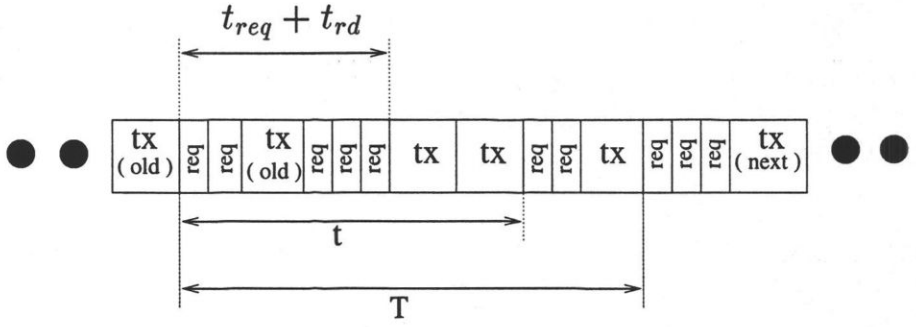


**Figure 5.6:** Example showing DRNC in presence of *network delay*

requesting the bandwidth. If any CM wants to send a data frame, it places its request in its request slot. When all CMs are polled, the CMTS fixes slots for data frames. Because of considerable round trip delay, there will be some gap between the last request frame and the first data frame. In that slot, the CMTS can allot the slots for backlog requests. Hence in this way, there won't be any wastage of bandwidth. In Fig. 5.6, it is seen that total time to complete one cycle is **t**. But total time to finish all the request is **T**. To simplify the situation, frame delay (D) can be written as the sum of cycle time ($t$) and round trip time ($t_{rd}$).

$$D = t + t_{rd} \tag{5.6}$$

Using Eq. 4.29, frame delay (D) for DRNC can be written as shown in Eq. 5.7.

$$D = \underbrace{\frac{L_{req}\, N_{cm}}{(W/8 - \Lambda\, L_{tx})}}_{t} + \underbrace{t_{rd}}_{round\ trip\ delay} \tag{5.7}$$

The effect of *network delay* on **DRC** can be calculated in similar fashion. Using Eq. 5.5, Eq. 4.43 is modified to include network delay.

$$D_1 = \tau_{req} + t_{nd} + \left(\frac{K+1}{2}\tau_{req} + t_{rd}\right)\left(e^{G_{req}} - 1\right) \tag{5.8}$$

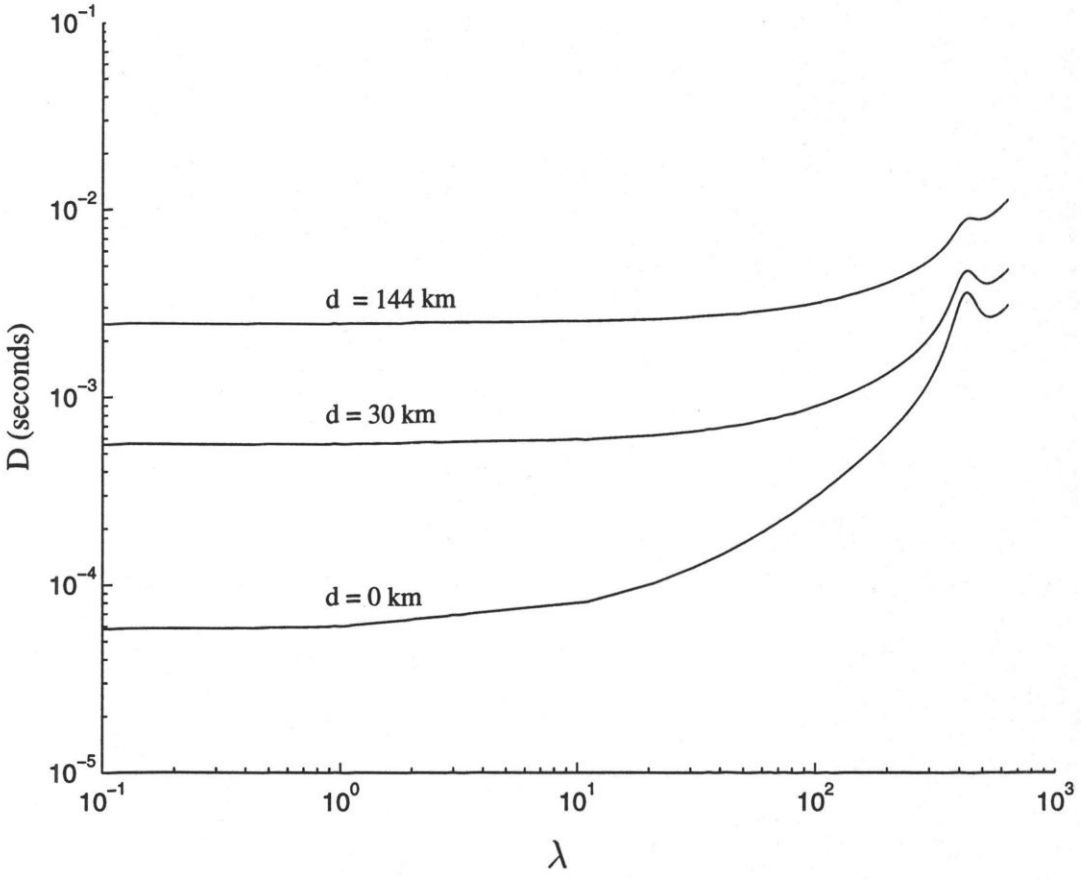


**Figure 5.7:** Effect of *network distance* on DRC

Similarly Eq. 4.44 is modified to include round trip delay.

$$D_2 = \frac{\left(1 - \frac{G_{tx}}{2}\right) \tau_{tx}}{1 - G_{tx}} + t_{rd} \tag{5.9}$$

Combining Eq. 5.8 and 5.9, total frame delay can be written as shown in Eq. 5.10.

$$D = \tau_{req} + 3\,t_{nd} + \left(\frac{K+1}{2}\tau_{req} + t_{rd}\right)\left(e^{G_{req}} - 1\right) + \frac{\left(1 - \frac{G_{tx}}{2}\right) \tau_{tx}}{1 - G_{tx}} \tag{5.10}$$

where $G_{tx}$ is the same as defined in Eq. 4.46. Eq. 4.68 can be modified to include network delay in **DRLC** as is done in Eq. 5.7 for DRNC.

$$D = \frac{L_{req}\, A_{cm}}{(W_a/8 - \Lambda\, L_{tx})} + t_{rd} \tag{5.11}$$

Fig. 5.7 shows the relation between *network distance* (d) and *frame delay* (D) at different users traffic ($\lambda$). Various other parameters used are $W = 48Mbit/s$, $P_A = 30\%$, $N_{cm} = 500$, $r = 0.99$, $L_{req} = 20$, $L_{tx} = 200$, and $K = 101$

In **M-DRLC**, the effect of *network delay* has to be calculated separately for *hyper* and *slack* CMs. Eq. 4.79 can be modified to include network delay for *hyper* CMs:

$$D_h = \frac{L_{req}\, H_{cm}}{(W_h/8 - \Lambda_h\, L_{tx})} + t_{rd} \tag{5.12}$$

Eq. 4.82 can be modified to include network delay for *slack* CMs

$$D_s = \tau_{req} + 3\, t_{nd} + \left(\frac{K+1}{2}\tau_{req} + t_{rd}\right)\left(e^{\Lambda_s\, \tau_{req}} - 1\right) + \frac{\left(1 - \Lambda_s\, \tau_{tx}\, e^{-\Lambda_s\, \tau_{req}} \Big/ 2\right) \tau_{tx}}{1 - \Lambda_s\, \tau_{tx}\, e^{-\Lambda_s\, \tau_{req}}} \tag{5.13}$$

Fig. 5.8 compares M-DRLC and DRC at various network distance. The value of $\kappa$ is 0.6 and other parameters used are used same as in Fig. 5.3.

## 5.3 Simulation Model for Slotted ALOHA

The simulation models are prepared using C++ language on unix workstations. The models are kept as simple as possible.

The simulation model for slotted ALOHA is as follows: it is assumed that there are many users, and they are generating new channel traffic at a Poisson mean rate of $G_n$ frames per frame time ($\Lambda_n$ frames per second). In the program it is considered that there is traffic coming from some source (all users). Which user is producing how much traffic is not considered. In this case it is also assumed that all users are generating fixed size frames ($L_{tx}$ bytes). The channel is divided into fixed size slots (slot length = frame length) by time division multiplexing. At every slot, the number of frames ready for transmission (new + backlog) is checked. If no frame

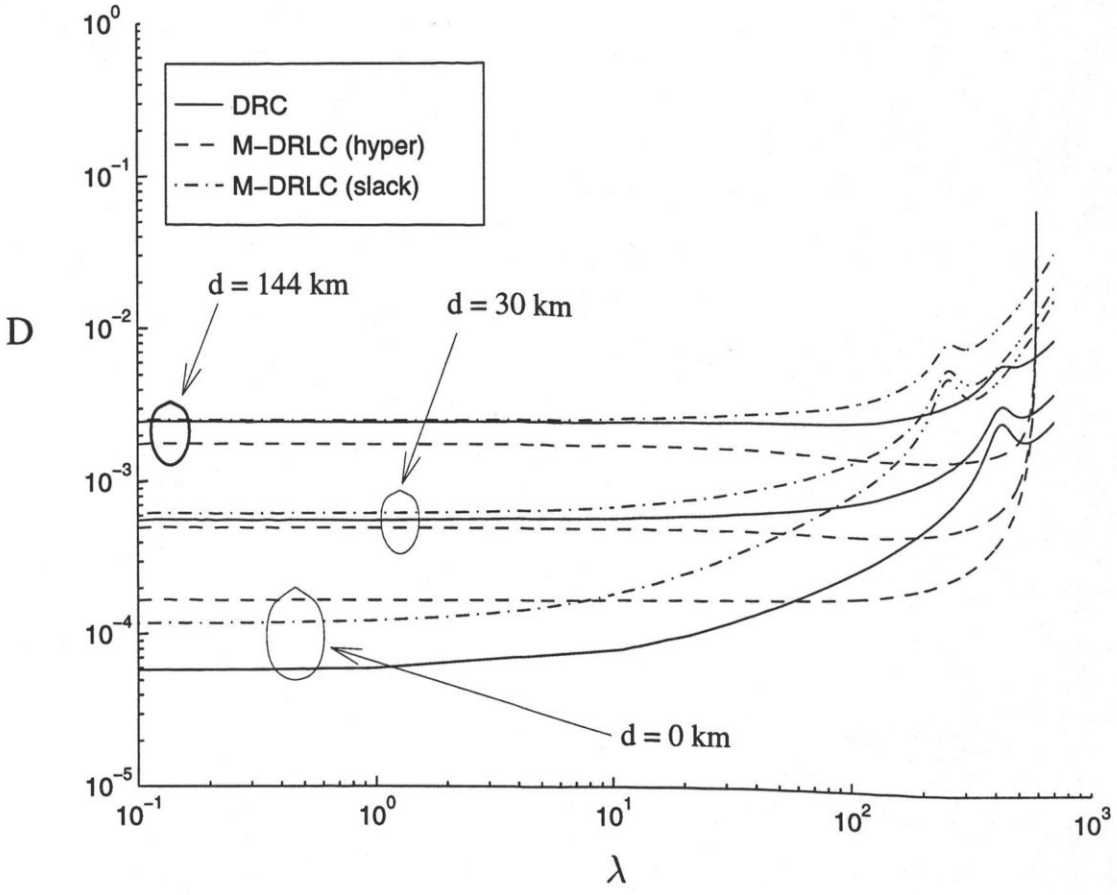


**Figure 5.8:** Effect of *network distance* on M-DRLC

is ready, then that slot goes idle. If only one frame is ready, then that frame is successfully transmitted. If more than one frame is ready, then it is considered a collision. As round trip delay and processing time by CM and CMTS is considered negligible, transmitting CMs will come to know about collisions immediately. All colliding frames will follow a contention resolution scheme as described in the next section. A record is kept for all colliding frames to calculate average frame delay.

### 5.3.1 Contention Resolution

When there is a collision, the station can follow two methods for contention resolution. These are *Randomization* and the *binary exponential back-off* algorithm.

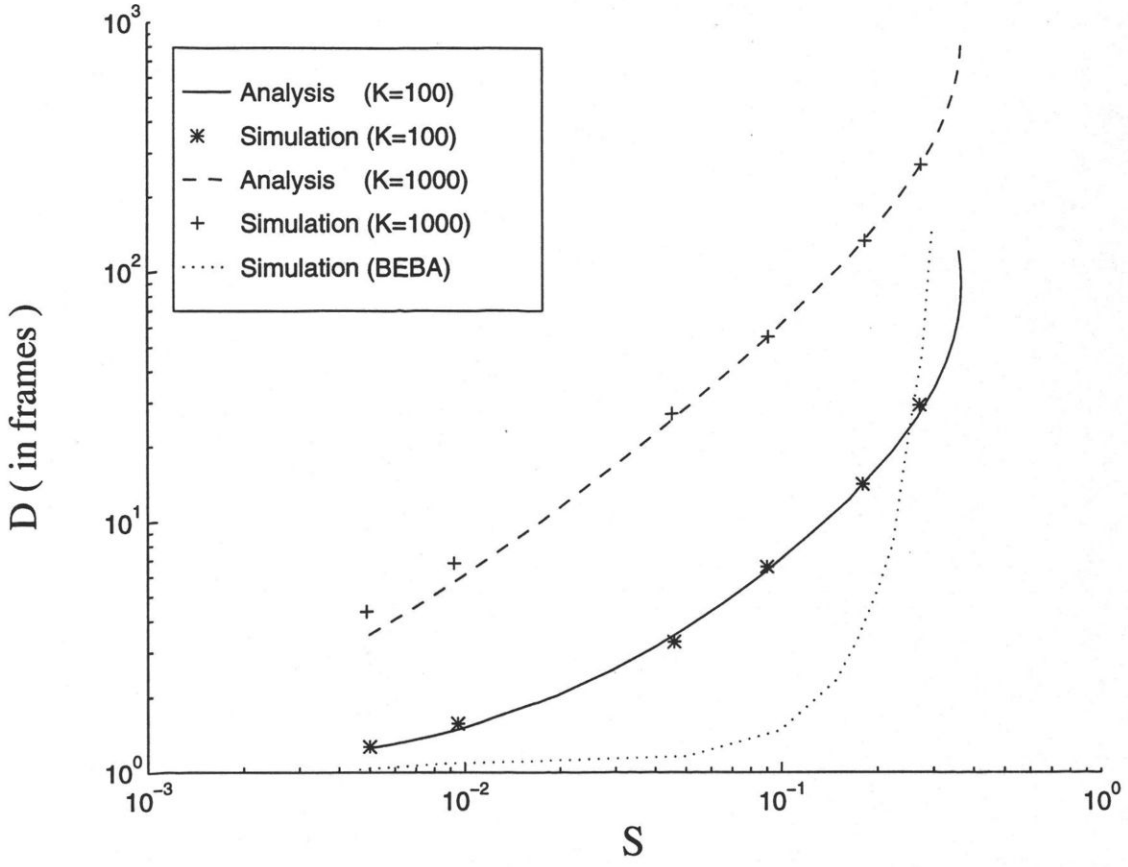


**Figure 5.9:** Comparison of Analytical results with Simulation results for Slotted Aloha

### Randomization

This is a simple method for contention resolution. Time is divided into discrete slots, one slot corresponding to one frame. When there is a collision, the station waits for a random slot between 0 and K. For example in Fig. 5.9, the value of K used is 100 and 1000. Analysis in Section 4.2 is done using randomization for contention resolution.

*The Binary Exponential Back-off Algorithm* **(BEBA)**

After the first collision, each station waits either 0 or 1 slots before trying again. If two stations collide and each one picks the same random number, they will collide

again. After the second collision, each one picks either 0, 1, 2 or 3 at random and waits that number of slots. If a third collision occurs, then the next time the number of slots to wait is chosen at random from the interval 0 to $2^3 - 1$. In general after $i$ collisions, a random number between 0 and $2^i - 1$ is chosen, and that number of slots is skipped. However after ten collisions have been reached, the randomization interval is frozen at a maximum of 1023 slots.

In Fig. 5.9, simulation results are presented and are compared with analytical ones. In simulation it is assumed that there is a very large number of active stations, each producing a small fraction of total channel traffic. The total channel traffic is the sum of new traffic ($G_n$) and old traffic, which is due to retransmissions of frames that previously suffered collision. At low load there will be few collisions, hence few retransmissions, so $G \approx G_n$. At high load there will be many collisions, so $G > G_n$. It is assumed that new channel traffic is *Poisson* at mean rate of $G_n$ frames per frame time. In analysis it was also assumed that channel traffic old and new combined is also *Poisson.* But in simulation, the nature of $G$ depends upon the contention and resolution schemes adopted. In simulation it was found that for $G_n > 0.3$, slotted ALOHA becomes unstable, with backlog traffic and frame delay both approaching infinity.

## 5.4 Simulation Model for DRNC and DRLC

It is assumed that there are $A_{cm}$ active CMs generating traffic at rate of $\lambda_n$ frames per second. As this protocol is a contention free protocol, there is no backlog traffic in other words $\lambda_n = \lambda$. If $\Lambda_n$ is the new channel traffic in frames per second, then for the DRNC protocol.

$$\Lambda_n = \Lambda \tag{5.14}$$

In this model, the channel is first divided into $N_{cm}$ slots of $L_{req}$ bytes as shown in Fig. 4.4. The CMTS polls all CMs to find out if there are any frames for transmission. When all CMs are polled, then the CMTS, depending upon the number of requests for data frames, reserves the bandwidth. For example, in one polling, if there are requests for 4 data frames, then the CMTS reserves the 4 next slots for data. Note

that data frames are of length $L_{tx}$ bytes. And it is also assumed that CMs request integer an number of data frames; i.e., they can request 0, 1, 2 and so on. They can not request 0.1 or 1.5 or any number which is not integer. This is done in order to keep the programs as simple as possible. As the channel is error free and contention free, these data frames are bound to be successfully transmitted. Also it is assumed

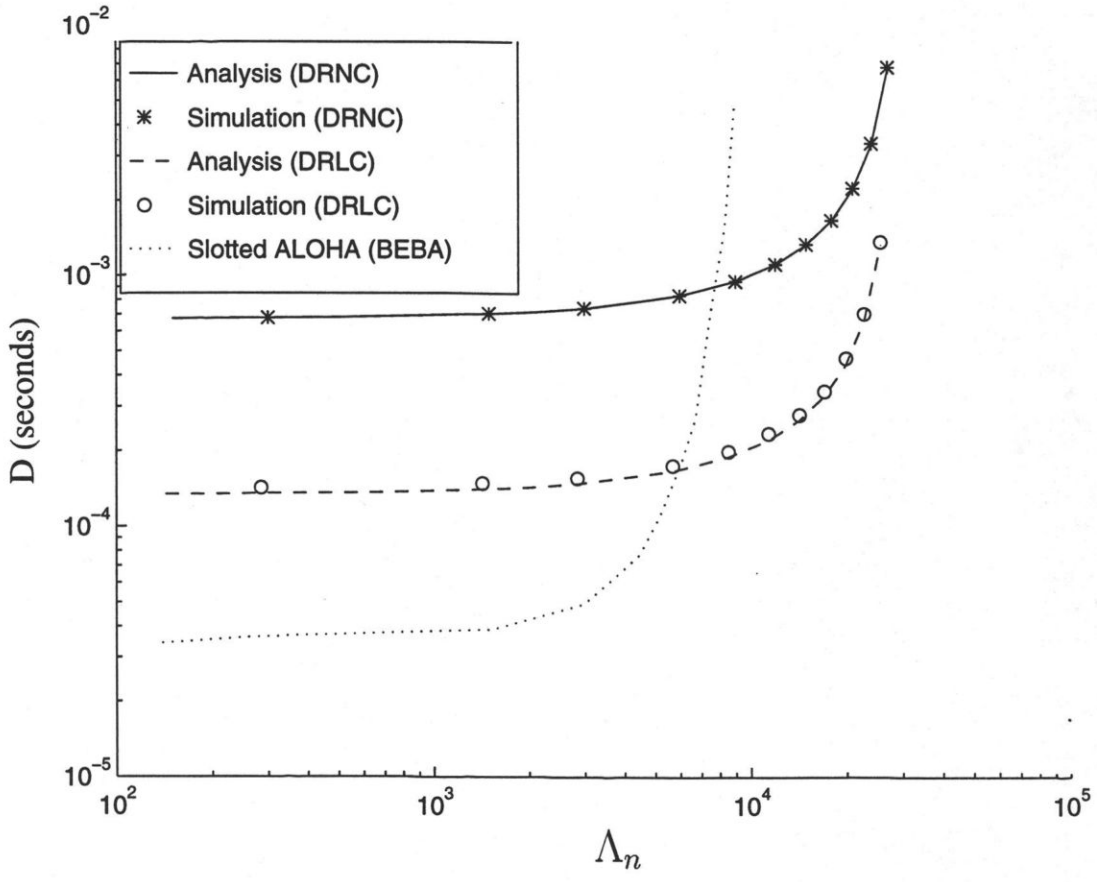


**Figure 5.10:** Simulation results for DRNC and DRLC protocols

that frame delay(D) is equal to one cycle as shown in Fig. 4.4. In Fig. 5.10, the following parameters are used: $W = 48$ Mbit/s, $L_{tx} = 20$ bytes, $L_{req} = 200$ bytes and $N_{cm} = 200$.

For the DRLC protocol, inactive users are not polled; they instead use the slotted ALOHA protocol. Active users use the DRNC protocol for bandwidth reservation. Bandwidth is divided in two parts by frequency division multiplexing. One part is given to inactive users and they use slotted ALOHA protocol in it; the rest of the bandwidth is given to active users. DRNC protocol is then employed on this part of the bandwidth for active users only. In Fig. 5.10, it is assumed that $\theta = 0.05$ and $P_A = 30\%$ and the rest of the parameters are the same as used for the DRNC protocol. Also in Fig. 5.10 DRLC and DRNC protocols are compared with Slotted ALOHA protocol which is using the *binary exponential back-off algorithm.* It is found that the slotted ALOHA protocol gives better frame delay at low channel traffic. At high channel traffic, the DRLC protocol gives better frame delay.

## 5.5 Simulation Model for DRC protocol

For DRC protocol, all users place requests for bandwidth using the slotted ALOHA protocol. It is also assumed that there are many users and a single user produces only a tiny fraction of the total channel traffic. BEBA or *Randomization* schemes can be employed for contention resolution. Once a request for bandwidth reaches the CMTS, the CMTS reserves bandwidth using a first come first served algorithm. The map for reserved upstream bandwidth is sent to users on the downstream channel. Section 4.4 explains more about the DRC protocol. Under stable conditions, the number of new requests arriving from all users ($\Lambda_n$) should be equal to the requests arriving at the CMTS ($\Lambda_{tx}$) as shown in Eq. 4.56. Also, due to collisions, the traffic at the request channel ($\Lambda_{req}$) will be larger than the new traffic ($\Lambda_n$).

$$\Lambda_{req} > \Lambda_n \tag{5.15}$$

In Fig. 5.11, simulation results for the DRC protocol are presented. Simulations are done using both contention resolution schemes, i.e. *Randomization* (K=100) and *The Binary Exponential Back-off Algorithm* (BEBA). The value of $r$ used is 1.08 and other parameters are the same as used in Section 5.4. The value of $r = 1.08$ does not mean anything special. While doing repeated simulations for different values of $r$ it was found that for $r = 1.08$, bandwidth utilization is maximum. The simulation

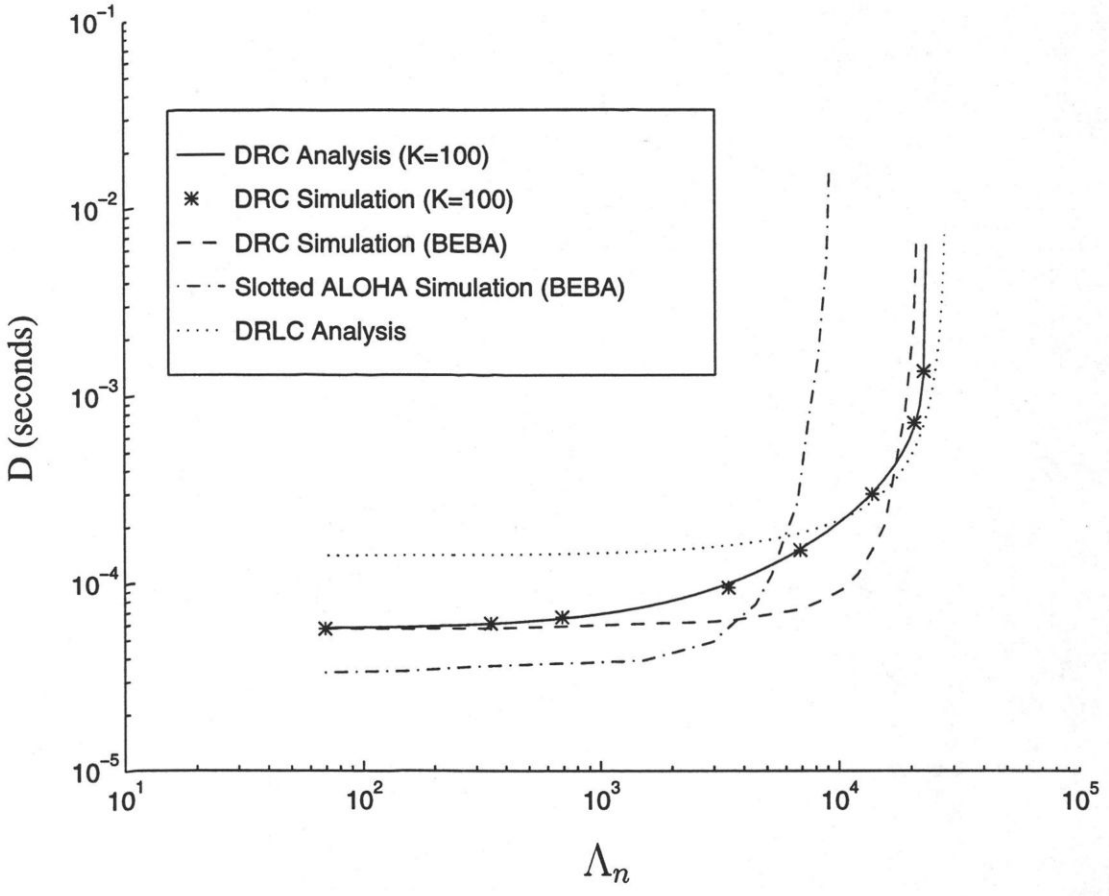


**Figure 5.11:** Simulation results for DRC protocols

results for the DRC protocol are compared with analytical ones and also with Slotted ALOHA (using BEBA for contention resolution) and the DRLC protocol and are shown in Fig. 5.11.

## 5.6 Simulation Model for M-DRLC

The M-DRLC protocol uses both DRC and DRLC protocols. M-DRLC is efficient if there are few CMs (hyper CMs) which are generating a considerable fraction ($f_h$) of channel traffic ($\Lambda_h = f_h\Lambda$). In other words, a few CMs are generating as much traffic as generated by the rest of the CMs $\{\Lambda_s = (1 - f_h)\Lambda = f_s\Lambda\}$.

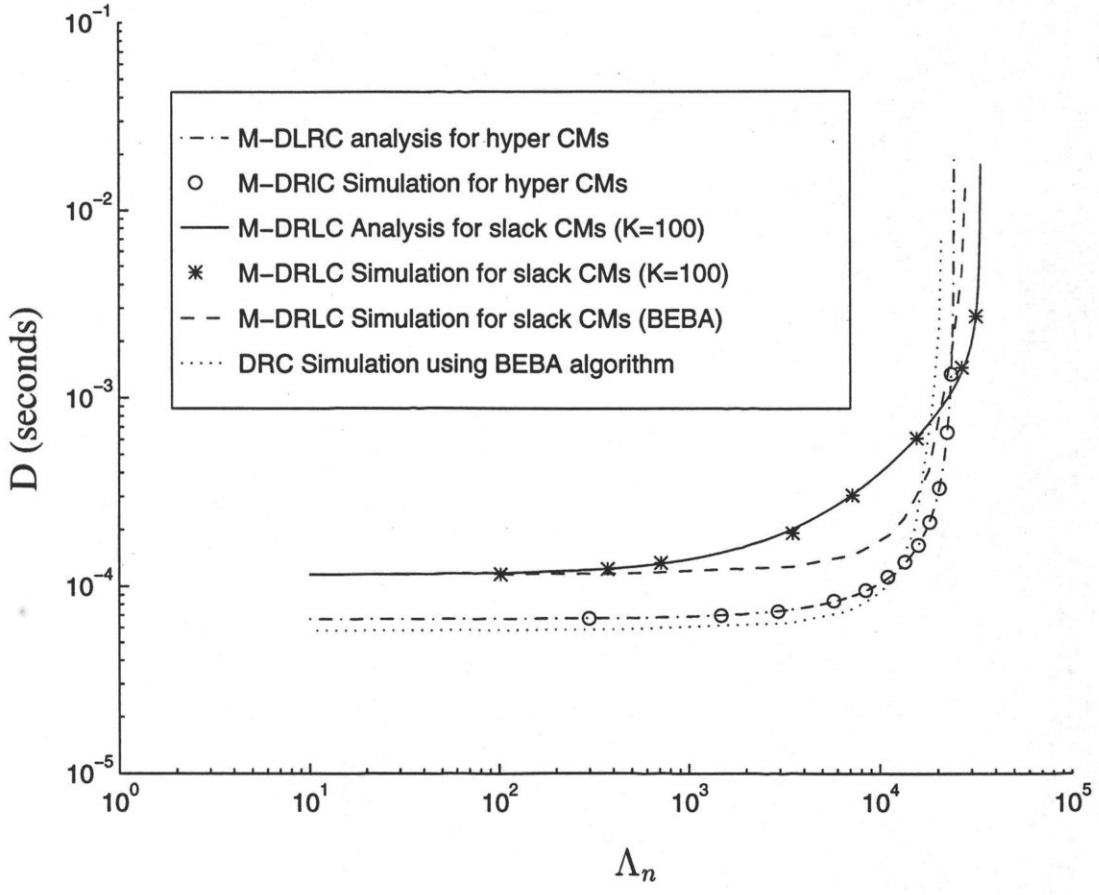


**Figure 5.12:** Simulation results for M-DRLC protocol

New traffic is less than channel traffic ($\Lambda_n < \Lambda$) as slack CMs are using the DRC protocol which creates extra traffic because of collisions of frames. In Fig 5.12, it is assumed that there are 200 CMs ($N_{cm}$) out of which 5% are hyper CMs ($P_H = 5\%$) and they are producing 50% of channel traffic ($f_h = 0.5$). Out of total channel bandwidth ($W = 48$ Mbit/s), 50% of bandwidth is given to hyper CMs ($\alpha = 0.5$). The value of $r = 1.08$ and $K = 100$. The request frame is 20 bytes long ($L_{req} = 20$ bytes) and the message frame is an average 200 bytes long ($L_{tx} = 200$ bytes). In Fig. 5.12, it is observed that when new channel traffic ($\Lambda_n$) is low, then performance of the DRC protocol is better than M-DRLC, but at high new channel traffic, M-DRLC is providing low frame delay to hyper CMs and also to slack CMs.

# Chapter 6

# The effect of White Noise and Impulse Noise on the performance

Hybrid fiber/coax is an emerging architecture for providing residential video and digital access. This architecture consists of optical fibers extending from the head-end or central office to remote fiber nodes. Extending from the fiber nodes is a coaxial cable distribution system that serves between a hundred and a thousand residences. Signals can be modulated and multiplexed at the head-end, transmitted by linear lasers in analog format on the fiber, then linearly converted to electrical signals for transmission on the coax. This architecture advantageously combines the long range of optical fiber with the simple electrical interfaces of coaxial cable [27].

## 6.1 Quadrature Amplitude Modulation (QAM)

QAM has emerged as the major contender for the upstream digital transmission on hybrid fiber/coax. It is bandwidth efficient and use multiple signal levels to send multiple bits/Hz. It conserves bandwidth by sending two orthogonal sine and cosine carriers in the same frequency band [27, 28, 29].

### 6.1.1 Probability of Error of QAM

In QAM, multiple signal phases and multiple signal amplitudes are used for transmitting $n$ information bits per symbol over the AWGN channel. It is observed that bandwidth efficiency of these digital modulations is proportional to $n = log_2 M$ [18].

If $n$ is even, then $M = 2^n$ signal points results in a symmetrical form of QAM which may be viewed as two separate PAM signals impressed on phase-quadrature carriers. Since the signals on the phase-quadrature carriers are perfectly separated by coherent detection, the error rate performance for QAM with a rectangular signal structure can be determined directly from the probability of error ($P_{\sqrt{M}}$) of a $\sqrt{M}$-ary PAM system [18, 28].

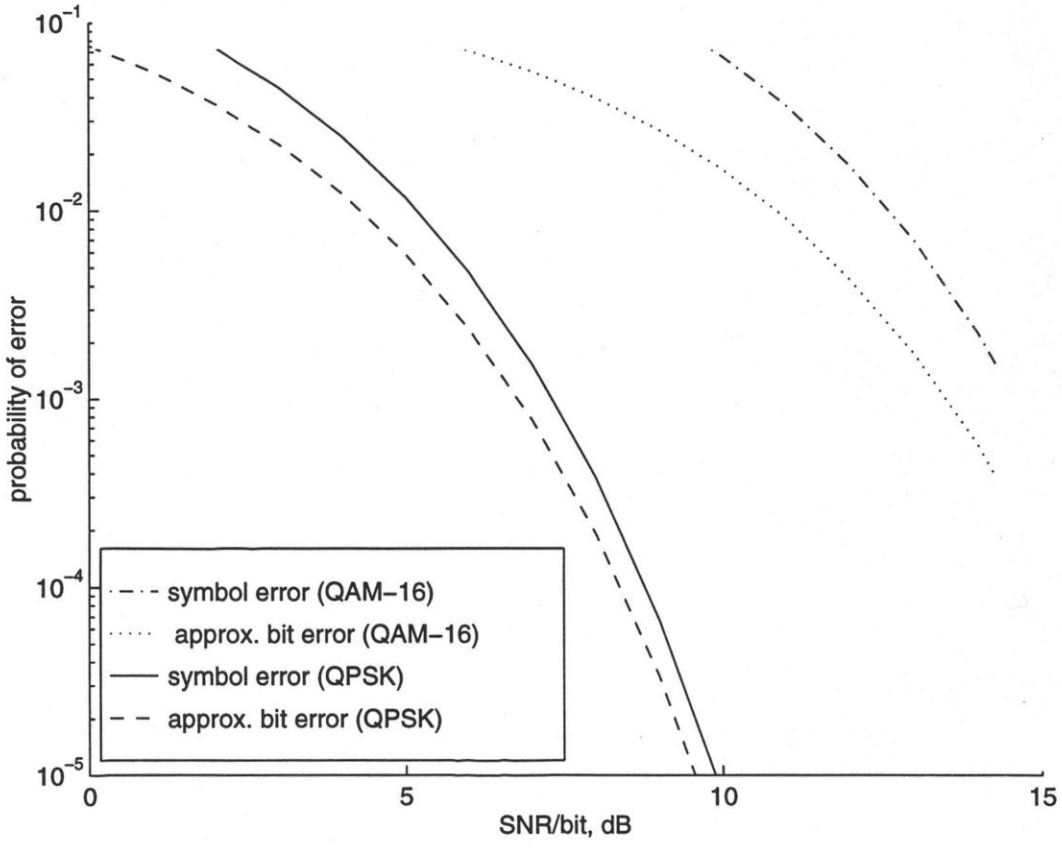


**Figure 6.1:** Probability of a symbol/bit error for QAM-16 and QPSK

$$P_{\sqrt{M}} = \left(1 - \frac{1}{\sqrt{M}}\right) erfc\left(\sqrt{\frac{3}{M-1}\frac{1}{2} n \gamma_b}\right) \tag{6.1}$$

where $\gamma_b$ is the SNR per bit. The probability of a correct decision ($P_c$) for the M-ary QAM system is calculated from Eq. 6.1,

$$P_c = \left(1 - P_{\sqrt{M}}\right)^2 . \tag{6.2}$$

Therefore the probability of symbol error ($P_M$) for the M-ary QAM system is given by Eq. 6.3,

$$P_M = 1 - {P_c}^2 = 1 - \left(1 - P_{\sqrt{M}}\right)^2 . \tag{6.3}$$

If the probability of symbol error ($P_M \approx 0$) is very small, then the probability of bit error ($\widehat{P_M}$) can approximated by $\frac{P_M}{n}$.

$$\widehat{P_M} \approx \frac{P_M}{n} = \frac{1 - \left(1 - P_{\sqrt{M}}\right)^2}{n} \tag{6.4}$$

Fig. 6.1 shows the probability of a symbol/bit error for QAM-16 and QAM-4 (QPSK) modulation techniques.

## 6.2 Error Control

The usual way to ensure reliable delivery is to provide the sender with some feedback about what is happening at the other end of the line. Typically the protocol calls for the receiver to send back special control frames bearing positive or negative acknowledgements about the incoming frames. If the sender receives a positive acknowledgement about a frame, it knows the frame has arrived safely. On other hand, a negative acknowledgement means that something has gone wrong, and the frame must be transmitted again.

An additional complication comes from the possibility that hardware troubles may cause a frame to vanish completely (e.g., in a noise burst or collision of frames). This possibility is dealt with by introducing timers. When the frame is lost, the timer will go off after a certain time, alerting the sender to a potential problem. The obvious solution is to just transmit the frame again.

**Table 6.1:** Comparison of different Block Codes

| **Property** | **BCH** | **Reed-Solomon** | **Hamming** | **Maximum-Length** |
|---|---|---|---|---|
| *Block Length* (n) | $n = 2^m - 1$ m=3,4,5 | $n = m(2^m - 1)$ bits | $n = 2^m - 1$ | $n = 2^m - 1$ |
| *Number of parity bits* ($\hat{r}$) | | $\hat{r} = m2t$ bits | $\hat{r} = m$ | |
| *Minimum distance* ($\hat{d}$) | $\hat{d} \geq 2t + 1$ | $\hat{d} = m(2t + 1)$ bits | $\hat{d} = 3$ | $\hat{d} = 2^m - 1$ |
| *Number of information bits* ($\hat{k}$) | $\hat{k} \geq n - mt$ | | | $\hat{k} = m$ |

## 6.3 Forward Error Correction(FEC)

Network designers have developed many strategies for dealing with errors. One way is to include enough redundancy information along with the data to enable the receiver to deduce what the transmitted character must have been. FEC can be done many ways; one way is by using linear block codes.

### 6.3.1 Linear Block Codes

Linear block codes can be characterised by the $(n, \hat{k})$ notation. The encoder transforms a block of $\hat{k}$ message digits (a message vector) into a longer block of $n$ codeword digits (a code vector). The ratio $\hat{k}/n \equiv R_c$ is defined as the rate of the code [30, 31, 32, 33]

The elements of a code word are selected from the alphabet having q elements. When the alphabet consist of two elements (q=2), 0 and 1, the code is called a binary code. When the elements of a code word are selected from an alphabet having q elements ($q > 2$), the code is non-binary. It is interesting to note that when q is a power of 2, i.e., $q = 2^m$ where $m$ is a positive integer, each q-ary element has an

equivalent binary representation consisting of m bits and thus a non-binary code of block length $N$ can be mapped into a binary code of block length $n = mN$.

### 6.3.2 Reed-Solomon(RS) block code

Reed-Solomon block codes are non-binary linear block codes. They are a subset of the BCH codes, which in turn are a class of cyclic codes [18]. A non-binary block code consists of a set of fixed-length code words in which the elements of the code words are selected from an alphabet of $q$ symbols, denoted as $\{0, 1, 2, \ldots, q-1\}$. Usually, $q = 2^m$ so that $m$ information bits are mapped into one of the $q$ symbols. The length of a non-binary code word is denoted as $N$ and the number of information symbols is denoted as $\hat{K}$. The minimum distance of the non-binary code is denoted as $D_{min}$.

The physical layer is concerned with transmitting raw bits over a communication channel. The physical layer of the cable network supports Reed-Solomon codes for FEC as shown in Fig. 6.2 [1]. These codes are described by the following parameters:

$$N = q - 1 = 2^m - 1 \tag{6.5}$$

$$\hat{K} = 1, 2, 3, \ldots, N - 1 \tag{6.6}$$

$$D_{min} = N - \hat{K} + 1\,, \quad and \tag{6.7}$$

$$R_c = \frac{\hat{K}}{N}. \tag{6.8}$$

Such a code is guaranteed to correct up to

$$t = \left[\frac{D_{min} - 1}{2}\right] = \left[\frac{N - \hat{K}}{2}\right] \tag{6.9}$$

symbol errors.

A systematic $(N, \hat{K})$ code can be shortened by setting a number of the information symbols to zero. That is a linear $(N, \hat{K})$ code which consist of $\hat{K}$ information symbols,

and $N - \hat{K}$ check symbols can be shortened into an $(N - l, \hat{K} - l)$ linear code by setting the first $l$ symbols to zero. These $l$ symbols are not transmitted. The $N - \hat{K}$ check symbols are computed in the usual manner, as in the original code.

As an example, take m=8 (One symbol = One byte) , then $N = 2^8 - 1 = 255$ symbols in a codeword. Suppose further that it is required that $t = 10$, then $D_{min} = 2 \times t + 1 = 21$ and $\hat{K} = N - D_{min} + 1$ is $255 - 21 + 1 = 235$ information symbols.

The code rate is

$R_c = \hat{K}/N = 235/255 \cong 12/13$

The total number of bits in the codeword is $255 \times 8 = 2040$ bits/codeword Since the RS code of this example can correct ten symbols it can correct a minimum burst of $10 \times 7 + 1 = 71$ consecutive bit errors.

It is interesting to note that while the (255,235) RS code can correct 71 consecutive bit errors it must then have an error-free 255 - 10 = 245 symbols (1960 bits). Further, if the errors are random, and there is, at most, one error per symbol, then the RS code can correct only ten bit errors in 2040 bits. Clearly the RS code is not an efficient code for correcting random errors.

One reason for the importance of the Reed-Solomon codes is their good distance properties specially against burst noise. A second reason for their importance is the existence of efficient hard decision decoding algorithms which make it possible to implement relatively long codes in many practical applications where coding is desirable.

## 6.4 Error Detection

The cable plant is a potentially harsh environment that may cause several different error conditions to occur. The physical layer uses FEC to correct the errors (Section 6.3) and the FEC overhead is spread throughout the MAC frame where it is assumed to be transparent to the MAC data stream (Section A.2).

FEC is not a fool proof method of removing all errors. It is up to higher layers to detect the errors. Higher layers (MAC layer and higher layers) prefer error detection followed by retransmission, because it is more efficient. The most widely used method for error detection is by polynomial codes (also known as cyclic redundancy codes or CRC codes).

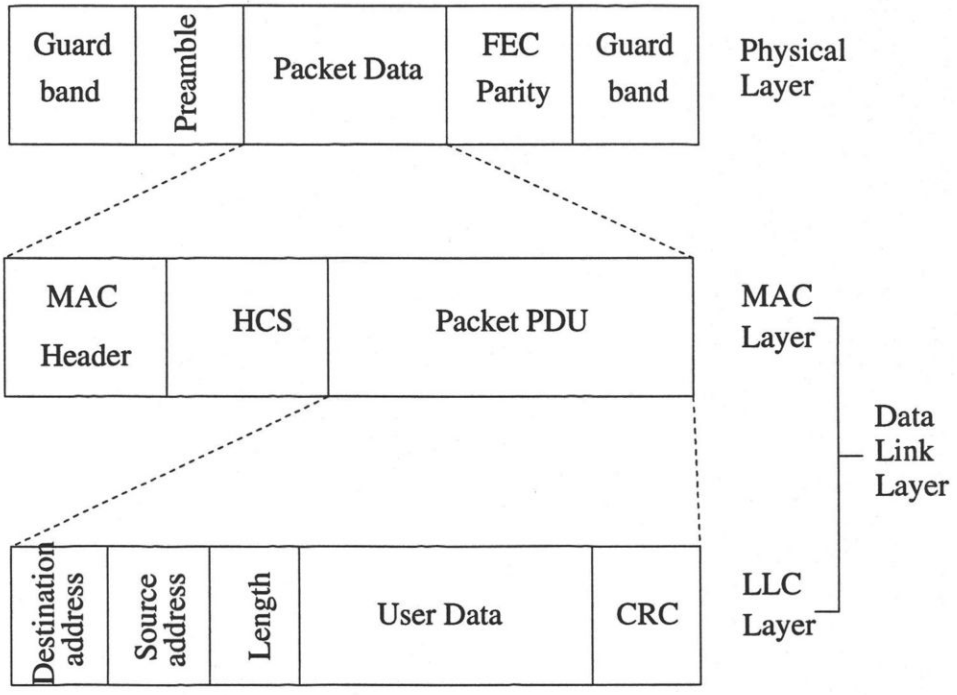


**Figure 6.2:** Data Link Layer and Physical Layer of cable modem

Polynomial codes are based upon treating bit strings as representations of polynomials with coefficients of 0 and 1 only. An r-bit frame is regarded as the coefficient list for a polynomial with r terms, ranging from $x^{r-1}$ to $x^0$. Such a polynomial is said to be of degree $r-1$. The high order (left most) bit is the coefficient of $x^{r-1}$, the next bit is the coefficient of $x^{r-2}$, and so on. Polynomial arithmetic is done modulo 2, according to the rules of algebraic field theory. When the polynomial code is employed, the sender and receiver must agree upon the generator polynomial, G(x), in advance. Both high order and low order bits of the generator must be 1. To compute the checksum for a frame with m bits, corresponding to the polynomial M(x), the

frame must be longer then the generator polynomial. The idea is to append a checksum to the end of the frame in such a way that the polynomial represented by the checksummed frame is divisible by G(x). When the receiver gets the checksummed frame, it tries dividing by G(x). If there is a remainder, there has been transmission error [3, 18, 30, 33].

### The HCS field

The MAC Header Check Sequence field is a 16-bit CRC that ensures the integrity of the MAC Header, even in a collision environment (Fig. A.2). The following widely-known CRC-16 polynomial is used [1].

$$\textbf{HCS Polynomial } \mathrm{G(x)} = x^{16} + x^{12} + x^5 + 1$$

The HCS field does not check *Packet PDU*. The integrity check of the *Packet PDU* is done by CRC at the LLC layer (Fig. 6.2).

## 6.5 The effect of White Noise on the performance

*White noise* is also known as Additive White Gaussian Noise (AWGN). Some of common causes of *white noise* are *thermal noise* (Section 3.1), *amplifier noise* (Section 3.1.2) and *ingress* (Section 3.2).

In Fig. 6.3, it is assumed that a channel has AWGN noise. If QPSK modulation is used and SNR ratio $\approx$ 9 dB, then from Eq. 6.3, the approximate BER under this condition is $10^{-4}$. The value of $m$ used is 8, so $N = 2^8 - 1 = 255$ and the frame length (including the physical header) is 200 bytes ($L_{tx} = 200$). In other words, the total number of information symbols in one code word is 200 ($\hat{K} - l = 200$). If RS can correct one symbol, then $t = 1$ and if RS is not used, then $t = 0$ and also in this example, one symbol is equal to one byte. If $t = 1$, then

$$N - l = \hat{K} - l + 2t = 200 + 2 = 202\ . \tag{6.10}$$

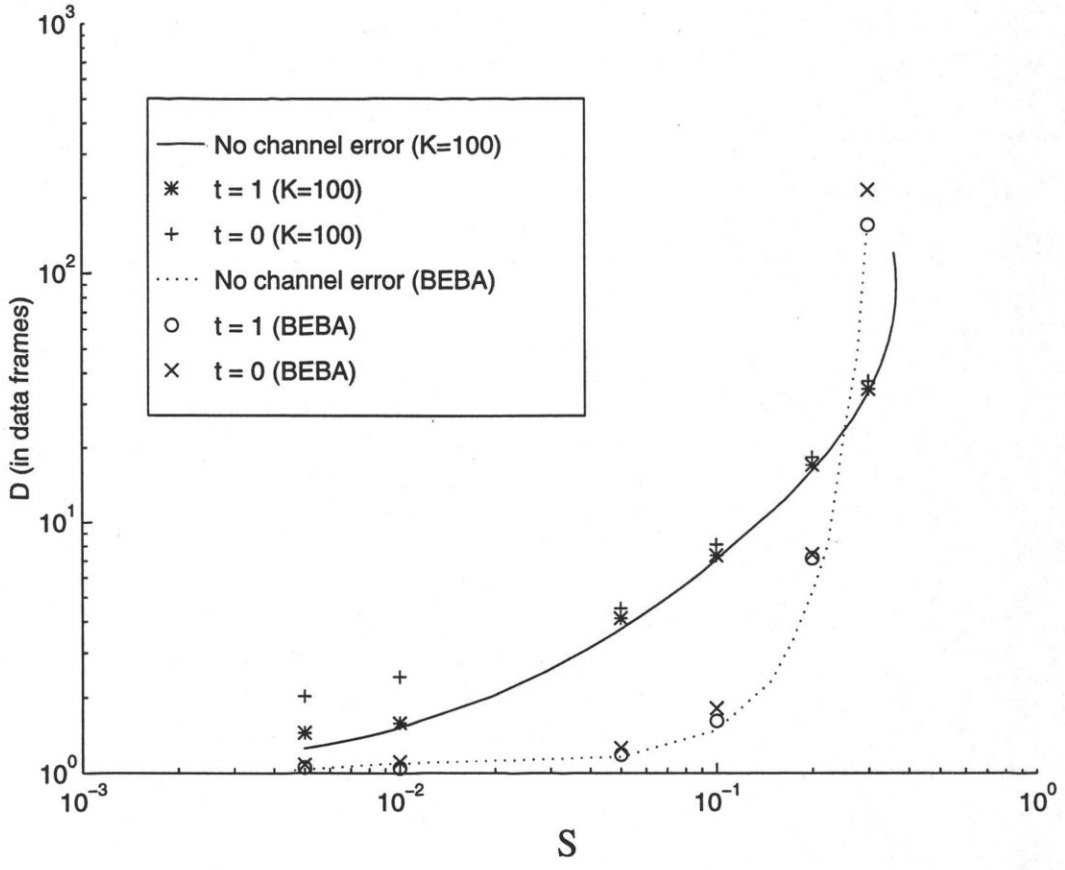


**Figure 6.3:** Performance of Slotted ALOHA in presence of AWGN noise

RS code is transmitted as a shortened codeword, with

$$l = N - 202 = 255 - 202 = 53 \; . \tag{6.11}$$

The length of the MAC and physical header combined is 20 bytes ($L_{req} = 20$ bytes). When a frame is transmitted by a CM, there are three possibilities considered:

1. The frame is transmitted successfully and is received by the CMTS and the HCS shows that the header is intact.

2. There is collision and the frame is lost.

3. There is no collision but the MAC header is corrupted (shown by HCS).

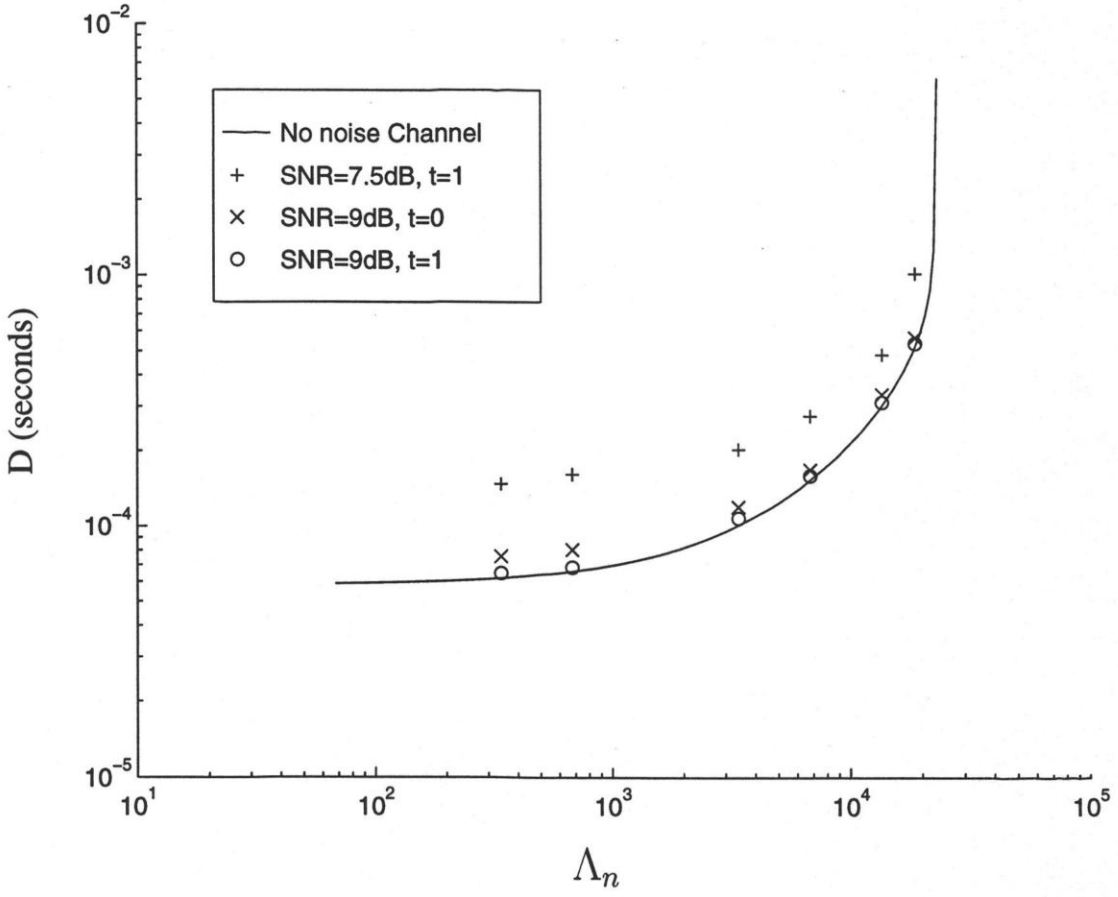


**Figure 6.4:** Effect of white noise on DRC protocol

In case of conditions 2 and 3, the CMTS will not send any acknowledgement. In this case the CM has to retry the frame again. For retransmission, the CM can use either *randomization* (K=100) or *The Binary Exponential Backoff Algorithm* (BEBA). The results in Fig. 6.3 show that there is very little increase in frame delay at $10^{-4}$ BER. By using RS codes ($t = 1$), frame delay further improves and approaches an ideal situation.

Fig. 6.4 shows the effect of white noise on the DRC protocol; the request frame is 20 bytes long and the data frame is 200 bytes long. In this example for the DRC protocol, the CM sends a request frame for reserving the bandwidth. This 20 bytes long frame consists only of the MAC header. The physical layer can use Reed-Solomon

FEC codes. If $r = 1$, then Reed-Solomon codes can correct one bit. If $r = 0$, then Reed-Solomon codes are not used. If there is collision or there is some error in the MAC header due to *white noise* (detected by the HCS) , then the CMTS will discard that frame. The CM uses randomization ($K = 100$) for frame retransmission.

If the request made by the CM is successful, then the CMTS reserves bandwidth for the CM at a particular instant as shown in Fig. A.4. The CM transmits a data frame in that slot. If due to *white noise*, the MAC header of the data frame gets corrupted, then the CMTS will discard that frame. The CMTS will again try to reserve bandwidth for the same CM in the next possible available slot. This process will continue until the CMTS receives the data frame with an error free MAC header. If QPSK modulation is used (Fig. 6.1), then by using Eq. 6.4, it is found that for the SNR = 9 dB, the system will give approximate BER $\approx 10^{-4}$ and for SNR = 7.5 dB, it will give approximate BER $\approx 10^{-3}$. It is found that at BER = $10^{-3}$, performance of the DRC protocol degrades substantially as seen in Fig. 6.4. The system performance remains close to ideal for BER = $10^{-4}$ as seen in Fig. 6.3 and Fig. 6.4.

## 6.6 The effect of Impulse Noise on the performance

Impulse noise consists of short duration pulses of unwanted signals which occur in a random pattern in the transmission medium. Impulse noise creates what appears as random transmission interruptions on multiple channels on both the upstream and downstream. Impulse noise appears on a spectral display as an increase in the noise floor across multiple channels, and possibly across the entire passband. It is usually of short time duration, less than 3 seconds [1, 14, 16, 34]. In this analysis only two parameters of impulse noise are considered (Section 3.3.3). These are *arrival rate* and *burst length.* It is further assumed that the density function of the arrival rate is *Poisson* and the density function of the burst length is *Uniform.*

Fig. 6.5 shows the effect of impulse noise on the DRC protocol; the modulation rate chosen is 200 kHz. The impulse noise incidence has burst length not longer than 100 $\mu$sec and the cycle rate is 10 Hz (type **A**) [1]. In the simulation, errors due to white noise are also introduced ($10^{-4}$ BER). Fig. 6.6 also shows the effect impulse noise on

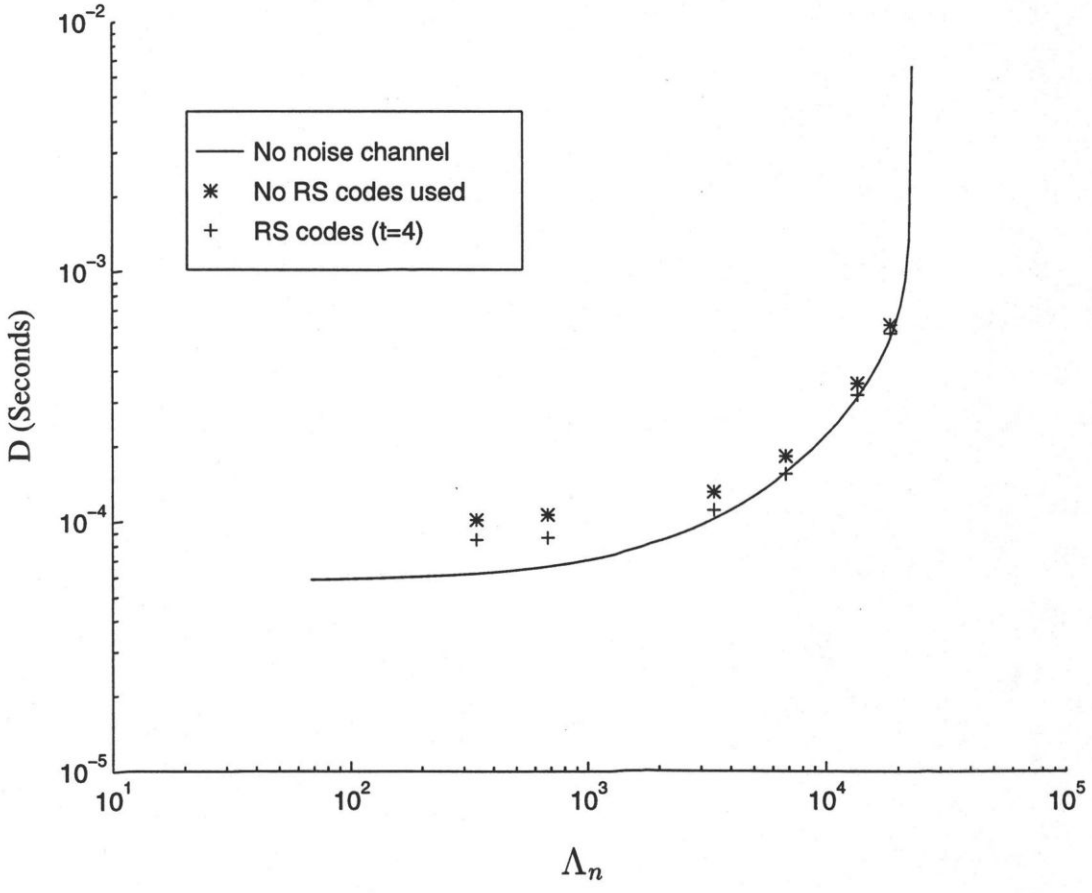


**Figure 6.5:** Effect of Impulse noise (type A) on DRC protocol

the DRC protocol but in this case, the impulse noise incidence has burst length not longer than 10 $\mu$sec and at a cycle rate of 1 kHz (type **B**) [1]. The other parameters are the same as used for Fig 6.4. In the simulation results, it is found that by using FEC, the performance degradation due to impulse noise can be controlled.

## 6.7 Summary

This chapter deals with the physical layer of the cable modems. Implementing the equipment with QPSK provides an economical, inherently robust format that has been proved over the years in the demanding environment of satellite communications and in field tests and preliminary installations over upstream HFC systems.

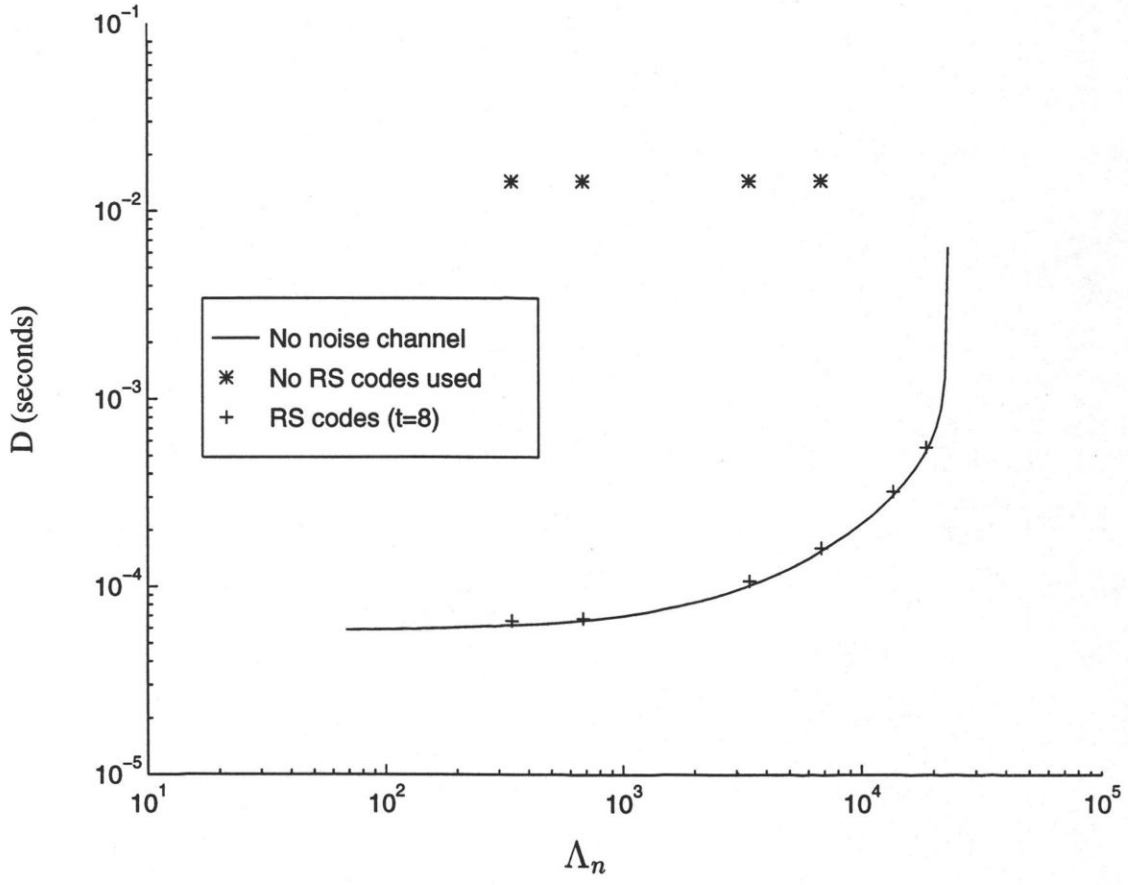


**Figure 6.6:** Effect of Impulse noise (type B) on DRC protocol

Forward Error Correction plays an important role. In this work, FEC at the physical layer is done using Reed-Solomon codes. As the frame length is not of fixed value, interleaving is not employed. RS codes add more information to the original data stream. This additional information tells the receiving modem how to correct the rest of its data in the event that an error occurs. Because RS codes add information, additional data bandwidth is required (or the throughput is reduced). One method that has been discussed is the ability to turn the FEC on and off. When the FEC is off, the data remain the same, but the throughput increases.

Error detection followed by retransmission is preferred at the MAC sublayer because it is more efficient. The total overhead is much less and the system becomes more robust. Polynomial codes (also known as a cyclic redunancy codes or CRC codes) are used for error detection. The *randomization* or *the binary exponential backoff algorithm* are used for retransmission.

From the simulation results, it is seen that the performance of the system remains at a satisfactory level at $10^{-4}$ random BER rate. At $10^{-3}$ random BER rate, the performance of the system degrades substantially. The system performance depends upon the nature of impulse noise. It is found that most of the impulse noise can be controlled using FEC.

# Chapter 7

# Summary and Conclusions

## 7.1 Summary

Conventional cable networks consist of a tree and branch architecture. A signal is originated at a cable headend and is sent to the cable subscriber through several bifurcations and a number of amplifiers spaced at pre-determined distances. Each amplifier receives a broadband signal and inserts enough gain and equalization such that a cascade of amplifiers have unity gain throughout the system. Reverse, or upstream, signal flow originates at a subscriber (CM) and terminates at the headend or hub (CMTS). Any signal transmitted over the reverse plant will eventually be re-processed at the headend for continuing distribution to subscribers over the forward cable plant.

A variety of cable systems ranging from a few hundred subscribers to several hundred thousand subscribers are present in North America. Equipment manufacturers for trunk amplifiers, distribution amplifiers, line extenders, passives, coaxial cables, lasers, etc., are often different from one cable system to another. Some cable systems consist solely of coaxial cable plants, while others have hybrid coaxial links with fiber nodes.

The upstream spectrum is limited, and this spectrum is shared by all users connected to the same coax drop. In addition, the upstream path is subject to interference, which enters the path and significantly degrades the transmission quality. The ingress in the cable return path is primarily due to broadcast signals which accumulate due to the noise funnelling effect of the cable return geometry. Although this

ingress can manifest itself in strong narrowband interferers which prevent the use of large bandwidth channels, a reduction of node size to nodes on the order of 500 homes or lower will reduce the amount of interference. Also, a well designed and properly maintained cable plant will be highly resistant to ingress problems. One of the entry points of ingress interference into the upstream path is from within the customer's home and this makes it extremely difficult to completely eliminate ingress.

Thermal noise level, carrier power level, channel frequency response, and interference due to ingress characterized by a statistical distribution of stationary disturbances in the cable environment provide useful information needed for both cost and performance optimization of the digital demodulator, as well as the cable system transmission equipment.

The coaxial cable network system still lacks standards to permit any cable modem to work with any headend equipment. Various independent groups are in the process of setting standards for the cable network system. MCNS specifications now define the physical layer, media access control layer, and operational support capabilities.

HFC, the new local distribution network solution currently being installed by cable TV providers, is different from other local distribution sytems. In HFC, only the final segment is shared coaxial cable and all users share common upstream spectrum. There is a strong need to have simple and efficient MAC protocols for this type of distribution system.

## 7.2 Conclusions

Some common impairments in the upstream channel of the hybrid fiber/coax cable network system have been discussed. New MAC protocols for the cable modem have been proposed in this work. The performance of these protocols when the users of the network have a variety of data rates have been analysed. The effects of *narrowband ingress* and *round trip* delay on the performance have been analysed. Most of the analytical results have been corroborated by preparing simulation models. The effect of *white noise* and *impulse noise* on the cable system performance have also been

studied by simulating the system. Below are the results of this work:

*Fixed assignment* using FDMA or TDMA is the simplest way to allocate bandwidth to all users. This protocol works fine if the traffic produced by all users is uniform and all users remain active at all times ($A_{cm} \approx N_{cm}$). But considering the bursty nature of much of the traffic, this protocol is highly inefficient and lots of bandwidth is wasted. The capacity assigned to inactive users is not utilised, whereas the active users experience relatively long delays due to the low capacity available to each user.

Slotted ALOHA is a simple and efficient way to allocate bandwidth at low channel traffic ($G < 0.36$ or $G_n < 0.33$). At higher channel traffic levels, the number of collisions increases and the system goes unstable. Another disadvantage of slotted ALOHA is that, for optimum performance, it demands fixed length data frames.

The DRNC protocol can utilize bandwidth to its full extent but at the cost of higher frame delay. If the system contains a very large number of users, ($N_{cm} \gg 200$), then this protocol is also highly inefficient; it also wastes bandwidth by polling inactive users. The DRLC protocol does not poll inactive users and hence its performance is better than DRNC. The performance of DRLC is even better than DRC at very high channel traffic ($G > 0.75$).

The DRC protocol gives very low frame delay even with considerable channel traffic ($G \approx 0.75$). DRC is highly efficient if the number of users is very large and user traffic is bursty. If it is assumed that a user can request all backlog traffic on a single request frame, then the efficiency of the DRC protocol can further be increased over that shown in the analysis and simulation models. In the DRC protocol, if there are some hyper active users, then there is a possibility that they can saturate the request channel. This problem is solved by the M-DRLC protocol. M-DRLC is a combination of DRC and DRLC protocols. Hyper users are alloted fixed bandwidth and they are unable to saturate the channel.

Ingress affects the cable system performance considerably. For example even narrowband ingress can make more than 15% of the upstream spectrum useless (Ta-

ble. 3.1). It is also seen that most of the noise is found between 5 and 18 MHz, while the band from 18 to 42 MHz is generally quiet spectrum. Large network distance also degrades the performance. It is seen that frame delay performance at $d = 30$ kms is almost ten times worse then at $d = 0$ kms (Fig 5.7).

The cable plant is a potentially harsh environment that may cause several different error conditions to occur. The system performance does not degrade substantially at $10^{-4}$ random BER (Fig. 6.6). If QPSK modulation is used and errors are only due to AWGN noise, then 9 dB SNR is sufficient for satisfactory performance. The impulse noise is sporadic in nature and the exact mechanisms involved in impulse noise generation are not completely known. In this thesis two types of impulse noise are simulated, (**a**), not longer than 100 $\mu$s at a 10 Hz average rate, (**b**), not longer than 10 $\mu$s at a 1 kHz average rate. It is found that errors due to impulse noise can be removed by using FEC (Fig. 6.6). By using proper Reed-Solomon codes, cable system performance can be maintained at a satisfactory level even in the presence of impulse noise.

## 7.3 Future Work

There are some impairments in cable plant which are not covered in this thesis. Some of them are: delay response distortion, hum modulation, plant micro-reflections and phase noise. Diplex filters in CATV amplifiers are one element that can introduce excessive delay variations over the frequency range of interest and which can impair digital transmission system performance. Hum modulation is the variation in the amplitude of a continuous wave carrier at the power line frequency of 60 Hz or its harmonics, induced throughout the cable network. Micro-reflections in the cable plant are generated when signals are reflected from component inputs and outputs as a result of return loss variations. Micro-reflections are generated by the trunk, the distribution system, and the subscriber environment. The resulting echoes will have the same content and frequency as the desired signal, but will be delayed relative to the desired signal. Phase noise is introduced by the high noise oscillators used in low quality cable modems. [8].

Synchronous code division multiple access is another MAC layer protocol which is not discussed in this thesis. This synchronous accessing scheme, with rigorous transmission schedules, is capable of producing very high throughput. S-CDMA is similar to the CDMA used in cellular and personal communication services networks, except that it exploits the fact that two-way cable modems communicate over fixed paths. While asynchronous CDMA networks treat other users on the same channel as noise, S-CDMA can eliminate the other users, providing enhanced noise and interference immunity. While dynamic channel allocation techniques described in this thesis search for narrow openings, S-CDMA uses the entire bandwidth and renders most of the noise harmless [35].

# References


[1] MCNS, "INTER COMM 97 - Global Communications Congress and Exhibition," Tech. Rep., Arthur D. Little Inc., 15/208 Acorn Park, Cambridge, Ma 02140, February 1997.

[2] D. Fleener, "Cable Modems To The Rescue," *Telephony*, vol. 232, pp. 21–26, June 1997.

[3] A. S. Tanenbaum, *Computer Networks.* Upper Saddle River, New Jersey 07458: Prentice Hall, third ed., 1996.

[4] A. Taylor, "Characterization of Cable TV Networks as the Transmission Media for Data," *IEEE Selected Areas In Communications*, vol. SAC-3, pp. 255–265, March 1985.

[5] C. A. Eldering, N. Himayat, and F. M. Gardner, "CATV Return Path Characterization for Reliable Communications," *IEEE Communication Magazine*, pp. 61–69, August 1995.

[6] SCTE, "Cable-Tec Expo' 96," Tech. Rep., Society of Cable Telecommunications Engineers, 140 Philips Road, Exton, PA 19341-1318, June 1996.

[7] SCTE, "Cable-Tec Expo' 97," Tech. Rep., Society of Cable Telecommunications Engineers, 140 Philips Road, Exton, PA 19341-1318, April 1997.

[8] CableLabs, "Two-Way Cable Television System Characterization," Tech. Rep., Cable Television Laboratories, Inc., 400 Centennial Parkway Louisville, CO 80027, April 1995.

[9] R. L. Freeman, *Telecommunication Transmission Handbook.* City College of New York, New York: John Wiley & Sons, Inc., third ed., 1991.

[10] R. L. Freeman, *Reference Manual For Telecommunications Engineering.* New York, 1985.

[11] F. Mazda, *Telecommunication Engineer's Reference Book.* Jordan Hill, Oxford: Butterworth Heinemann Ltd, 1993.

[12] F. Connor, *Noise, Introductory topics in Electronics and Telecommunication.* Edward Arnold, second ed., 1982.

[13] G. F. Donald and C. Donald, *Electronics Engineers Handbook.* MacGraw-Hill Book Company, third ed., 1989.

[14] J. Fennick, "A report on some characteristics of impulse noise in telephone communication," *IEEE Transactions on Communication and Electronics*, pp. 700–704, November 1964.

[15] J. Fennick, "Amplitude distribution of telephone channel noise and a mode for impulse noise," *Bell System Tech. Journal*, pp. 3243–3263, December 1969.

[16] J. Fennick, "Understanding impulse noise measurement," *IEEE Transaction on Communication*, pp. 247–251, 1972.

[17] H. Werner, T. Kessler, and H. Chung, "Coded 64-CAP ADSL in an impulse-noise environment," *IEEE Selected areas in Communications*, vol. 13, pp. 1610–1621, December 1995.

[18] J. G. Proakis, *Digital Communications.* 1221 Avenue of Americas, New York, NY 10020: McGraw-Hill, Inc., third ed., 1995.

[19] C. Shannon, "A mathematical theory of communication," *Bell System Tech. J.*, vol. 27, pp. 379–423 and 623–656, July and Oct. 1948.

[20] L. Tobagi, Fouad A. and. Kleinrock, "Packet Switching in Radio Channels: Part 3-Polling and, (Dynamic) Split-Channel Reservation Multiple Access," *IEEE Transactions on Communications*, vol. 24, pp. 832–844, August 1976.

[21] J. Bellamy, *Digital Telephony.* New York: John Wiley & Sons Inc., second ed., 1991.

[22] N. Abramson, *Multiple Access Communications, Foundations , for Emerging Technologies.* New York: The Institute of Electrical and Electronics Engineers, first ed., 1992.

[23] P. E. Green, *Computer Network Architecture and Protocols.* New York and London: Plenum Press, first ed., 1982.

[24] V. Paxson and S. Floyd, "Wide-Area Traffic: The Failure of Poisson Modeling," *SIGCOMM '94*, pp. 257–268, August 1994.

[25] M. F. Arlitt and C. L. Williamson, "A Synthesis Workload Model For Internet Mosaic Traffic," *Proceedings of the SCSC '95*, pp. 852–857, July 1995.

[26] W. Willinger, M. S. Taqqu, R. Sherman, and D. V. Wilson, "Self-Similarity Through High-Variability: Statistical Analysis of Ethernet Lan Traffic at the Source Level," *SIGCOMM '95*, pp. 100–113, 1995.

[27] K. Kerpez, "A Comparison of QAM and VSB for Hybrid Fiber/Coax Digital Transmission," *IEEE Transactions on Broadcasting*, vol. 41, pp. 9–15, March 1995.

[28] L. W. Couch, *Digital And Analog Communication Systems.* Toronto: Maxwell Macmillan Canada, fourth ed., 1993.

[29] R. E. Zeimer and R. L. Peterson, *Digital Communications And Spread Spectrum Systems.* New York: Macmillan Publishing Company, first ed., 1985.

[30] B. Sklar, *Digital Communications, Fundamentals and Applications.* Englewood Cliffs, N.J. 07632: Bernard Sklar, first ed., 1988.

[31] E. R. Berlekamp, *Algebraic Coding Theory.* New York: McGraw-Hill, first ed., 1968.

[32] S. Lin, *An introduction to error-correcting codes.* Englewood Cliffs, N.J. 07632: Prentice-Hall, first ed., 1970.

[33] R. E. Blahut, *Theory and practice of error control codes.* Addison-Wesley, first ed., 1983.

[34] W. Henkel, T. Kessler, and H. Chung, "Coded 64 - CAP ADSL in an impulse-noise environment-modeling of impulse noise and first simulation results," *IEEE J. Sel. Ar. Comm., Dec. 1995*, pp. 168–171, Dec. 1995.

[35] Y. Jong, R. Wolters, and P. Henrie, "A CDMA Based Bidirectional Communication System for Hybrid Fiber-Coax CATV Networks," *IEEE Transactions on Broadcasting*, vol. 43, pp. 127–135, June 1997.

# Appendix A

# Media Access Control Layer (*From MCNS Specifications*)

## A.1 Introduction

A MAC-sublayer domain is a collection of upstream and downstream channels for which a single MAC Allocation and Management protocol is run. Its attachments include one CMTS and some number of CMs. The CMTS MUST service all of the upstream and downstream channels; each CM may access one or more upstream and downstream channels.

### A.1.1 Service ID

The CMTS may assign one or more Service IDs (SIDs) to each CM, corresponding to the classes of service required by the CM. Service IDs provide both device identification and quality-of-service management. Within a MAC sublayer domain, all Service IDs MUST be unique. The length of the Service ID is 14 bits.

### A.1.2 Mini-Slots

The upstream transmission time-line is divided into intervals by the upstream bandwidth allocation mechanism. Each interval is an integral number of mini-slots. A mini-slot is the unit of granularity for upstream transmission opportunities. Each interval is labeled with a usage code which defines both the type of traffic that can be transmitted during that interval and the physical layer modulation encoding. A mini-slot is an integer multiple of 6.25 $\mu$sec increments.

## A.2 Frame

A frame is a unit of data exchange between two(or more) entities at the Data Link Layer. By IEEE convention, the Data Link Layer is divided into the LLC and the MAC sublayers. An LLC frame consists of a pair of 48-bit addresses, data and a CRC sum, and is normally encapsulated in a MAC frame. A MAC frame consists of a MAC header and an LLC frame; MAC frames are variable in length.

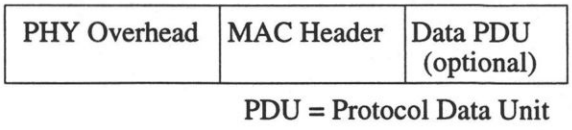


**Figure A.1:** Generic MAC Frame Format

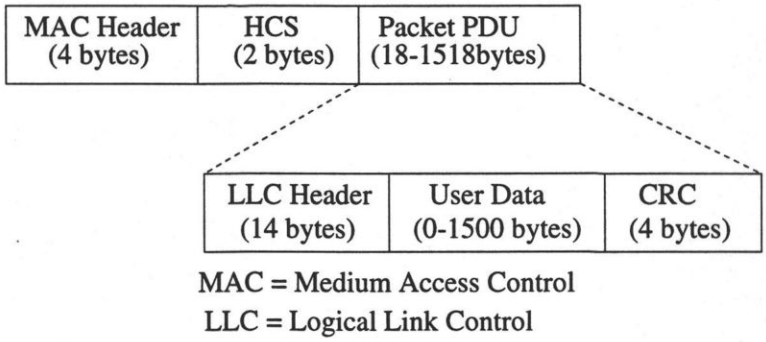


**Figure A.2:** Variable Length Packet PDU Frame

The length of a MAC frame is equal to 6 + n + PHY, where n is the length of the packet PDU in bytes. There are three distinct regions to consider as shown in Fig. A.1. The MAC Header uniquely identifies the contents of the MAC frame. The MAC sublayer must support a variable-length Ethernet type Packet Data PDU. The Packet PDU may be passed across the network in its entirety, including its original CRC. A unique Packet MAC Header is appended to the beginning. The frame format is shown in Fig. A.2. The MAC Header Check Sequence field is a 16-bit CRC that ensures the integrity of the MAC Header, even in the collision environment. The

**Table A.1:** PHY Overhead

| PHY Field | Usage | Size |
|---|---|---|
| Guard Band | Ensures that transmissions do not overlap | xbits |
| Preamble | Allows PHY to synchronize to new TX | ybits |
| Unique Word | Allows PHY to provide indication of start of MAC Frame | 16 bits |
| FEC | Error correction | Variable |

PHY overhead region provides a means for the PHY layer to indicate the start of the MAC frame. The PHY layer indicates the start of the MAC frame to the MAC sublayer. This is accomplished through a Unique Word pattern. The PHY layer may also introduce other overhead; a summary of the PHY overheads is given in Table A.1. The value of x and y are dependent on the specific burst profile in use. The FEC overhead is spread throughout the MAC frame and is assumed to be transparent to the MAC data stream. The MAC sublayer does need to be able to account for the overhead when doing the Bandwidth Allocation.

### A.2.1 MAC Frame Transport

The transport of MAC frames by the PHY layer for upstream transmission is shown in Fig. A.3.

## A.3 Upstream Bandwidth Allocation

The upstream channel is modeled as a stream of mini-slots. The CMTS generates the time references for identifying these slots. It also controls access to these slots by the cable modems. For example, it grants some number of contiguous slots to a CM for it to transmit a data PDU. The CM times its transmission so that the CMTS receives it in the time reference specified. This section describes the element of protocol used in requesting, granting, and using upstream bandwidth. The basic mechanism for assigning bandwidth management is the allocation map as shown in Fig. A.4.

The allocation map is a MAC Management message transmitted by the CMTS

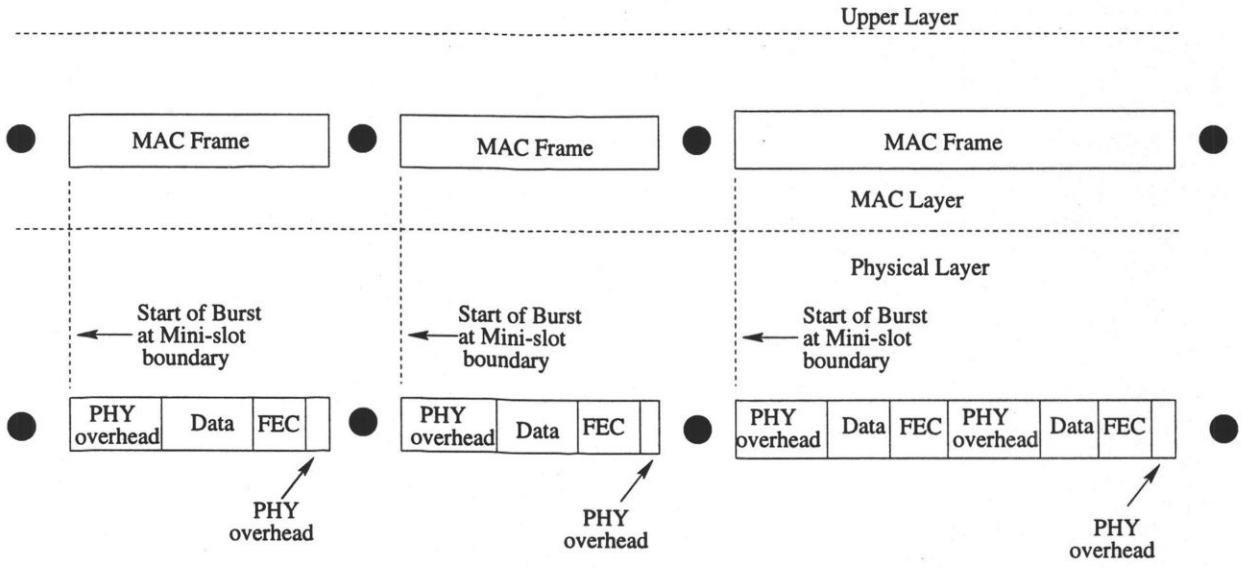


**Figure A.3:** Upstream MAC/PHY Convergence

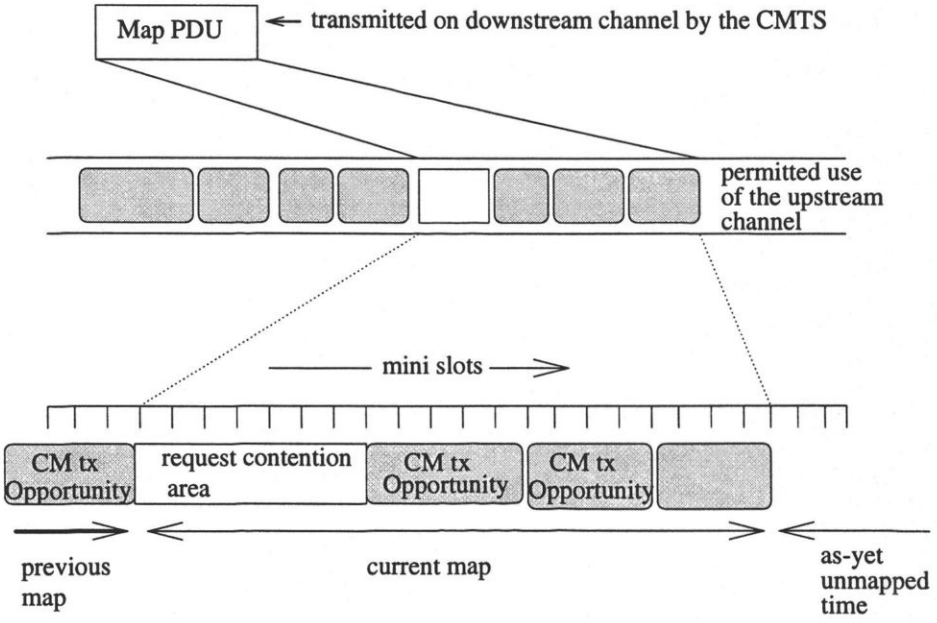


**Figure A.4:** Allocation Map

on the downstream channel which describes, for some interval, the uses to which the upstream mini-slots are put. A given map describes some slots as grants for particular stations to transmit data in; other slots are available for contention transmission, and other slots as an opportunity for new stations to join the link.

Many different scheduling algorithms may be implemented in the CMTS.

The bandwidth allocation includes the following basic elements.

- Each CM has one or more short(14-bit) service identifiers as well as a 48-bit address
- Upstream bandwidth is divided into a stream of mini-slots. Each mini-slot is numbered relative to a master reference maintained by the CMTS. The clocking information is distributed to the CMs by means of SYNC packets.
- CMs issue requests to the CMTS for upstream bandwidth.

# Appendix B

# Protocol Example (*From MCNS Specifications*)

Suppose a given CM has a data PDU available for transmission.

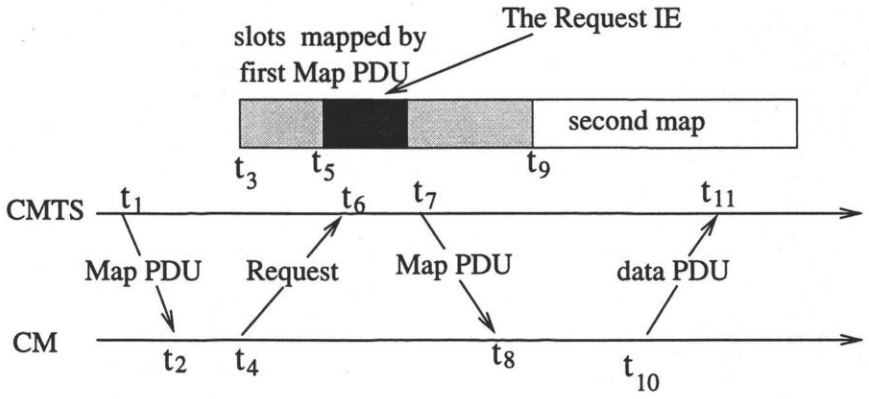


**Figure B.1:** Protocol Example

1. At time $t_1$, the CMTS transmits a map whose effective starting time is $t_3$. Within this map is Request IE which will start at $t_5$. The difference between $t_1$ and $t_3$ is needed to allow for:

   - downstream propagation delay(including FEC),
   - processing time at the CM, and
   - upstream propagation delay.

2. At $t_2$, the CM receives this map and scans it for request opportunities. In order to minimize request collisions, it calculates $t_6$ as a random offset from $t_5$ within the interval described by the Request IE.

3. At $t_4$, the CM transmits a request for as many mini-slots as needed to accommodate the PDU. Time $t_4$ is chosen based on the ranging offset so that the request will arrive at the CMTS at $t_6$.

4. At $t_6$, the CMTS receives the request and schedules it for service in the next map.

5. At $t_7$, the CMTS transmits a map whose effective starting time is $t_9$. Within this map, a data grant for the CM will start at $t_{11}$. The grant will be for the entire request unless fragmentation is used.

6. At $t_8$, the CM receives the map and scans for its data grant.

7. At $t_{10}$, the CM transmits its data PDU so that it will arrive at the CMTS at $t_{11}$. Time $t_{10}$ is calculated from the ranging offset.

Steps 1 and 2 need not contribute to access latency if CMs routinely maintain a list of request opportunities.

At Step 3, the request may collide with requests from other CMs and be lost. The CMTS does not directly detect the collision. The CM determines that a collision occurred when the next map fails to include acknowledgment of the request. The CM then performs a back-off algorithm and retries.

At Step 4, the CMTS scheduler may fail to accommodate the request within the next map. If so, it will reply with a zero length grant in that map. It continues to report this zero-length grant in all succeeding maps until the request is granted. This signals to the CM that a request is still pending.

**Contention Resolution** The CMTS allow collisions on either Requests or Data PDUs. When the CM tries a contention transmission, it randomly chooses one of the available transmit opportunities as defined in the Request IE or Request/Data IE in the allocation map. The CM determines that the contention transmission is lost when it finds that in a subsequent map, Data Grant or Data Grant Pending is missing. The CM then uses the contention resolution scheme to defer and re-try at a later transmit opportunity.

The contention resolution scheme is based on a truncated binary exponential back-off; the back-off window and maximum back-off window are controlled by the CMTS and represents a power of two value. For example a value of 4 indicates a window between 0 and 15, a value of 10 indicates a window between 0 and 1023. After each subsequent collision, the cable modem must increase its back off window by a factor of two, as long as it is less than the maximum back off window. The CM randomly selects a value within the new back-off window and defers this number of contention opportunities before retrying. This continues until the maximum number of retries has been reached, at which time the PDU is discarded.

If the CM receives the unicast Request at any time while deferring for this SID, it must stop the contention resolution process and use the explicit opportunity.